108

THERMAL WATERS ALONG THE NORTH ANATOLIAN FAULT ZONE (NAFZ): GEOCHEMISTRY AND GEOTHERMOMETRY APPLICATIONS

A THESIS SUBMITTED TO
THE GRADUATE SCHOOL OF NATURAL AND APPLIED SCIENCES
OF
THE MIDDLE EAST TECHNICAL UNIVERSITY

BY

JÜLİDE YAPMIŞ

119269

T.C. YÜKSEKÖĞRETİM KURULU
DOKÜMANTASYON MERKEZİ

119269

IN PARTIAL FULFILLMENT OF THE REQUIREMENTS FOR THE DEGREE OF

MASTER OF SCIENCES

IN

THE DEPARTMENT OF GEOLOGICAL ENGINEERING

SEPTEMBER 2002

Approval of the Graduate School of the Natural and Applied Sciences

Prof. Dr. Tayfur Öztürk
Director

I certify that this thesis satisfies all the requirements as a thesis for the degree of Master of Sciences.

Prof. Dr. Nurkan Karahanoğlu
Head of Department

This is to certify that we have read this thesis and that in our opinion it is fully adequate, in scope and quality, as a thesis for the degree of Master Sciences.

Prof. Dr. Nilgün Güleç
Co-Supervisor

Prof. Dr. Nurkan Karahanoğlu
Supervisor

Examining Committee Members

Prof. Dr. Nurkan Karahanoğlu

Prof. Dr. Nilgün Güleç

Prof. Dr. Mahmut Parlaktuna

Assoc. Prof. Dr. Kadir Dirik

Assoc. Prof. Dr. Zeki Çamur

ABSTRACT

THERMAL WATERS ALONG THE NORTH ANATOLIAN FAULT ZONE (NAFZ): GEOCHEMISTRY AND GEOTHERMOMETRY APPLICATIONS

Yapmış, Jülide

M.S., Department of Geological Engineering

Supervisor: Prof. Dr. Nurkan Karahanoğlu

Co-Supervisor: Prof. Dr. Nilgün Güleç

September 2002, 96 pages

This study is concerned with determination of geochemical characteristics and assessment of geothermal potential of fields located along the North Anatolian Fault Zone (NAFZ), which Gölyaka-Efteni (Bolu), Mudurnu-Babas (Bolu), Seben-Pavlu (Bolu), Bolu (town center), Kurşunlu-Çavundur (Çankırı), Gözlek (Amasya) and Reşadiye (Tokat). Water samples were collected in two different periods, June 2000 and April 2001.

Discharge temperature of thermal waters ranges between 38 and 73°C, pH values are between 5.6 and 7.5. TDS content varies from 11074 to 433 mg/l. The majority of thermal waters are Na-HCO_3. Chemical composition of waters, when examined with their discharge temperature, suggests occurrence of subsurface mixing and conductive cooling in Kurşunlu, Seben and Mudurnu.

Geothermometry applications and silica-enthalpy, chloride-enthalpy mixing models, which could be applied to Kurşunlu, Mudurnu and Seben, yielded reservoir estimates ranging from 88-115 °C for Kurşunlu, 85-88 °C for Bolu, 143-150 °C for Efteni, 77-101 °C for Mudurnu, 110-149 °C for Seben, 97-99 °C for Reşadiye and 67-72 °C for Gözlek.

Fluid-mineral equilibria calculations were performed for carbonate, sulphate and quartz minerals. These calculations revealed that all waters are supersaturated with respect to calcite and silica. As, however, no saturation state assessment could be done with respect to feldspar, mica and clay minerals (due to lack of Al^{+3} data), no equilibrium temperature could be obtained from these calculations.

Kurşunlu, Efteni, Mudurnu, Seben and Reşadiye are more promising for geothermal energy development. However, they may require some precautions to be taken against possible silica and calcite scaling during utilisation of these thermal waters.

Keywords: Thermal Waters, North Anatolian Fault Zone, Geothermal, Geothermometry, Geochemistry

ÖZ

KUZEY ANADOLU FAYI HATTINDA YER ALAN TERMAL SULARDA JEOKİMYA VE JEOTERMOMETRE UYGULAMALARI

Yapmış, Jülide

Yüksek Lisans, Jeoloji Mühendisliği Bölümü

Tez Yöneticisi: Prof. Dr. Nurkan Karahanoğlu

Ortak Tez Yöneticisi: Prof. Dr. Nilgün Güleç

Eylül 2002, 96 sayfa

Bu çalışma Kuzey Anadolu Fay hattında yer 7 jeotermal alanın, Gölyaka-Efteni (Bolu), Mudurnu-Babas (Bolu),Seben-Pavlu (Bolu), Bolu (merkez), Kurşunlu-Çavundur (Çankırı), Gözlek (Amasya) ve Reşadiye (Tokat), jeokimyasal karakteristiğini ve jeotermal potansiyelini belirlemeyi konu almaktadır. Örnekleme işlemleri Haziran 2000 ve Nisan 2001 olmak üzere 2 farklı dönemde gerçekleştirilmiştir.

Termal suların sıcaklıkları 38 ile 73 °C arasında, pH'ları 5.6 ile 7.5 arasında, TDS içerikleri 11074 ile 433 ppm arasında değişmektedir. Ca-SO_4 tipinde olan Bolu ve Ca-HCO_3 tipinde olan Mudurnu dışında, termal sular Na-HCO_3 tipindedir. Kurşunlu, Seben ve Mudurnu alanlarında termal suların kimyasal bileşimleri

sıcaklıkları ile birlikte değerlendirildiğinde soğuk su ile karışmış oldukları veya kondüktif soğumaya maruz kaldıkları ileri sürülebilir.

Jeotermometre uygulamalarından ve Kurşunlu, Seben ve Mudurnu alanlarına uygulanabilen silika-entalpi ve klorit-entalpi karışım modellerinden elde edilen rezervuar sıcaklıkları Kurşunlu'da 88-115 °C, Bolu'da 85-88 °C, Efteni'de 143-150 °C, Mudurnu'da 77-101 °C, Seben'de 110-149 °C, Reşadiye'de 97-99 °C ve Gözlek'de 67-72 °C arasında değişmektedir .

Kabuklaşma problemi olasılığını ortaya koymak ve elde edilen rezervuar sıcaklığının bir de bu yöntemle kontrolünü yapmak için karbonat, sülfat ve kuvars mineralleri için akışkan-mineral dengesi hesaplamaları yapılmıştır. Bütün termal suların kalsit ve silika minerallerine doygun olduğu ortaya çıkmıştır. Ancak, Al^{+3} verisi olmadığı için feldspar, mika ve kil minerallerine ilişkin doygunluk hesapları yapılamadığından, mineral akışkan dengesi hesapları ile denge sıcaklıklarının belirlenmesi mümkün olmamıştır.

Jeotermal enerji açısından Kurşunlu, Efteni, Mudurnu, Seben ve Reşadiye alanlarının daha umut verici alanlar olduğu gözükmektedir. Ancak, bu termal suların kullanımı sırasında silika ve kalsit kabuklaşması için önlem alınmalıdır.

Anahtar Kelimeler: Termal Sular, Kuzey Anadolu Fay Hattı, Jeotermal, Jeotermometre, Jeokimya.

ACKNOWLEGEMENTS

I would like to express my sincere gratitude to my supervisor Prof. Dr. Nurkan Karahanoğlu and my co-supervisor Prof. Dr. Nilgün Güleç, for their guidance, kind criticism and insight throughout the research.

This thesis research was carried out under the financial support by METU Research Fund Project AFP No: 99-03-09-02 which I acknowledge with thanks.

I would also like to express my gratitude to Assoc. Prof. Dr. Zeki Çamur for his kind help.

Finally, I am appreciative to my parents for their all kind support and thrust throughout this study.

TABLE OF CONTENTS

ABSTRACT..... iii

ÖZ..... v

ACKNOWLEDGEMENTS..... vii

TABLE OF CONTENTS..... viii

LIST OF TABLES..... x

LIST OF FIGURES..... xi

CHAPTERS

1. INTRODUCTION..... 1

1.1. Purpose and Scope..... 3

1.2. Methods of Study.....3

2. GEOTHERMAL FIELDS..... 5

2.1. Tectonic Setting: The North Anatolian Fault Zone..... 5

2.2. Geologic and Hydrogeologic Setting.....8

2.2.1. Kurşunlu-Çavundur (Çankırı).....8

2.2.2. Bolu-Town Centre..... 10

2.2.3. Efteni-Gölyaka (Bolu)..... 12

2.2.4. Babas-Mudurnu (Bolu)..... 15

2.2.5. Seben-Kesenözü-Pavlu (Bolu).....15

2.2.6. Gözlek-Amasya..... 17

2.2.7. Reşadiye-Tokat.....20

3. HYDROGEOCHEMICAL CHARACTERISTICS.....23

3.1. Methods of Study.....23

3.1.1. Sampling.....23

3.1.2. Analytical Techniques.....26

3.2. Results.....27

3.3. Discussion.....30

3.3.1 Water Type.....30

3.3.2 Evaluation of Subsurface Processes.....36

4. GEOTHERMOMETRY APPLICATIONS.....46

4.1. Principles.....46

4.2. Silica Geothermometers.....46

4.3. Cation Geothermometers.....49

4.4. Results of Chemical Geothermometer Calculations.....52

4.5. Na-K-Mg Diagram and Na-K-Mg-Ca Diagram.....56

4.6. Mixing Models.....58

5. FLUID-MINERAL EQUILIBRIA.....70

5.1. Theory.....70

5.2. Saturation Index Calculations for Geothermal Fields.....73

6. CONCLUSIONS.....77

REFERENCES.....79

APPENDICES

A. METHODS OF ANALYSES.....87

B. CALCULATION OF BOILING TEMPERATURE.....93

C. CALCULATION OF CBE AND TDS.....94

D. EXAMPLE OUTPUT FILE FOR PROGRAM WATSPEC.....95

LIST OF TABLES

TABLE

3.1.a. Information relevant to the samples and sample localities (June 2000)..... 24

3.1.b. Information relevant to the samples and sample localities (April 2001)..... 25

3.2.a. The results of the chemical analyses of water samples collected in June 2000..... 28

3.2.b. The results of the chemical analyses of water samples collected in April 2001..... 29

3.3. Correlation coefficients between ions of water samples 40

4.1. Temperature equations for silica geothermometers 47

4.2. Temperature equations of cation geothermometers 50

4.3. Results of silica geothermometery applications of collected waters (°C)..... 53

4.4. Results of cation geothermometery application of collected waters (°C)..... 55

T.C. YÜKSEKÖĞRETİM KURULU
DOKÜMANTASYON MERKEZİ

LIST OF FIGURES

FIGURES

1.1. Map showing distribution of geothermal fields in Turkey..... 2

2.1. Map showing sample location and distinctive structural Units in Anatolia..... 6

2.2. Geologic map of Kurşunlu geothermal field..... 9

2.3. Geologic map of Bolu geothermal field..... 11

2.4.a. Geologic map of Efteni geothermal field..... 13

2.4.b. Geologic map of Derdin geothermal field..... 14

2.5. Geologic map of Mudurnu geothermal field..... 16

2.6. Geologic map of Seben geothermal field..... 18

2.7. Geologic map of Gözlek geothermal field..... 19

2.8. Geologic map of Reşadiye geothermal field..... 22

3.1.a. Piper diagram showing major ion distribution for samples collected in June 2000..... 31

3.1.b. Piper diagram showing major ion distribution for samples collected in April 2001..... 32

3.2.a. Schoeller diagrams for samples collected in June 2000..... 34

3.2.b. Schoeller diagrams for samples collected in April 2001..... 35

3.3 Variation diagrams in ionic concentration of samples collected in June 2000 and April 2001..... 37 and 38

3.4.a. Ionic abudance vs. discharge temperature diagrams for Kurşunlu samples..... 42

3.4.b. Ionic abudance vs. discharge temperature diagrams for Mudurnu samples..... 44

3.4.c. Ionic abudance vs. discharge temperature diagrams for Seben samples..... 45

4.1. Graphical evaluation (Giggenbach, 1988) of the water-rock equilibration temperatures using relative Na, K and Mg concentrations (mg/kg) of thermal water in the studied areas..... 57

4.2. Plot of 10K/(10K+Na) vs. 10Mg/(10Mg+Ca) of thermal water (mg/kg) in the studied areas (Giggenbach, 1988)..... 59

4.3. Silica-enthalpy mixing model for samples of Seben..... 61

4.4. Silica-enthalpy mixing model for samples of Mudurnu..... 62

4.5. Silica-enthalpy mixing model for samples of Kurşunlu..... 64

4.6. Entalpy-chloride mixing model for samples of Seben..... 65

4.7. Entalpy-chloride mixing model for samples of Kurşunlu..... 68

5.1. Mineral equilibrium diagrams for samples collected in June 2000 and April 2001..... 74 and 75

CHAPTER 1

INTRODUCTION

Geothermal energy is the natural heat of the Earth. From earliest times, people have used this energy for bathing, cooking, medicine and heat building. Today, geothermal energy appears as an alternative energy in many places and it is used to generate electricity or for direct uses.

Many geothermal fields are localized in active tectonic and volcanic areas, especially along active plate boundaries such as the spreading ridges and the subduction zones.

Turkey is located in the tectonically active Alpine-Himalayan belt and characterized by a widespread geothermal activity. This activity manifests itself as numerous hot springs, fumaroles and recent mineralization. The distribution of hot springs in Turkey roughly parallels the distribution of the fault systems (Figure 1.1).

Geological, geophysical, geochemical and drilling studies carried on until these days pointed out that high enthalpy systems (>150 °C) are concentrated in West Anatolian Region under extensional tectonic regime in Turkey (Mutlu and Güleç, 1996). Intermediate and low enthalpy systems are found in North, Central and East Anatolia, the latter two being a volcanicly active region recently.

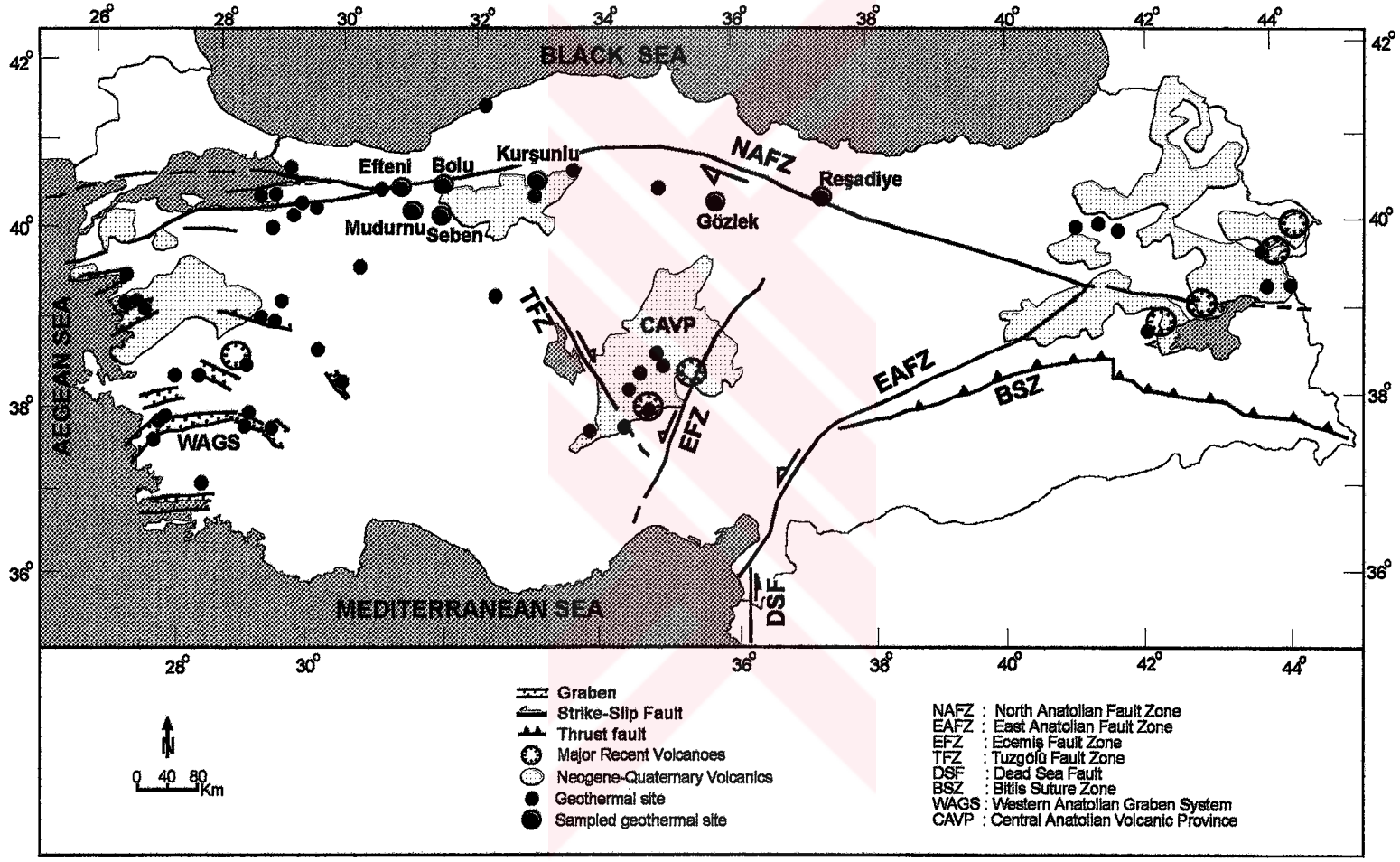


Figure 1.1. Map showing distribution of geothermal fields in Turkey (Şaroğlu, et al., 1992).

The present study is concerned with the geothermal fields located along the North Anatolian Fault Zone (NAFZ), studied by several researchers (Canik, 1971; Şahinci, 1971; Canik, 1972; Koçak, 1974; Ünlü and Balkaş, 1975; Şentürk and Ünay, 1976; Özcan and Ünay, 1978; Yücel et al, 1994) in terms of geological, geophysical or geochemical characteristics.

1.1. Purpose and Scope

The purpose of this study is to determine geochemical characteristics and geothermal potential of the geothermal fields along the North Anatolian Fault Zone (NAFZ).

Study fields include a total of 7 geothermal fields along NAFZ (E-W transect of 530 km long from Bolu to Reşadiye-Tokat). These geothermal fields are Gölyaka-Efteni (Bolu), Bolu (Town Center), Mudurnu-Babas (Bolu), Seben-Kesenözü-Pavlu (Bolu), Kurşunlu-Çavundur (Çankırı), Gözlek (Amasya) and Reşadiye (Tokat) (Figure 1.1).

1.2. Methods of Study

The study includes three steps: i) sampling, ii) laboratory analysis, iii) data interpretation. Sampling was performed in two different periods, June 2000 and April 2001. 15 samples were collected from both natural springs and the production wells in the first, and 16 samples were collected in the second sampling periods. Laboratory analyses were conducted by titration, spectrophotometer and flame photometer in the laboratories of the Department of Geological Engineering. The

results of analyses were evaluated to determine chemical characteristics of the thermal waters and to estimate reservoir temperature of the geothermal fields.

CHAPTER 2

GEOTHERMAL FIELDS

2.1 Tectonic Setting: The North Anatolian Fault Zone

This study includes the geothermal fields located on North Anatolian Fault Zone which is a major structural unit originated as a result of northward movement of Afro-Arabian plate during neotectonic period of Anatolian Block (McKenzie, 1972; Dewey and Şengör, 1979).

Post collisional convergence between the Afro-Arabian and Eurasian Plates has resulted in the formation of several neotectonic provinces (Şengör et al., 1979) characterized by distinctive structures like Bitlis Suture Zone, East Anatolian Fault Zone (EAFZ), North Anatolian Fault Zone (NAFZ) and West Anatolian Graben System (WAGS) (Figure 2.1).

The Bitlis Suture Zone is the manifestation of the collision between the Afro-Arabian and Eurasian Plates, which occurred in about the Middle Miocene (Dewey and Şengör, 1979). The diffuse seismic activity throughout eastern Turkey (Mc Kenzie, 1972; Rotstein and Kafka, 1982; Jackson and Mc Kenzie, 1984) and the folding and thrusting of recent sediments onto the Arabian platform suggest that the convergence is still in progress (Şengör and Canıtez, 1982).

T.C. YÜKSEKÖĞRETİM KURULU
DOKÜMANTASYON MERKEZİ

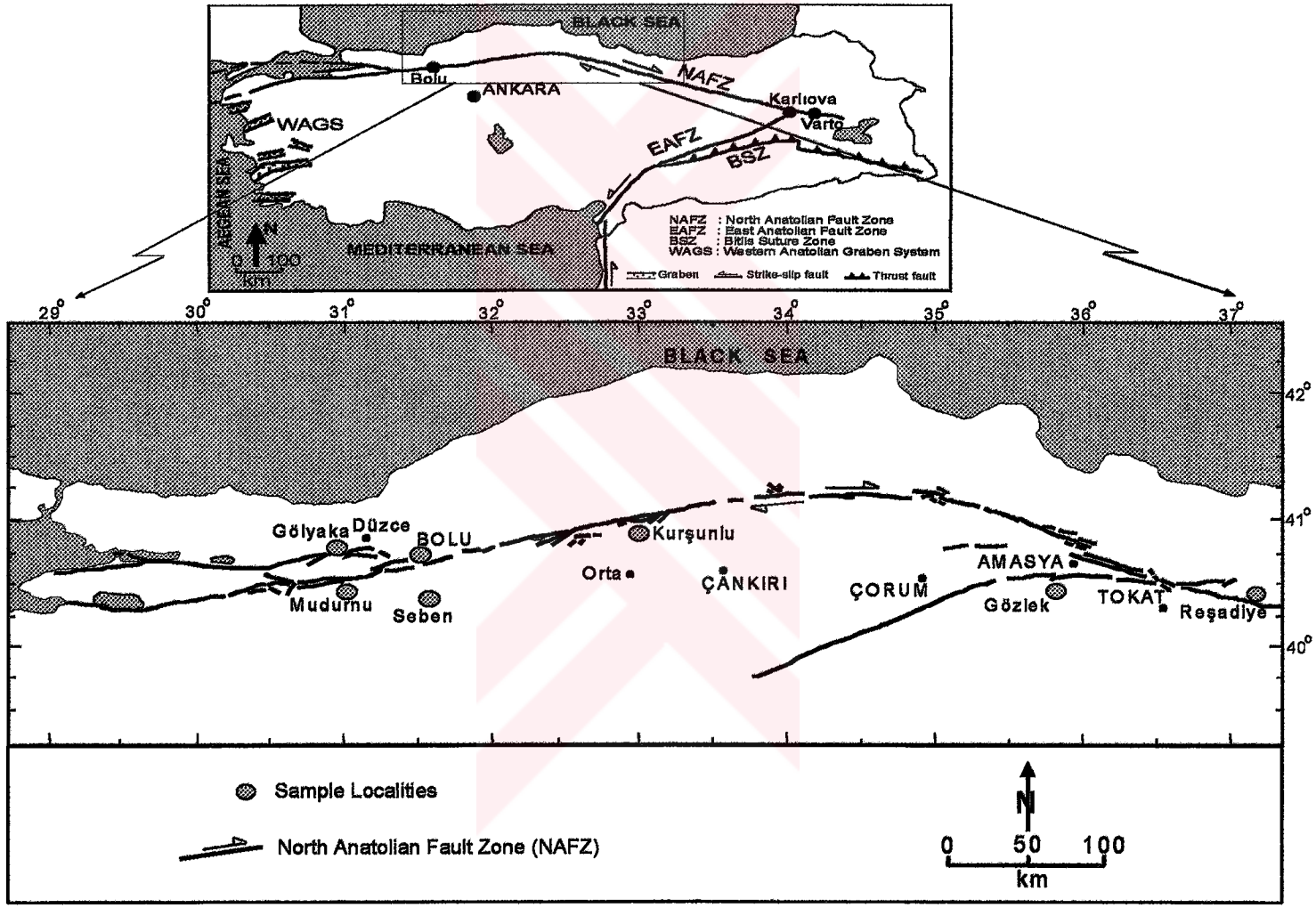


Figure 2.1. Map showing sample location and distinctive stuctural units in Anatolia (Çemen et al., 2000).

The North Anatolian Fault Zone and the East Anatolian Fault Zone and are strike-slip faults (with right-lateral and left-lateral sense, respectively) originated in response to the northward movement of the Arabian Plate (McKenzie, 1972; Dewey and Şengör, 1979). The faults are not single rupture, but are narrow zones consisting of small faults of en-echelon geometry. Starting from the Karlıova junction in the east, the EAFZ extends southwestward where it is connected to the Dead Sea Fault (Arpat and Şaroğlu, 1972). The NAFZ extends westwards and, to the west of 31 longitude, is split into several branches characterized by dominant normal faulting component along with strike-slip component (Canıtez and Üçer, 1967; Mc Kenzie, 1972; Dewey and Şengör, 1979).

The NAFZ is about 1500 km long, broad arc-shaped, dextral strike-slip fault system that extends from eastern Turkey in the east to Greece in the west, a few hundred meters to 40 km wide and is an active dextral fault zone consisting numerous parallel to subparallel, sometimes anastomosing fault segments (Bozkurt, 2001). The fault zone has a mostly single fault trace for about 900 km between Karlıova in the east and Dokurcun town in the west. To the west of Dokurcun town, the NAFZ bifurcates into two major strands, the Geyve fault in the south and the Adapazarı fault zones in the north. The age of NAFZ is Early Pliocene (Barka and Kadinsky-Cade, 1988). Geological works along NAFZ estimate a total offset ranging from 85 ± 5 km to 20-25 km (Seymen, 1975; Tatar, 1978; Şengör, 1979; Toprak, 1988; Barka, 1992; Koçyiğit, 1988; Şaroğlu, 1988; Koçyiğit, 1990; Tüysüz et al., 1998).

2.2. Geologic and Hydrogeologic Setting

2.2.1. Kurşunlu-Çavundur (Çankırı)

Kurşunlu-Çavundur geothermal field is located 45 km northwest of Çankırı. Çavundur bath is 13 km west of Kurşunlu town (Figure 2.2).

The oldest units in the field are Neogene tuff, tuffite and volcanics composed of altered basalt. Pliocene sediments, including marl, clay, silt and locally conglomerate which is intercalated with the volcanics, extend in large areas. The lava that belongs to a later volcanic phase locally covers these Pliocene units. Volcanic and sedimentary units are covered by Quaternary alluvium and travertine (Koçak, 1974; Erişen et al., 1996) (Figure 2.2).

Major structural units in the field are E-W and NE-SW trending faults and NNE-SSW trending fissure (Figure 2.2).

Jointed Neogene volcanics form the reservoir rock for the hot water, whereas, the Pliocene conglomerate is the reservoir rock for the cold water (Koçak, 1974; Erişen et al., 1996). Pliocene sedimentary units are the cap rocks in the field.

Hot waters in Kurşunlu-Çavundur field emerge in the vicinity of Çavundur bath. Temperature of waters are about 30-38 °C, flow rates range between 0.1 and 0.2 l/sec (Koçak, 1974; Erişen et al., 1996). There are 11-20 °C cold water and mineral water in the vicinity of the bath (Koçak, 1974). There is one production well which was drilled by General Directorate of the Turkish Mineral Research and Exploration (Maden Tetkik ve Arama, MTA) in 1987. The depth of this well is 270 m. The flow rate of water is 47 l/sec and its temperature is 54 °C (Erişen et al., 1996). The well has still been used for water supply for the bath.

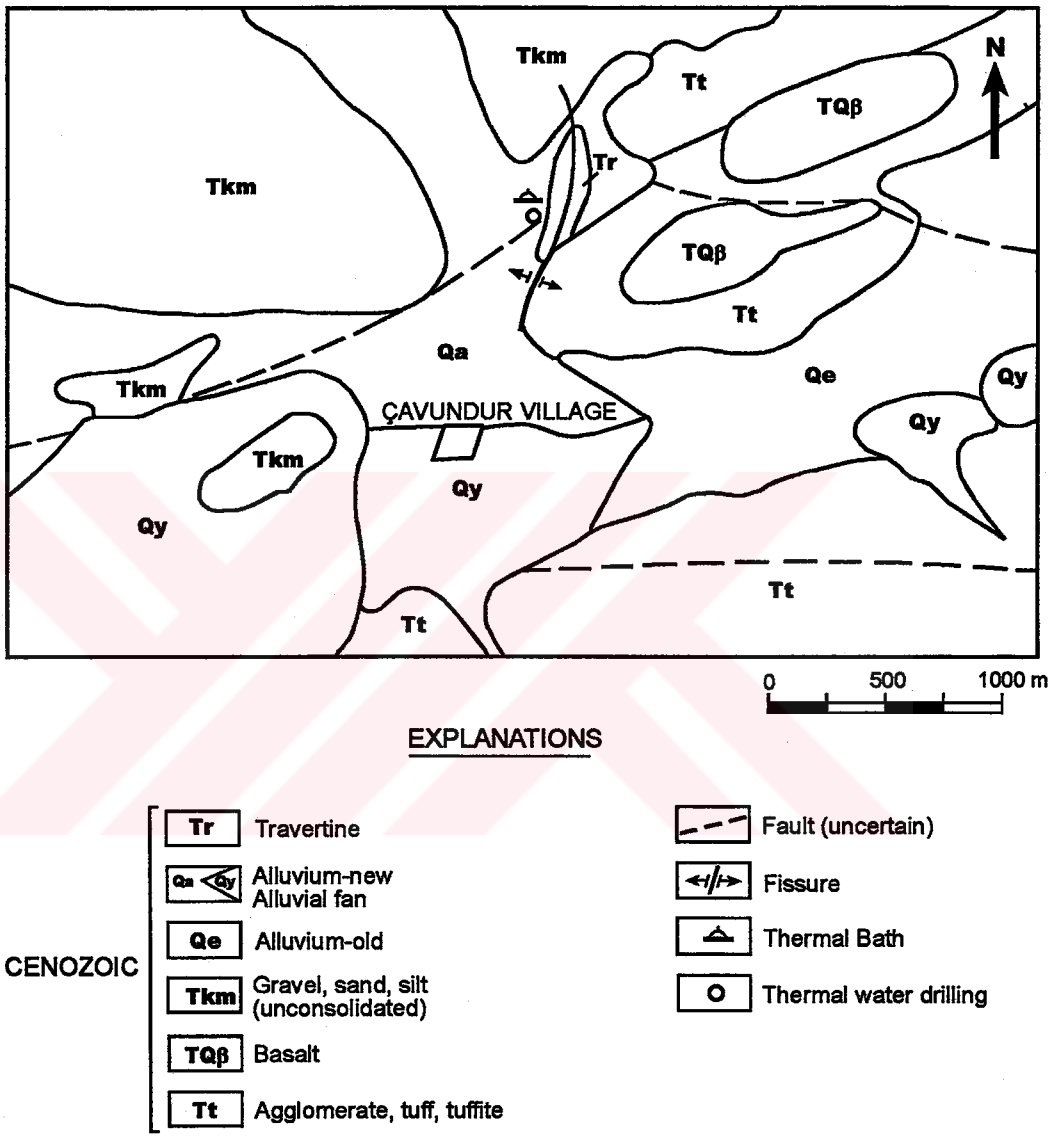


Figure 2.2. Geologic map of Kurşunlu geothermal field (Erişen et al., 1996).

2.2.2. Bolu-Town Center

The geothermal field is located 5 km south of Bolu (Figure 2.3). The oldest unit is Mesozoic olistostromal sedimentary series in flysch facies (Upper Cratecous) (Erişen et al., 1996). At the upper level of this series, intercalation of Upper Cretaceous limestone-sandstone-marl is observed. Cenozoic is composed of Neogene volcanics (agglomerate and tuff), lacustrine sediments (intercalation of conglomerate, sandstone and siltstone) and Quaternary debris and alluvium (Canik, 1971; Erişen et al., 1996) (Figure 2.3).

The major structural units trend ENE-WNW direction (Figure 2.3).

The reservoir rock is composed of Upper Cretaceous limestone and sandstone, and impervious clayey levels form the cap rock (Canik, 1971; Erişen et al., 1996).

Temperature of hot waters in the field is 44 °C, total flow rate is about 15 l/sec (Canik, 1971; Erişen et al., 1996). Five drillings have been performed in the field (Yücel et al., 1994). Two wells were drilled in 1971 by MTA. Their temperatures are 43 °C and 45 °C, flow rates are 4.25 l/sec and 4.63 l/sec, depths are 83 m and 97 m, respectively (Erişen et al., 1996 – B. Bath and K. Bath drilling). These wells supply water for present bath and Physical Therapy and Rehabilitation Centre. One hot water drilling was made in 1980s by a private firm called Petrokent but it was stopped since water of the bath had been effected negatively in terms of flow rate. One more well was drilled in 1993 by MTA. The depth of the well is 758.5 m, the temperature is 40 °C and the flow rate is 1.1 l/sec (Yücel et al., 1994; Erişen et al., 1996 – B-1 drilling). One more well was drilled 4 m from the B. Bath

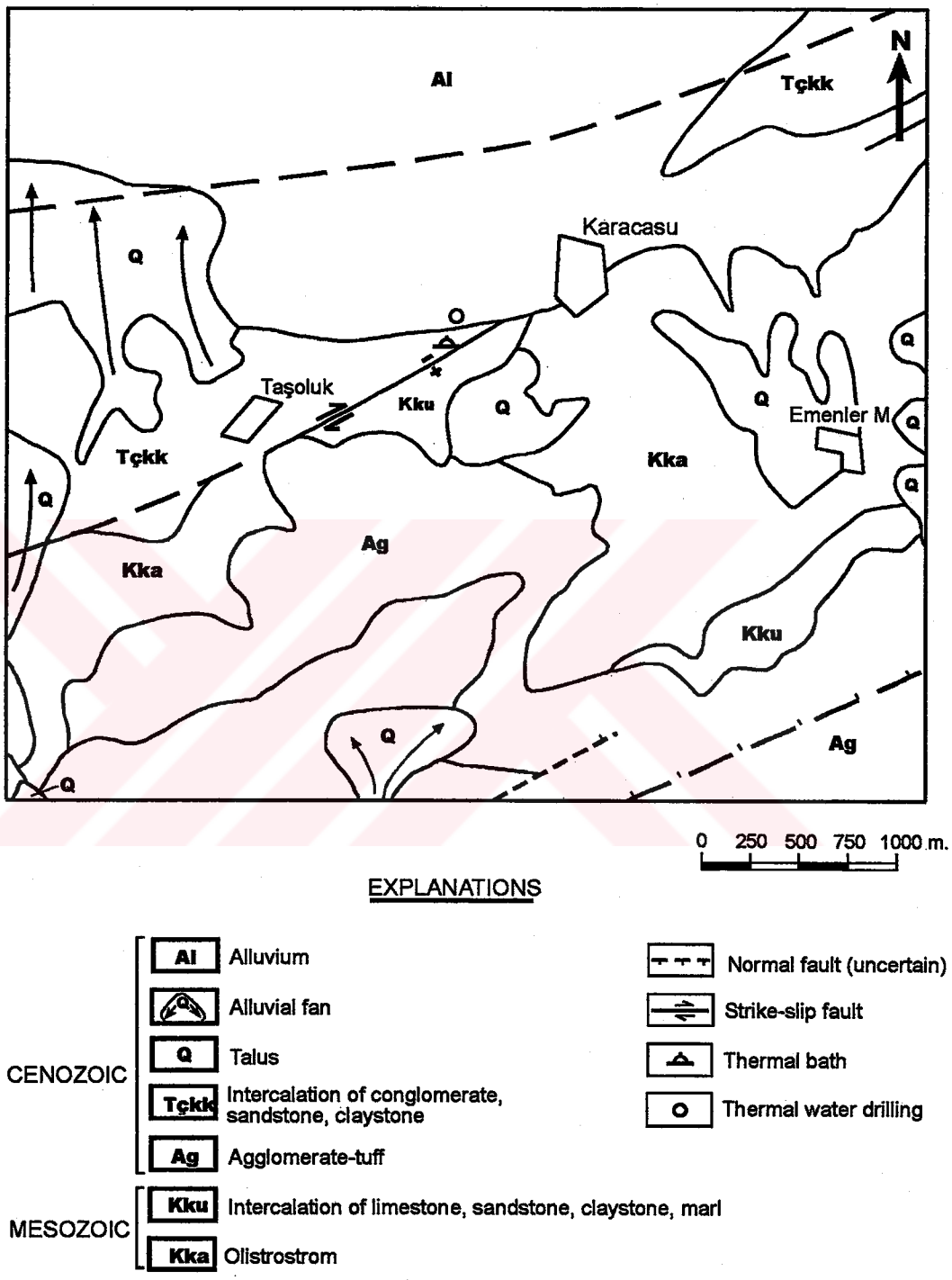


Figure 2.3. Geologic map of Bolu geothermal field (Erişen et al., 1996).

Well in June 2000. The depth is 150 m and the flow rate is 30 l/sec. During the production of this well, other wells do not supply water.

2.2.3. Efteni-Gölyaka (Bolu)

Efteni-Gölyaka geothermal field is 45 km WNW of Bolu town centre. It is called Efteni-Derdin geothermal field in geothermal literature since Efteni is 4-5 km east of Derdin geothermal field.

The basement is composed of flysch containing Cretaceous sedimentary (clay-sandtone-sandy limestone) and locally volcanics material. Eocene lava, volcano-sedimentary and sedimentary (sandstone-clay) units overlie this unit unconformably (Figure 2.4 a,b). At the uppermost level, Pliocene fluvial deposits composed of clay-sandstone-siltstone is observed (Figure 2.4 a,b) (Canik, 1972; Erişen et al., 1996).

The major structural units in the field are E-W, NE-SW and NW-SE trending faults (Figure 2.4 a,b).

Limestone and sandstone levels comprise the reservoir rocks, whereas impervious clayey levels form cap rocks in the field (Canik, 1972; Erişen et al., 1996).

Efteni and Derdin Springs are sources of thermal water in the field. Their temperatures are 42 °C and 31 °C, and the flow rates are 2-3 l/sec and 4 l/sec, respectively (Erişen et al., 1996). Any drilling has not been performed yet in the field. Thermal water has been used for bathing.

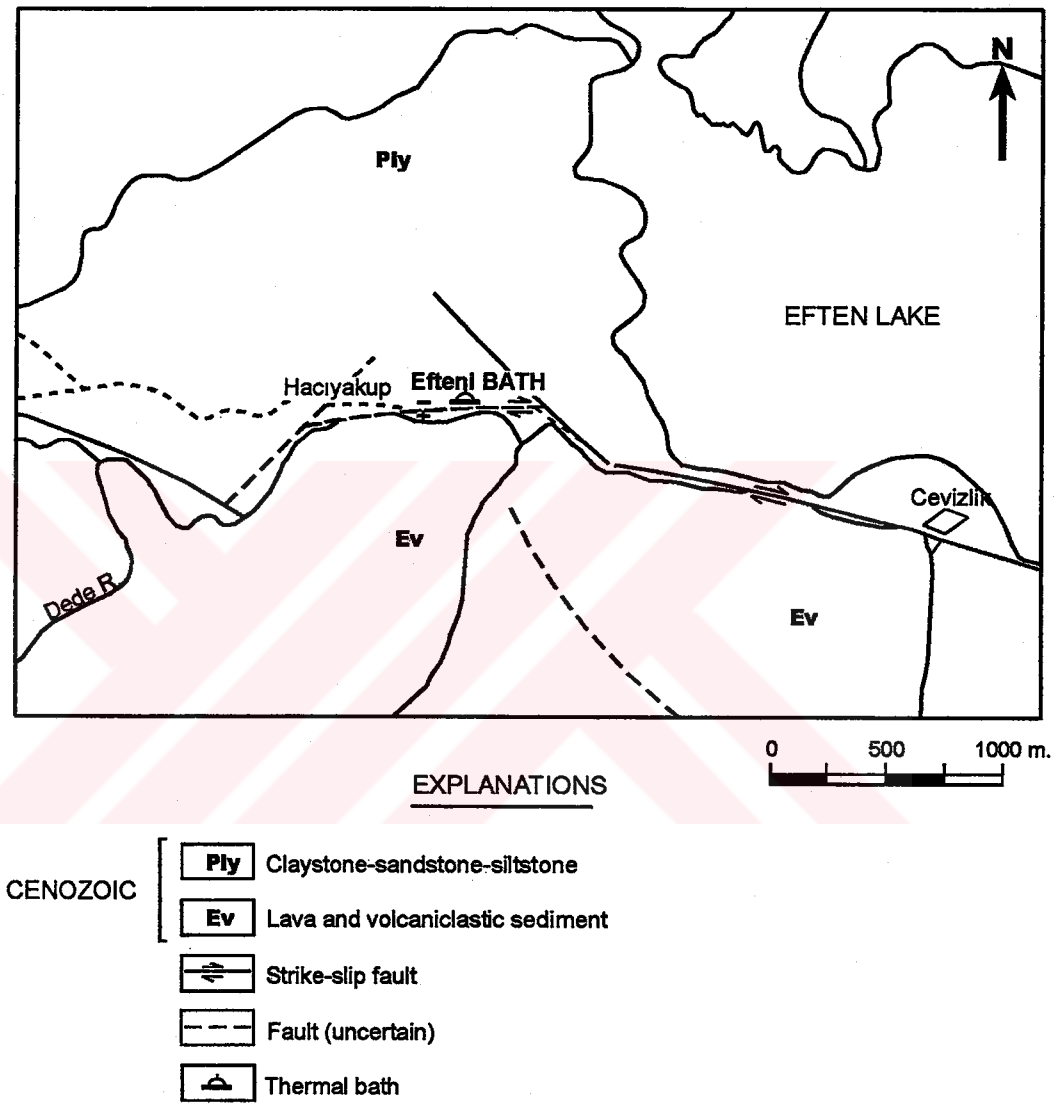


Figure 2.4.a. Geologic map of Efteni geothermal field (Erişen et al., 1996).

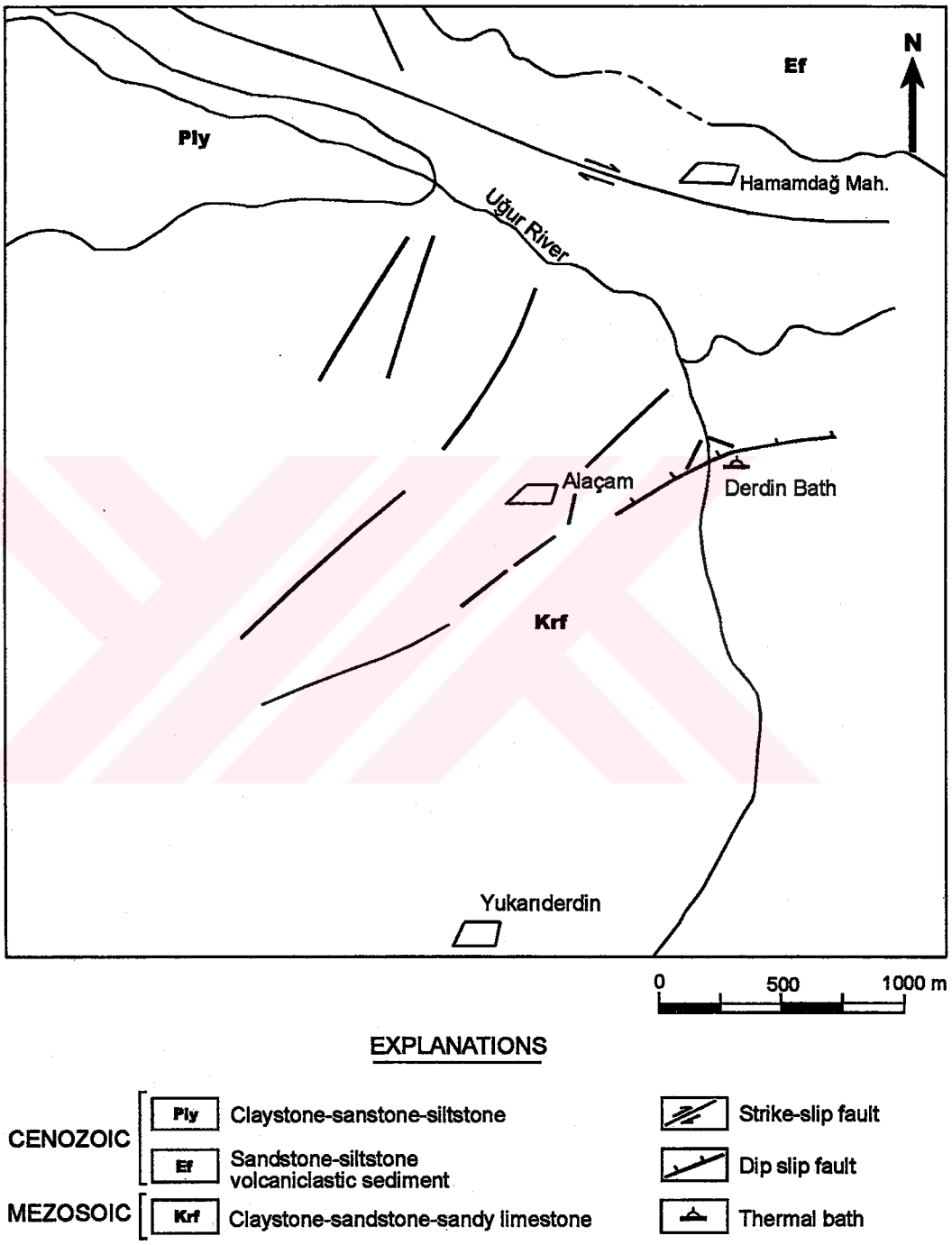


Figure 2.4.b. Geologic map of Derdin geothermal field (Erişen et al., 1996).

2.2.4. Babas-Mudurnu (Bolu)

Babas-Mudurnu geothermal field is located about 40 km southwest of Bolu, and about 4 km SW of Mudurnu town centre.

The oldest unit is Middle Jurassic – Lower Cretaceous limestones in the field. It is overlain conformably by sedimentary units composed of intercalation of limestone-sandstone-marl-claystone. The age of the upper levels of this unit extends to Upper Cretaceous. The youngest units are travertine and alluvion (Erişen et al., 1996) (Figure 2.5).

The trends of normal faults are NE-SW and that of reverse fault is E-W in the field (Figure 2.5).

The reservoir rock is composed of Middle Jurassic – Lower Cretaceous limestones. The impervious levels of sedimentary unit form cap rock (Şahinci, 1970; Erişen et al., 1996).

There are two drilling wells in Babas field. The wells are artesian type and 25-30 m away from each other. Their depths are 80 m and 125 m; the temperatures are 38 °C and 40 °C, respectively. Thermal water is used in bathing purposes.

2.2.5. Seben-Kesenözü-Pavlu (Bolu)

Seben-Kesenözü-Pavlu geothermal field is located 40 km south of Bolu town centre. Pavlu bath is about 10 km southwest of Seben.

Upper Cretaceous Kesenözü formation which is composed of alternation of sandstone, limestone, siltstone and marl, comprises the oldest unit in the field. Palaeocene-Pliocene detrital sedimentary rock and Quaternary alluvium cover this

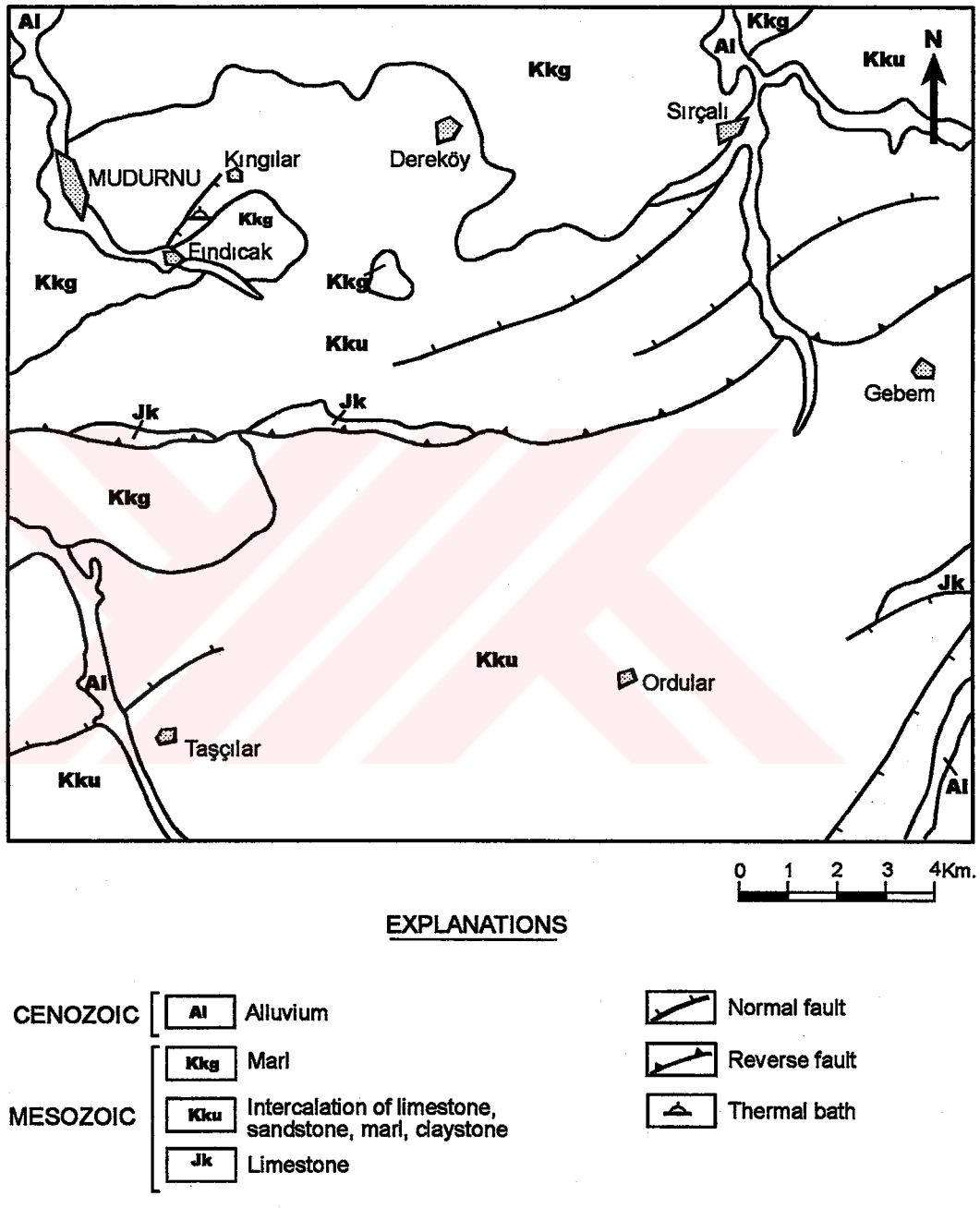


Figure 2.5. Geologic map of Mudurnu geothermal field (Erişen et al., 1996).

T.C. YÜKSEKÖĞRETİM KURULU
DOKÜMANTASYON MERKEZİ

Mesozoic unit (Ünlü and Balkaş, 1975; Özcan and Ünay, 1978; Müftüoğlu and Akıncı, 1989; Erişen et al., 1996) (Figure 2.6).

The major structural units in the field are E-W trending folds and faults (Figure 2.6).

Geothermal energy related studies began in 1975 by MTA in the field. Then, resistivity studies conducted between 1976 and 1977 (Özcan and Ünay, 1978). Seismic studies performed in 1988 (Müftüoğlu and Akıncı, 1989). 750 m-drilling well had been suggested after seismic studies. Shallow gradient studies conducted together with seismic studies indicated that there was no increase in temperature to the north of the bath (Müftüoğlu and Akıncı, 1989).

The reservoir rock is Cretaceous limestone and sandstone, whereas impervious clayey levels are cap rock in the field.

Thermal spring in Seben-Kesenözü-Pavlu geothermal field has temperature of about 74 °C and flow rate of about 4 l/sec. There are two production wells in the field whose depths are 2.5-3 m and 3.5-4 m, and temperatures are 51 °C and 58 °C, respectively. Thermal waters are used for bathing.

2.2.6. Gözlek-Amasya

Gözlek is located about 20 km southwest of Amasya.

Paleozoic schist forms the basement. Jurassic-Cretaceous recrystallised massive limestones overlie the schist (Figure 2.7). Eocene Nummulitic flysch series composed of intercalation of conglomerate-sandstone-marl-claystone cover Paleozoic and Mesozoic units unconformably. Quaternary alluvium is the youngest

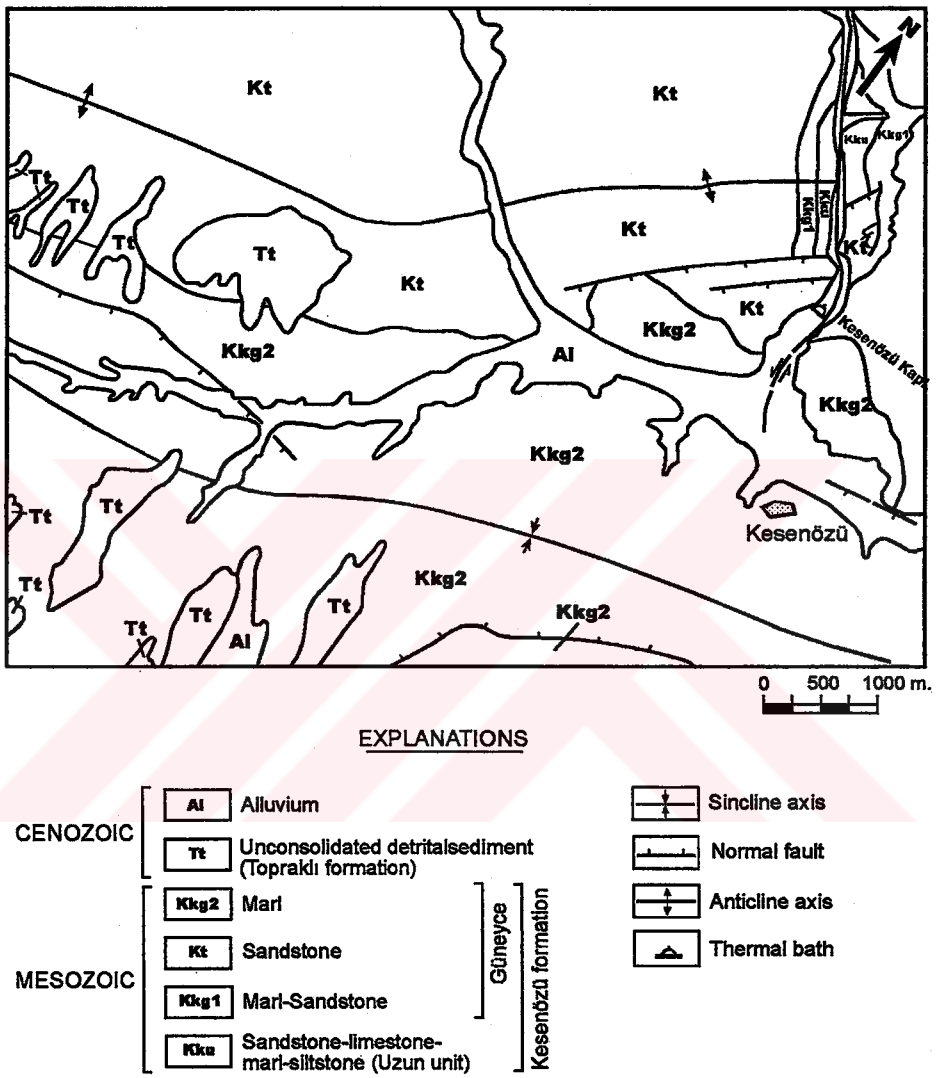


Figure 2.6. Geologic map of Seben geothermal field (Erişen et al., 1996).

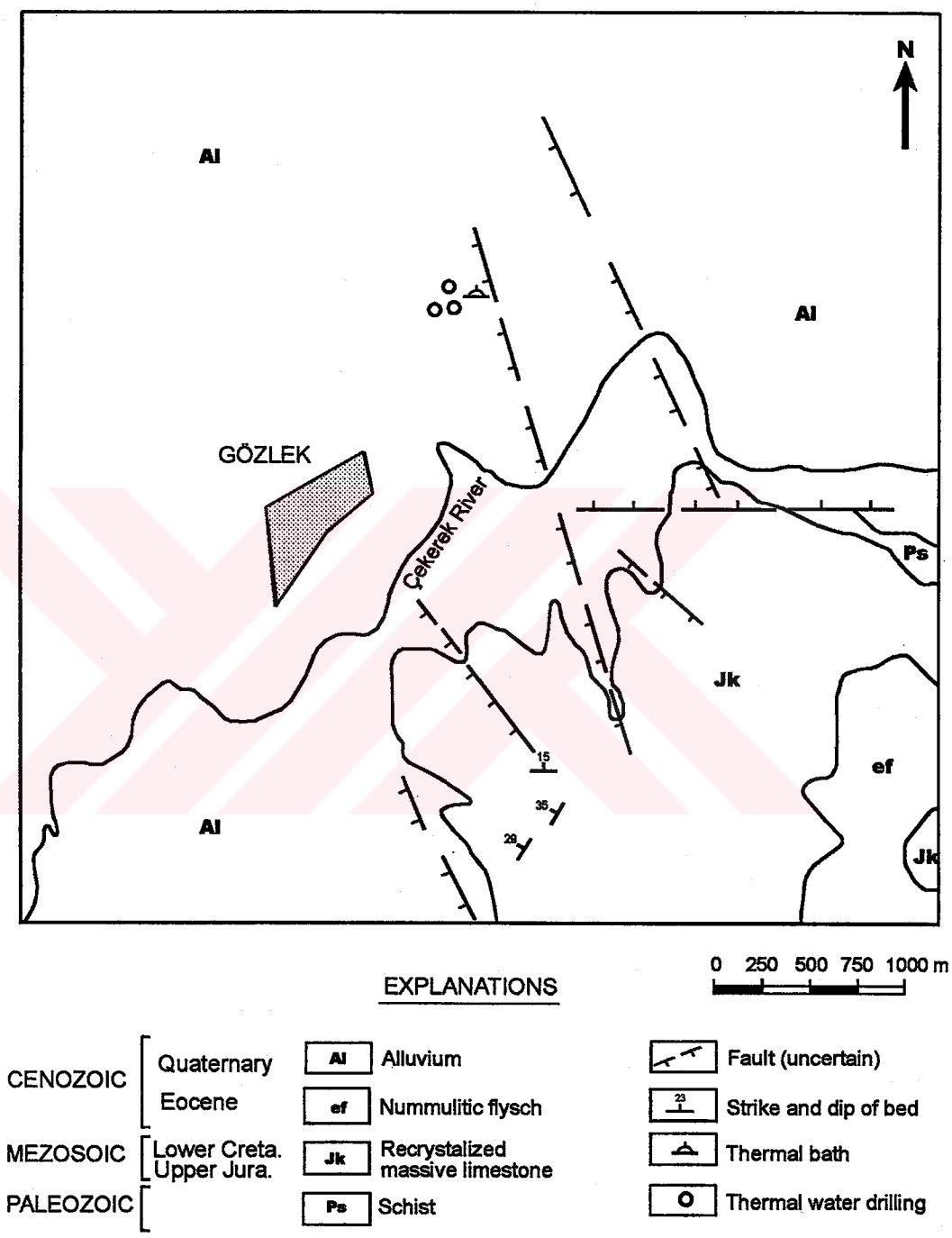


Figure 2.7. Geologic map of Gözlek geothermal field (Erişen et al., 1996).

unit and gives extensive outcrops in the field (Şentürk and Ünay, 1976; Erişen et al., 1996) (Figure 2.7).

Resistivity studies were performed by MTA (Şentürk and Ünay, 1976) in order to determine faults including thermal water. The dominant fault direction is NNW-SSE in the field (Figure 2.7).

The reservoir rock is composed of recrystallised massive limestones and the impervious layers form the cap rock.

The temperature of thermal water is 39 °C and flow rate is 2 l/sec.

Three wells were drilled during 1988-1991 by MTA in the field. The first (artesian) well was completed at depth of 398.5 m in 1988. The temperature and the flow rate were 40.5 °C and 10.5 l/sec, respectively. The second (pumping) well was drilled to depth of 393 m in 1989, temperature and flow rate of which were 40.5 °C and 0.1 l/sec, respectively. The third (pumping) well was drilled in 1991 to depth of 530.3 m. Temperature was 35.5 °C and flow rate was 0.8 l/sec. The bath in the Gözlek field is currently fed by an artesian type well which is producing water from a depth of 800 m with a temperature at 40 °C and a flow rate of 16 l/sec (personel communication with local people, 2000).

2.2.7. Reşadiye-Tokat

Reşadiye is located about 65 km ENE of Tokat.

The basement is Jurassic-Cretaceous limestones. Campanian limestones intercalated with claystone and siltstone overlie this unit unconformably. The uppermost unit of Mesozoic deposits is Upper Cretaceous flysch. Palaeocene limestones cover unconformably Mesozoic units. Quaternary alluvium and

travertine overlie Palaeocene limestone. Volcanic activity began in Upper Cretaceous is represented by andesite overlying Upper Cretaceous flysch and intercalated with the flysch, tuff and agglomerate (Erişen et al., 1996) (Figure 2.8).

NAFZ passes through Reşadiye geothermal field. There is a fissure with the axis of NW-SE in the vicinity of the bath (Figure 2.8).

In Reşadiye geothermal field thermal waters are located along the fissure. Their temperatures range between 39 and 49 °C, flow rates range between 0.1 and 0.9 l/sec. There is one well drilled in 1989 by MTA. Its depth is 238.9 m, temperature is 46.5 °C and flow rate is 30 l/sec. It is an artesian type well (Erişen et al., 1996). Thermal waters are used in baths.

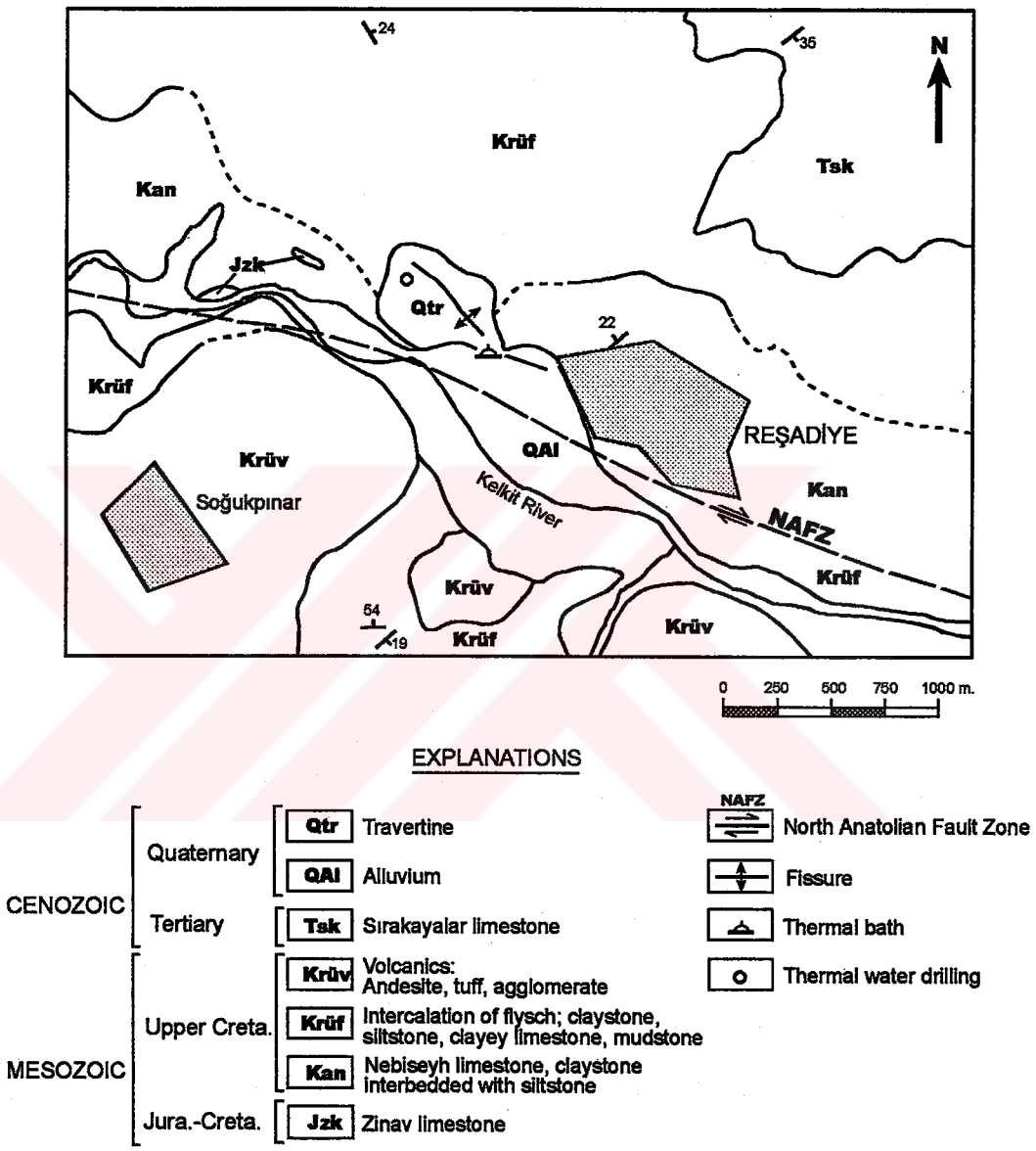


Figure 2.8. Geologic map of Reşadiye geothermal field (Erişen et al., 1996).

CHAPTER 3

HYDROGEOCHEMICAL CHARACTERISTICS

3.1. Methods of Study

This study consists of three major steps: sampling, laboratory analysis and data interpretation.

3.1.1. Sampling

In this study sampling was performed in two sampling periods, in June 2000 and April 2001. During both periods, samples were collected from a total of 7 localities, namely, Çavundur-Kurşunlu-Çankırı, Bolu (town centre), Efteni-Gölyaka (Bolu), Mudurnu-Babas (Bolu), Seben-Pavlu (Bolu) Gözlek-Amasya and Reşadiye-Tokat (Table 3.1.a and Table 3.1.b). Both natural-springs and production wells were utilised during sampling. During the sampling in June 2000, a total of 15 samples were collected from the localities concerned, comprising 10 hot water, 4 cold water and 1 mineral water samples (Table 3.1.a). During the sampling in April 2001, samples were collected from the same localities. However, in Bolu town centre, sampling was performed from a different (recently drilled) well since the previous well was already out of production at the time of sampling (Table 3.1.b). In

Table 3.1.a. Information relevant to the samples and sample localities (June 2000).

Locality	Sample No.	*Temperature (°C)	Sample Type (Production well – production depth / spring)
Kurşunlu-Çavundur	1a	57	Production Well – 165 m
Kurşunlu-Çavundur	1b	16	Spring (mineral water)
Kurşunlu-Çavundur	1c	13	Spring
Bolu Hamamları	2	45	Production Well – 83 m
Efteni-Gölyaka	3a	44	Spring
Efteni-Gölyaka	3b	19	Spring
Babas-Mudurnu	4a	38	Production Well – 80 m
Babas-Mudurnu	4b	40	Production Well – 125 m
Babas-Mudurnu	4c	18	Spring
Seben-Pavlu	5a	73	Spring
Seben-Pavlu	5b	58	Production Well – 4 m
Seben-Pavlu	5c	51	Production Well – 2.5 m
Seben-Pavlu	5d	17	Spring
Reşadiye-Tokat	6	47	Spring
Gözlek-Amasya	7a	40	Production Well – 800 m

*Temperatures of samples taken from production wells are well head temperature.

Table 3.1.b. Information relevant to the samples and sample localities (April 2001).

Locality	Sample No.	*Temperature (°C)	Sample Type (Production well – production depth / spring)
Kurşunlu-Çavundur	1a	54	Production Well – 165 m
Kurşunlu-Çavundur	1b	16	Spring (mineral water)
Kurşunlu-Çavundur	1c	15	Spring
Bolu Hamamları	2'	45	Production Well – 150 m
Efteni-Gölyaka	3a	44	Spring
Efteni-Gölyaka	3b	19	Spring
Babas-Mudurnu	4a	40	Production Well – 80 m
Babas-Mudurnu	4b	40	Production Well – 125 m
Babas-Mudurnu	4c'	17	Spring
Babas-Mudurnu	4d	25	Spring
Seben-Pavlu	5a	73	Spring
Seben-Pavlu	5b	58	Production Well – 4 m
Seben-Pavlu	5c	43	Production Well – 2.5 m
Seben-Pavlu	5d	16	Spring
Reşadiye-Tokat	6	44	Spring
Gözlek-Amasya	7a	41	Production Well – 800 m

*Temperatures of samples taken from production wells are well head temperature.

T.C. YÜKSEKÖĞRETİM KURULU
DOKÜMANTASYON MERKEZİ

addition, the cold water spring sampled in 2000 from Mudurnu was dried in 2001; instead, 1 warm and 1 cold water samples were collected from newly emerged springs encountered during the excavation studies performed by local people in 2001.

During sampling, 250 ml polyethylene bottles were used for the collection of waters. The bottles were first rinsed with water to be sampled in the field before sample collection. Water samples were then collected – via filtering – into the bottles. The temperature and pH of the waters were measured in the field.

3.1.2. Analytical Techniques

Analyses were performed within a month following sample collection. Samples were analysed at the laboratories of the Department of Geological Engineering at Middle East Technical University (METU). Na^+ and K^+ ions were analysed by Flame Photometry (Jenway PFP7). Total hardness and Ca-hardness analyses for determination of Ca^{++} and Mg^{2+} ions, and the Phenolpthaline and total alkalinity analyses for determination HCO_3^- and CO_3^{2-} ions were performed by Titration method (HACH Digital Titrator-MK120). $SO_4^=$ and Cl^- ions, and the SiO_2 contents were analysed by Spectrophotometry (HACH DR/2000 Direct Reading Spectrophotometer for $SO_4^=$ and Cl^-, UNICOM SP600 Series 2 for SiO_2). The details of the analytical procedures are given in Appendix A.

3.2. Results

The results of chemical analyses of samples collected from the concerned geothermal fields are given in Table 3.2 (a, b). The SiO_2 analyses of samples collected in 2001 could not be performed owing to technical problems with UNICAM SP600 Series 2 Spectrophotometer. The temperatures of the waters collected from hot springs and production wells range between 38 and 73 °C; the waters sampled from cold-springs have temperatures ranging between 13 and 19 °C. The thermal waters are slightly acidic to neutral in character with pH values ranging from 5.6 to 7.5 (Table 3.2 a, b).

As can be seen from Table 3.2, the hot waters are generally characterised by high TDS contents ranging from 960 to 11074 ppm, with the exception of Gözlek hot water (sample no. 7a) which, despite its high temperature, has considerably low TDS content around 433 ppm. The cold waters, on the other hand, have TDS contents ranging between 362 to 866 ppm. The highest TDS content belongs to the hot water and mineral water samples (sample no. 1a and 1b) from Kurşunlu field. The hot water sample from Seben field, with the highest temperature (73 °C) recorded so far, has a TDS content around 2000 ppm which is lower by a factor of about 5 than that obtained from the Kurşunlu hot water.

Table 3.2.a. The results of the chemical analyses of water samples collected in June 2000. Concentrations are in mg/l. CBE: charge balance error, TDS: total dissolved solid (Appendix C).

Locality	Sample no	T (°C)	pH	Na^+	K^+	Ca^{2+}	Mg^{2+}	HCO^-_3	Cl^-	SO^{2-}_4	SiO_2	CBE	TDS
Kurşunlu	1a	57	7.4	2425	270	78	17.1	5791	732	5	37.1	0.87	9355
Kurşunlu	1b	16	5.9	1750	97	110	2.4	3962	480	20	30.8	3.31	6453
Kurşunlu	1c	13	7.3	11	1	58	9.8	268	4	1	48.7	-3.72	402
Bolu	2	45	4.0	53	22	224	114.8	268	140	750	34.6	-0.99	1607
Efteni	3a	44	6.2	400	17	126	146.5	1664	200	1	124.0	4.69	2679
Efteni	3b	19	6.9	33	6	54	17.1	317	9	25	24.7	-2.4	486
Mudurnu	4a	38	6.2	29	9	136	50.1	695	3,3	39	28.6	0.41	990
Mudurnu	4b	40	6.2	29	8	140	33.0	677	3,3	38	32.3	-3.5	960
Mudurnu	4c	18	7.1	30	3	72	23.2	293	25	40	19.1	4.16	505
Seben	5a	73	6.5	560	38	44	3.7	1122	100	195	60.8	4.83	2123
Seben	5b	58	6.5	520	38	54	7.3	1085	75	215	65.7	4.9	2060
Seben	5c	51	6.6	500	35	60	12.2	1097	75	195	61.2	4.89	2036
Seben	5d	17	6.9	80	8	90	30.5	287	9	315	13.5	-3.7	833
Reşadiye	6	47	6.4	810	47	278	89.1	1646	880	240	45.5	0.74	4036
Gözlek	7a	40	7.5	84	6	18	7.3	250	11	40	22.2	0.79	438

Table 3.2.b. The results of the chemical analyses of water samples collected in April 2001. Concentrations are in mg/l. CBE: charge balance error, TDS: total dissolved solid.

Locality	Sample no	T (°C)	pH	Na^+	K^+	Ca^{2+}	Mg^{2+}	HCO^-_3	Cl^-	SO^{2-}_4	CBE	TDS
Kurşunlu	1a	54	7.3	3160	230	16	17.1	7071	570	9	4.82	11074
Kurşunlu	1b	16	6.3	2480	170	86	5.9	6157	394	6	2.12	9299
Kurşunlu	1c	15	7.6	9	1	76	0	269	5	2	-4.42	362
Bolu	2'	45	5.7	42	16	336	87.9	751	9	780	-4.66	2022
Efteni	3a	44	5.9	345	13	220	114.8	2042	26	1	2.2	2762
Efteni	3b	19	6.5	30	5	78	4.4	329	12	24	-4.41	483
Mudurnu	4a	40	5.6	22	6	165	41.8	783	7	36	-3.79	1060
Mudurnu	4b	40	5.6	23	6	177	36.4	773	7	36	-2.43	1058
Mudurnu	4d	25	6.5	21	4	141	27.4	627	10	36	-4.68	866
Mudurnu	4c'	17	7.8	18	3	100	15.4	416	8	31	-3.71	592
Seben	5a	73	6.2	475	36	50	3.9	1238	20	200	-1.24	2022
Seben	5b	58	5.8	475	40	60	17.8	1280	21	340	-4.57	2234
Seben	5c	43	6.6	460	38	66	17.3	1234	24	350	-4.65	2189
Seben	5d	16	6.9	78	6	100	36.9	293	12	340	-2.62	866
Reşadiye	6	44	6.2	670	42	336	80.6	1975	262	520	2.9	3886
Gözlek	7a	41	6.9	80	6	18	6.8	263	15	43	-4.84	433

3.3. Discussion

3.3.1. Water Type

Water types of samples are presented on the piper diagram (Piper, 1944) (Figure 3.1.a and Figure 3.1.b). According to the diagram, Kurşunlu hot water is Na-HCO_3 type. Kurşunlu cold water is Ca-HCO_3 type water. In Bolu field the water is Ca-Mg-SO_4 in first sampling period whereas it is Ca-SO_4 in second sampling period. In Efteni the hot water shows Na-Mg-HCO_3 character in first sampling period however it is Na-Ca-HCO_3 in second sampling period. The cold water has Ca-Na-HCO_3 character. In Mudurnu both hot and cold waters have Ca-HCO_3 character. Hot waters from Seben field are Na-HCO_3 in nature whereas cold water is a mixed water namely Ca-Na-Mg-SO_4-HCO_3 type. In Reşadiye hot water sample is Na-HCO_3-Cl in first sampling period whereas it is Na-HCO_3 type in second sampling period. In Gözlek thermal water is Na-HCO_3 type water in first sampling period and Na-HCO_3 type in second sampling period.

When compared to the results of previous geochemical studies (Canik, 1971; Şahinci, 1971; Canik, 1972; Koçak, 1974; Ünlü and Balkaş, 1975; Şentürk and Ünay, 1976; Özcan and Ünay, 1978) performed in these fields, it appears that the hydrogeochemical facies did not change in time in Kurşunlu, Seben (Na-HCO_3) and Mudurnu (Ca-HCO_3) fields whereas in Efteni, as Mg and Ca content increased so the water type change from Na-HCO3 to Na-Mg-HCO_3. In Bolu field, HCO_3 content decreased and so water type changed from Ca-HCO_3-SO_4 to $CaSO_4$.

Schoeller diagrams (Schoeller, 1977) are also useful to distinguish different water types. In these diagrams, different ions are plotted against the relevant ionic

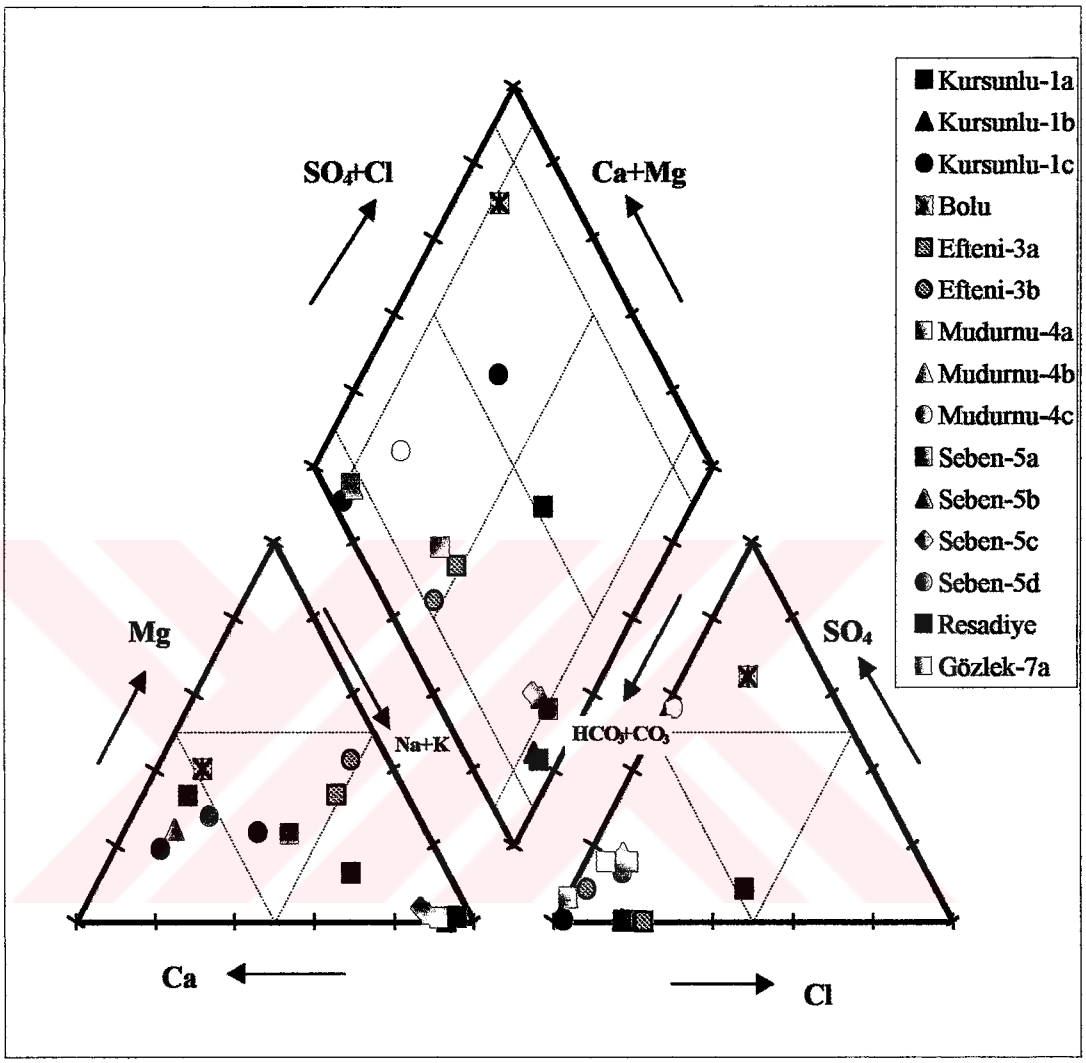


Figure 3.1.a. Piper diagram showing major ion distribution for samples collected in June 2000.

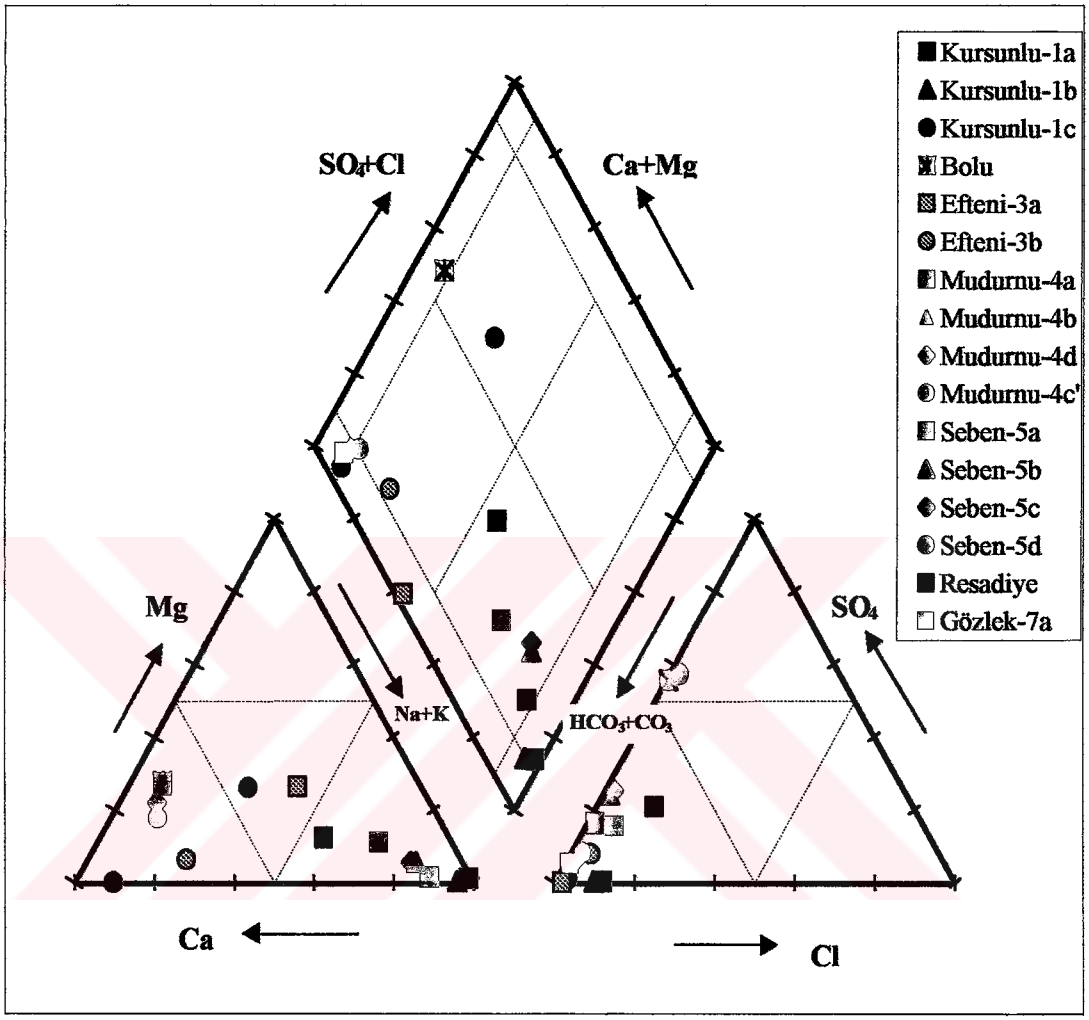


Figure 3.1.b. Piper diagram showing major ion distribution for samples collected in April 2001.

concentrations. The waters of similar nature and/or waters coming from the same reservoir yield similar ionic profiles. The ionic compositions of the waters analyzed in this study are evaluated here in terms of Schoeller diagrams (Fig. 3.2 a, b) prepared separately for each field. As can be seen from these diagrams, in Kurşunlu field, hot water sample from production well (sample no. 1a) and the mineral water collected from a spring (sample no. 1b) have similar ionic profiles pointing to the same source for both samples. The cold water, on the other hand, has a different profile and considerably low concentration levels (particularly for Na+K, Cl, SO_4, HCO_3) suggesting a different source.

For Bolu field, Schoeller diagram can give information only about the water type as there is only one sample collected from this field.

In Efteni, hot and cold water profiles are different.

In Mudurnu, both hot waters (collected from two different wells) and the cold water have similar ionic profiles. The similarity between hot and cold water compositions is particularly apparent in the samples collected in April 2001 (Fig. 3.2.b). The slight difference (between hot- and cold waters) observed in samples collected in 2000 seems to be due to the higher Cl^- content of the cold water which can be due to analytical error. In this respect, both hot and cold waters seem to have originated from the same source; the low temperature of the cold-water can then be ascribed to the conductive cooling for this sample with no change in composition.

In Seben, both thermal water and cold water have similar ionic profiles but thermal waters have higher Na-HCO_3 content whereas cold waters have higher Ca and Mg content. It can be concluded that thermal and cold waters have different reservoir.

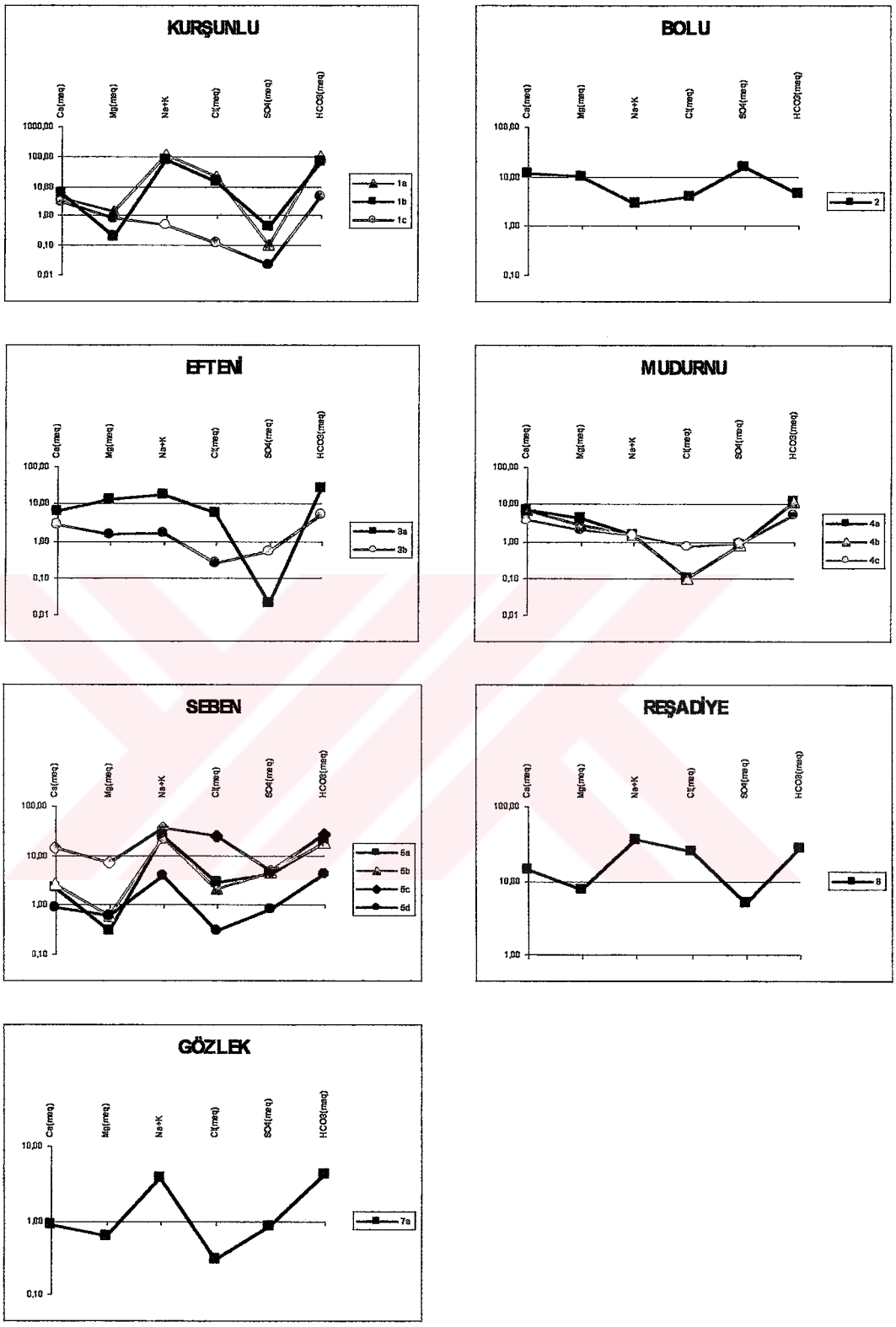


Figure 3.2.a. Schoeller diagrams for samples collected in June 2000.

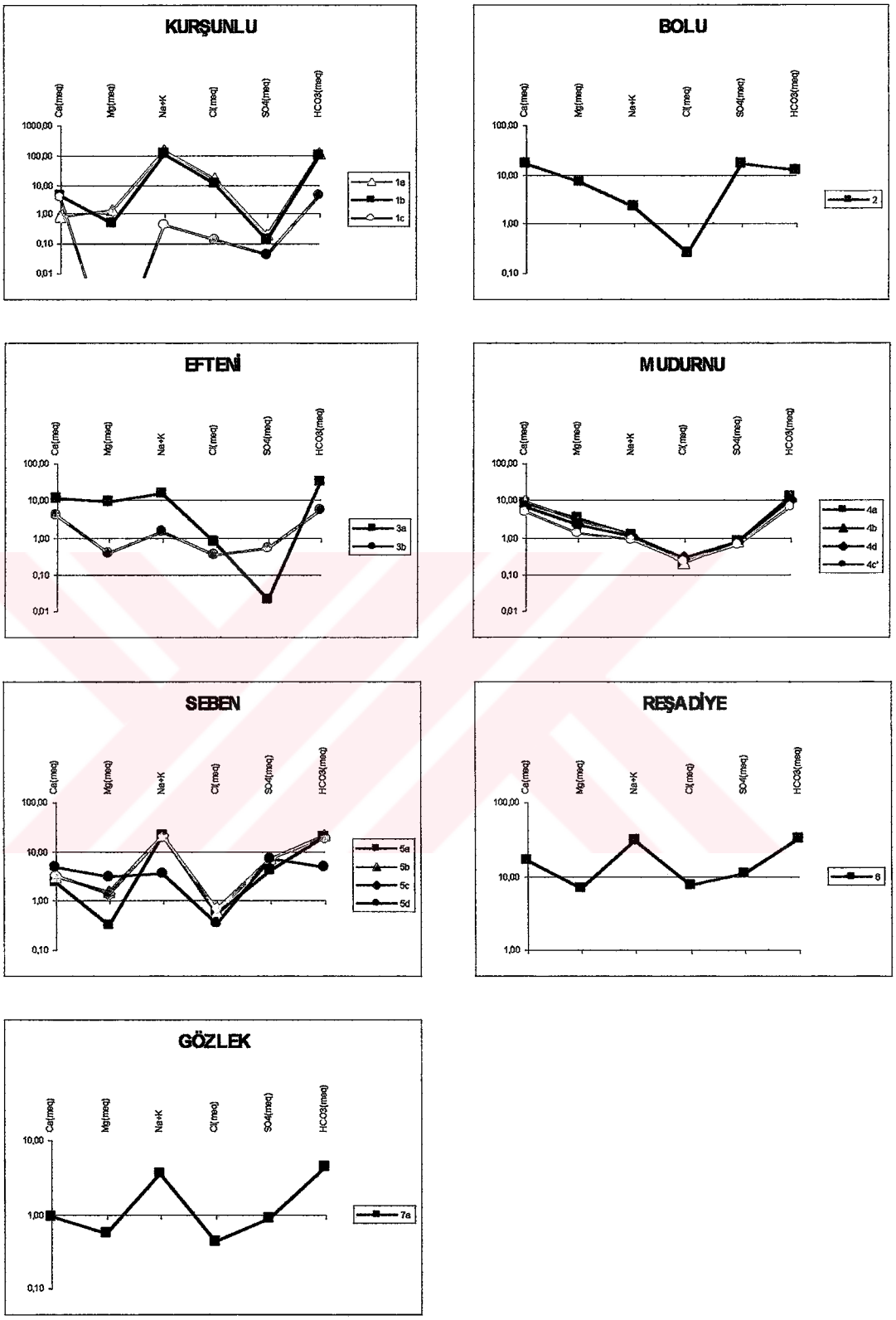


Figure 3.2.b. Schoeller diagrams for samples collected in April 2001.

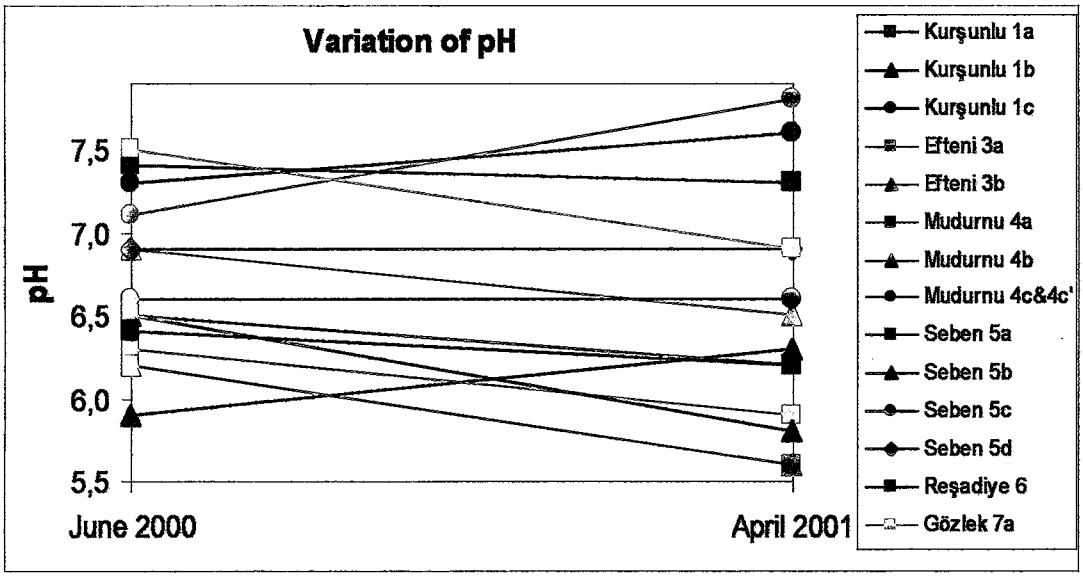
In Reşadiye and Gözlek, since one sample was collected, Schoeller diagrams give information about only water type.

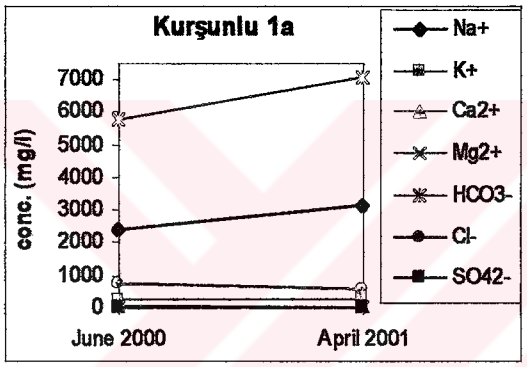
Comparison between two sampling periods, June 2000 and April 2001, as variation in ionic content of samples, is presented in Figure 3.3. In Bolu field, in spite of samples 2 and 2' were collected from different wells, they were compared. Similarly, in Mudurnu field, cold water samples (sample 4c and 4c') were collected in different source but they were compared. Moreover, sample 4d is not indicated in the figure since it was collected only in April 2001.

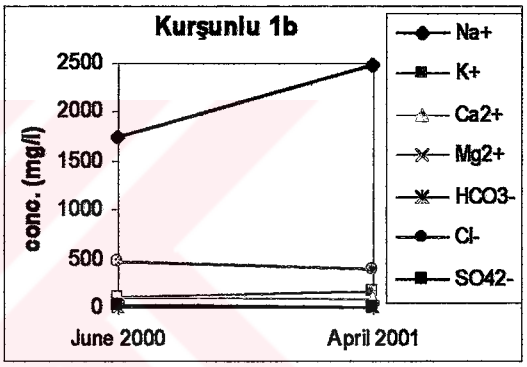
There appears to be a general decrease in pH values and accompanying increase in Ca, HCO_3 and TDS contents of the samples collected in April 2001, as compared to those collected in June 2000 (except sample 1b and 1c in Kurşunlu). Overall however, there is no change in the hydrogeochemical facies of thermal waters as defined by dominant anions and cations in Kurşunlu, Mudurnu and Seben, whereas there is slight difference in Bolu, Efteni, Reşadiye and Gözlek (see Figure 3.1.a and 3.1.b).

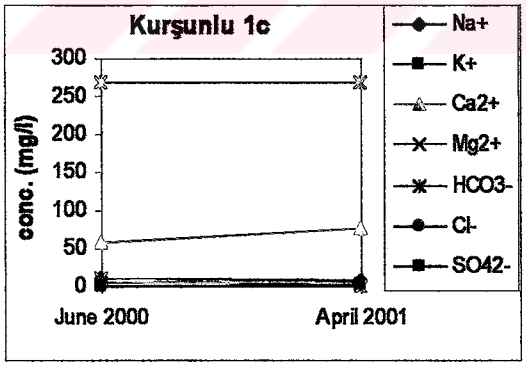
3.3.2. Evaluation of Subsurface Processes

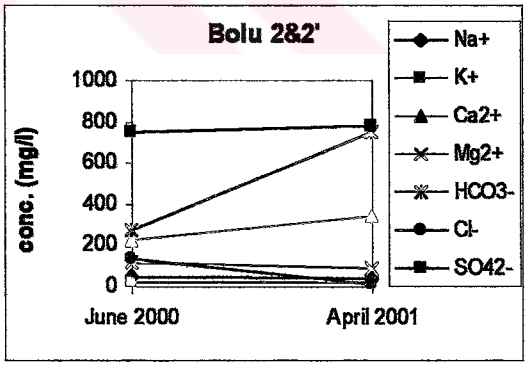
The type of water is determined by interaction between water and the rocks through which it travels. Majority of the studied thermal water has Na-HCO_3 character; while HCO_3 character seems to be compatible with the type of reservoir rocks that are dominated by limestones, the dominancy of Na cation is probably be responsible by ion exchange with the overlying lacustrine sediments including clay-marl.

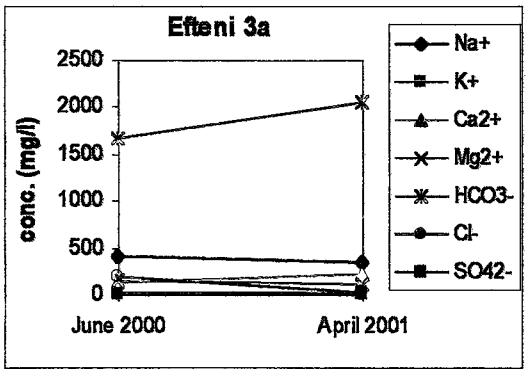


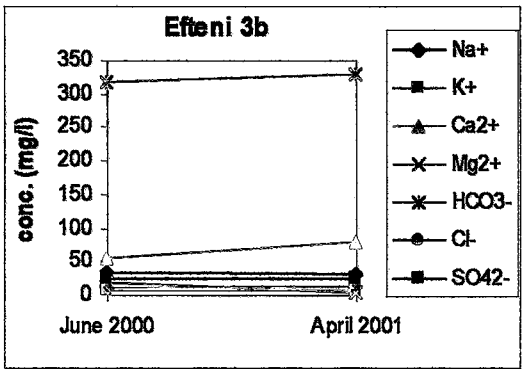












T.C. YÜKSEKÖĞRETİM KURULU
DOKÜMANTASYON MERKEZİ

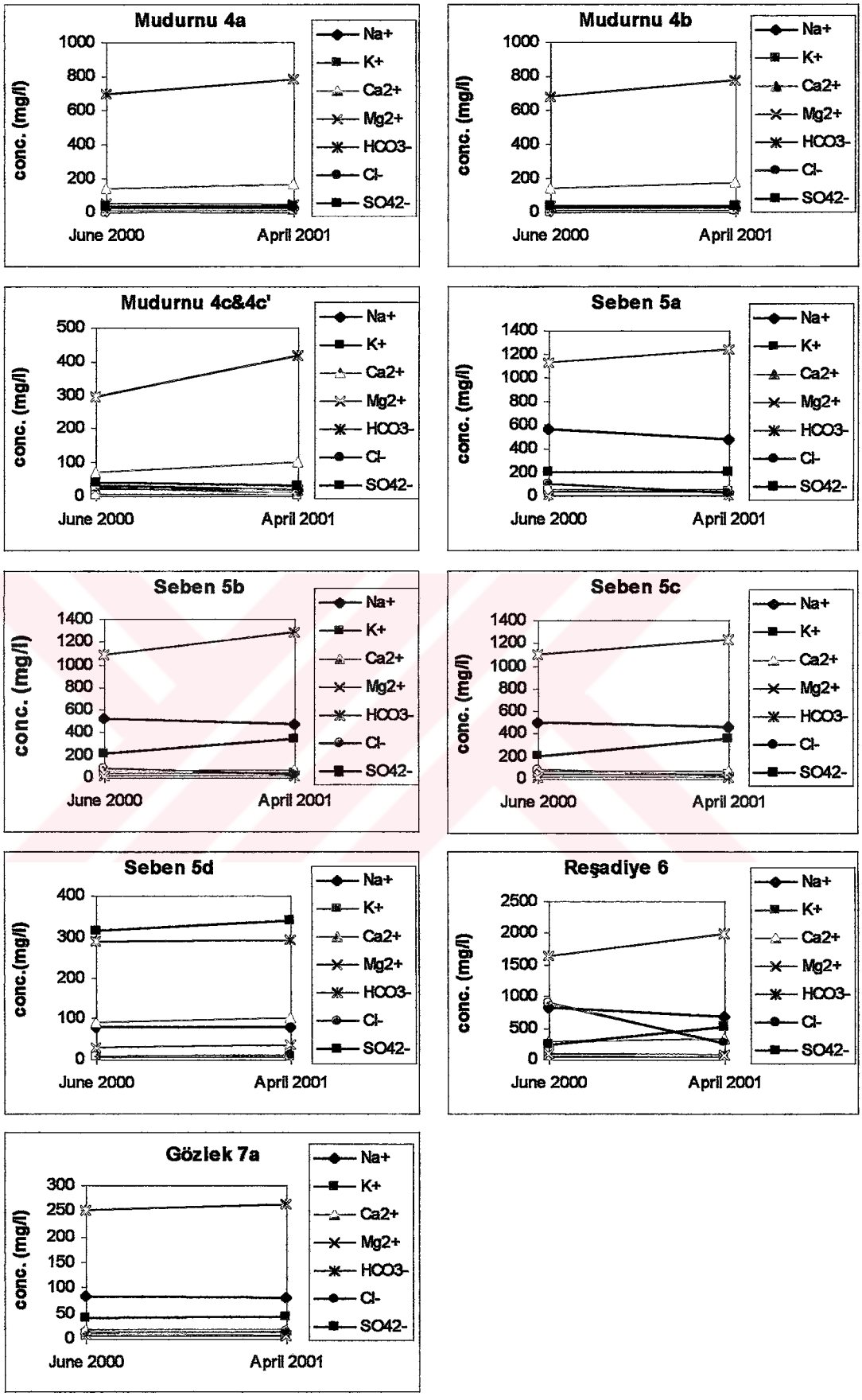


Figure 3.3. Variation diagrams in ionic concentration of samples collected in June 2000 and April 2001.

The correlation coefficients were calculated between ions by using two sampling periods result for fields where more than one samples were collected (Kurşunlu, Mudurnu and Seben) (Table 3.3). 4 samples were used in Kurşunlu field, 5 samples were used in Mudurnu field and 6 samples were used in Seben field. The f-test was performed for the results of correlation coefficient for each field. The f-test indicated that when correlation coefficient was higher than 0.85 and number of sample was 4, the correlation coefficient was in critical area and so significant. In Kurşunlu and Seben, there is strong positive correlation ($r > 0.95$) between Na and HCO_3, whereas there is negative correlation between Ca and HCO_3. In Mudurnu, there is a positive correlation ($r > 0.95$) between Ca and HCO_3 but negative correlation between Na and HCO_3. It can be interpreted that the effective process in hydrogeochemical evolution of samples in Mudurnu geothermal field is the dissolution process. However, instead of dissolution processes, ion exchange processes are effective in Kurşunlu and Seben fields. In other words, concentration of Ca ion increases by dissolution of carbonate rocks in Kurşunlu and Seben, then, during the circulation of thermal water, it is exchanged by Na ion of clay minerals of Neogene units.

The physicochemical processes are examined by means of diagrams on which the ionic abundances of the samples are plotted against their discharge temperatures for fields where more than two samples could be collected (Kurşunlu, Seben and Mudurnu) (Figure 3.4.a,b,c). The arithmetic averages of results of two sampling periods were used to draw these diagrams. The cold water and the hot water are taken as end members so the line connecting them can be regarded as a mixing line. The possible position of hot water component is indicated on this plot together with the effects of mixing, conductive cooling and steam-heating. In a

Table 3.3. Correlation coefficients between ions of water sample for fields where more than one samples were collected.

Kurşunlu

	Na	K	Ca	Mg	HCO_3	Cl	SO_4	pH	TDS
Na	1	0,930	-0,226	0,589	0,997	0,902	0,432	-0,319	0,998
K		1	-0,229	0,742	0,935	0,944	0,220	-0,067	0,946
Ca			1	-0,648	-0,199	-0,019	0,384	-0,605	-0,187
Mg				1	0,580	0,617	-0,165	0,378	0,595
HCO_3					1	0,895	0,395	-0,323	0,998
Cl						1	0,492	-0,264	0,921
SO_4							1	-0,785	0,424
pH								1	-0,317
TDS									1

Mudurnu

	Na	K	Ca	Mg	HCO_3	Cl	SO_4	pH	TDS
Na	1	0,487	-0,245	0,395	-0,102	0,227	0,923	-0,198	-0,025
K		1	0,561	0,862	0,714	-0,712	0,424	-0,652	0,730
Ca			1	0,635	0,973	-0,710	-0,091	-0,861	0,965
Mg				1	0,766	-0,512	0,498	-0,811	0,806
HCO_3					1	-0,774	0,029	-0,885	0,994
Cl						1	0,307	0,420	-0,718
SO_4							1	-0,393	0,119
pH								1	-0,925
TDS									1

Seben

	Na	K	Ca	Mg	HCO_3	Cl	SO_4	pH	TDS
Na	1	0,981	-0,960	-0,921	0,953	0,666	-0,580	-0,644	0,964
K		1	-0,927	-0,867	0,987	0,526	-0,436	-0,732	0,992
Ca			1	0,981	-0,897	-0,657	0,686	0,636	-0,884
Mg				1	-0,836	-0,672	0,784	0,526	-0,809
HCO_3					1	0,412	-0,383	-0,772	0,986
Cl						1	-0,750	-0,031	0,492
SO_4							1	0,081	-0,348
pH								1	-0,733
TDS									1

search for the origin and reservoir characteristics of geothermal systems, Cl^- is usually considered to be one of the most useful tracers owing to its relatively "conservative" nature. For this reason, the nature of distinct compositions can best be studied using the plot of Cl^- concentration vs. discharge temperature.

In Kurşunlu area, three water samples are plotted on the figure 3.4.a. Hot water (sample 1a) and cold water (sample 1c) are considered as end members. Mineral water (sample 1b) deviates from the mixing line. It can be claimed that conductive cooling happened following mixing process between cold and hot water. The cold water component seems to be higher in the mineral water. Other alternative is that the mineral water represents a residual liquid from a boiling process, which occur at about 97 °C at the elevation of Kurşunlu (see Appendix B). Boiling of the geothermal fluid results in the separation of a steam phase leaving the residual liquid relatively cold and enriched in non-volatile constituents. However, a temperature as low as 16 °C suggests, once more conductive cooling following boiling. On Na, K and HCO_3 vs. temperature diagrams, the position of mineral water indicates again conductive or adiabatic cooling following mixing. However, it is not clear whether cooling is conductive or adiabatic. SO_4 vs. temperature diagram seems to support the adiabatic cooling. However, since temperature of mixed water will be less than 60 °C, the possibility of adiabatic cooling is not considered. It can be considered alternatively that there is hotter water in deeper levels. Ca and Mg vs. temperature diagrams are not reliable since their solubilities increase with decreasing temperature so their concentrations easily change during ascent of water. In addition, calcite precipitation in the vicinity of the well indicates that measured Ca concentration does not reflect Ca content in the reservoir. The hot and mineral water samples have less SiO_2 content with respect to cold water on SiO_2 vs.

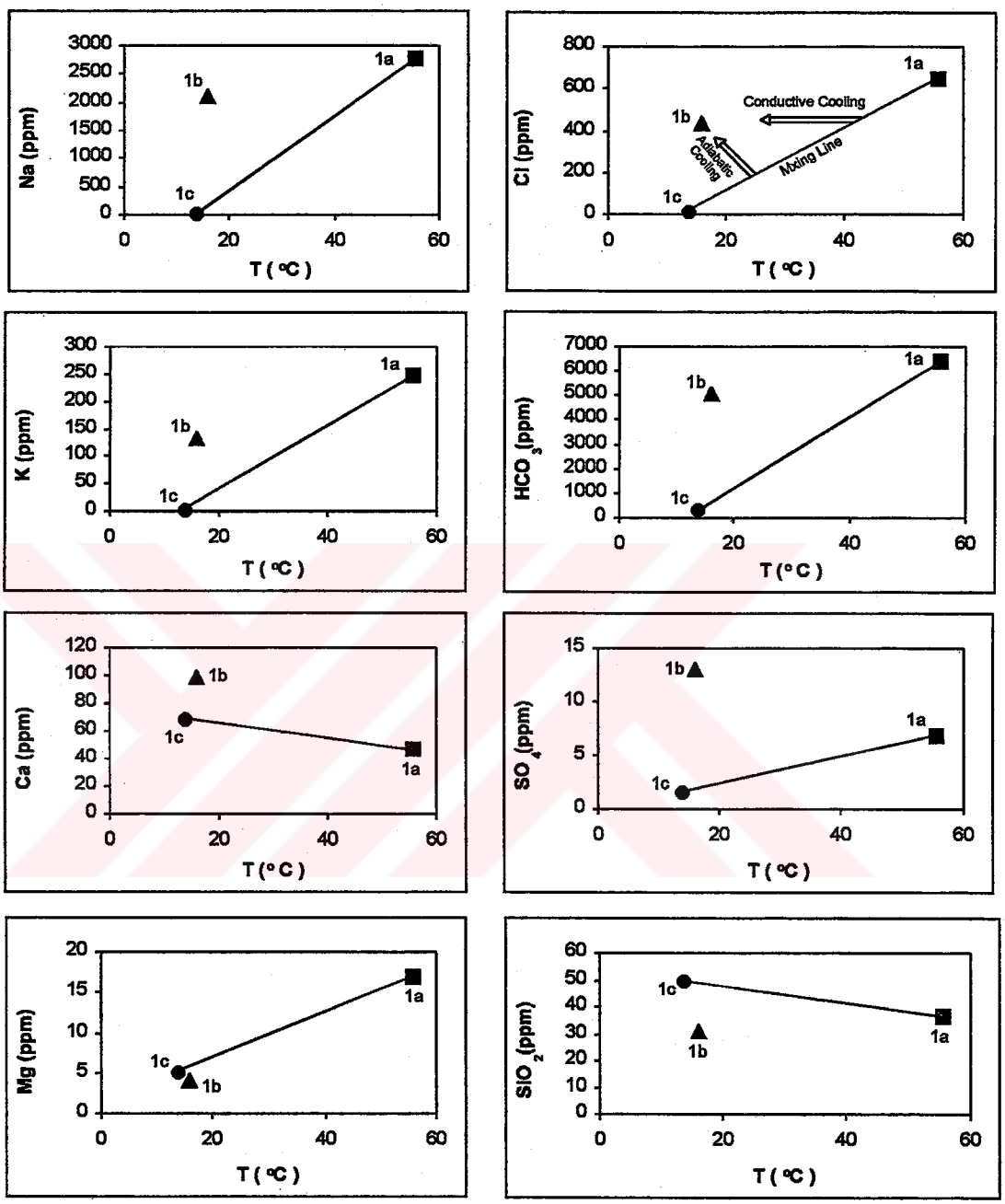


Figure 3.4.a. Ionic abundance vs. discharge temperature diagrams for Kurşunlu samples.

temperature diagram. It can be due to possible precipitation of silica before or after sampling.

In Mudurnu geothermal field, there are two cold water (sample 4c and 4c') end members collected in two different sampling periods (Figure 3.4.b). Cl content of cold water (sample 4c) collected during first sampling period is higher than that of hot waters (sample 4a and 4b). Cl content of cold, warm (sample 4c' and 4d, respectively) water collected during second sampling period and hot waters are similar to each other. It can be interpreted that hot waters have also meteoric origin as cold waters and it circulates deeper and gets higher temperature.

In Seben geothermal field, cold water (sample 5d) and the hottest water (sample 5a) were taken as end members (Figure 3.4.c). Cold water is rich as Ca, SO_4 and Mg ions. All hot waters possibly come from single reservoir. Two hot waters (samples 5b and 5c) can be resulted by the process of mixing between cold and hot waters (sample 5a) or there can be conductive cooling following mixing.

Although quantitative evaluation of mineral-water reactions is out of the scope of this thesis, the waters appear to gain) their chemical composition by processes of dissolution of lithologic units in the fields or ion exchange process between waters and these lithologic units. In addition, temperature of waters and ionic concentration indicate possible mixing between cold and hot waters and conductive or adiabatic cooling following mixing.

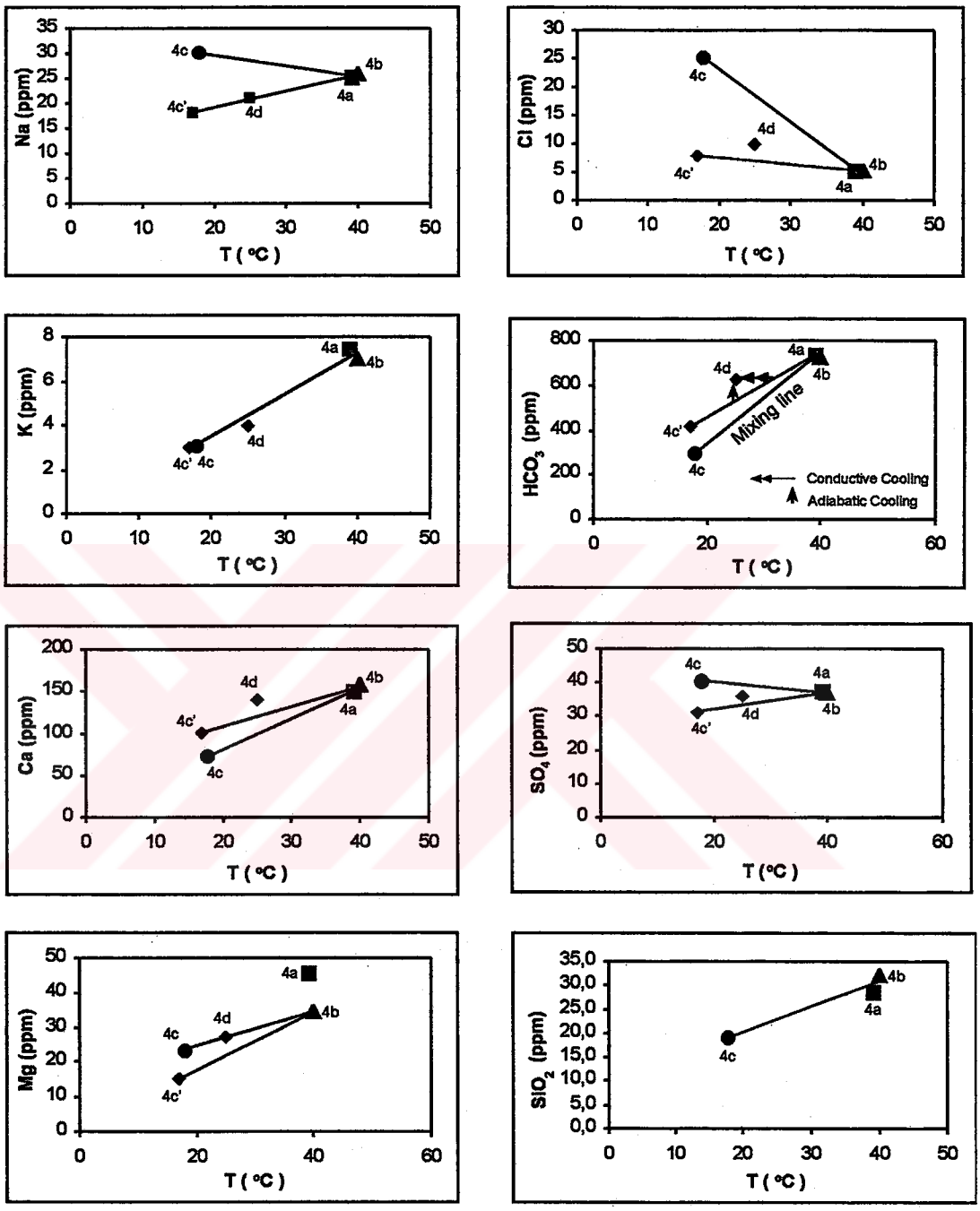


Figure 3.4.b. Ionic abundance vs. discharge temperature diagrams for Mudurnu samples.

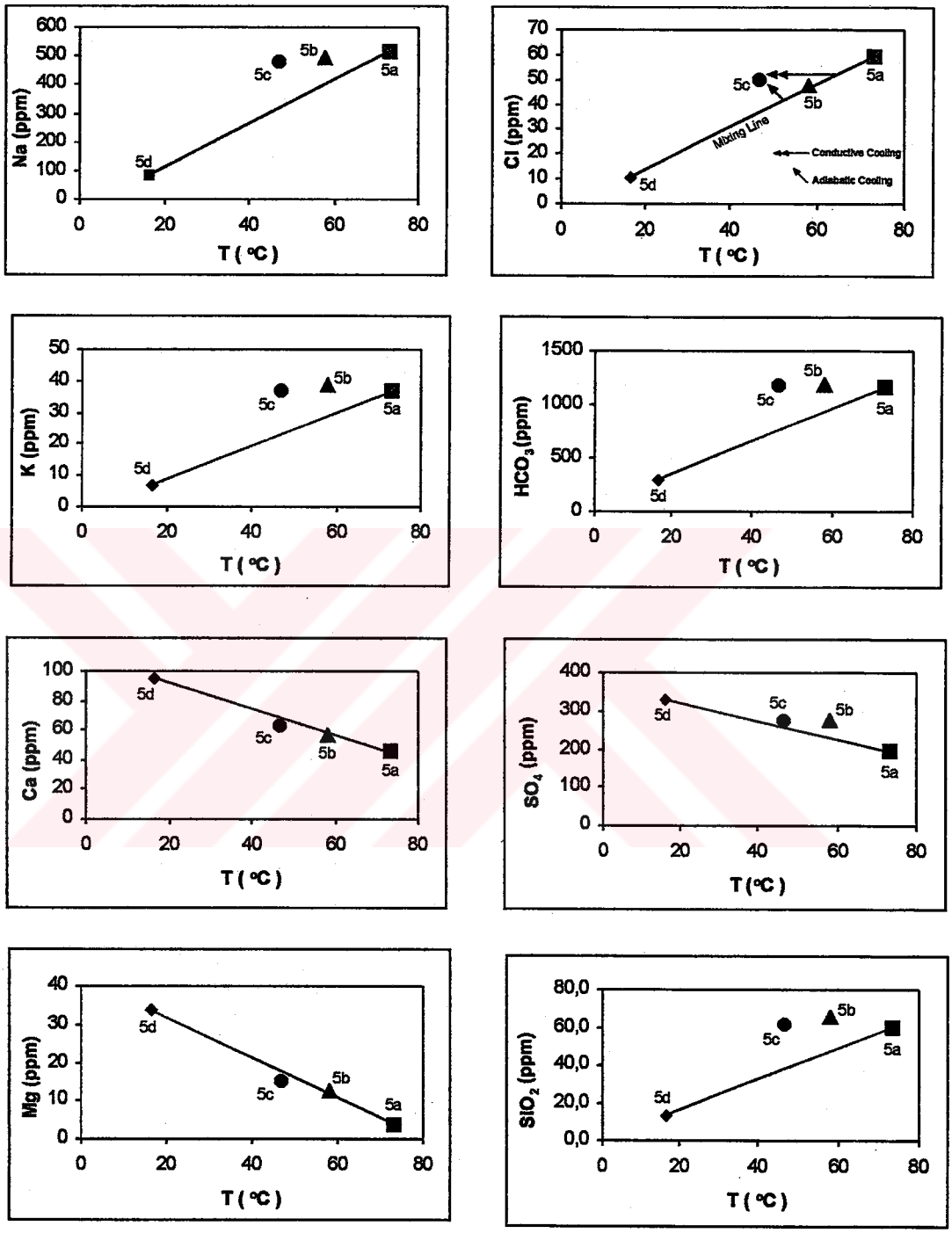


Figure 3.4.c. Ionic abundance vs. discharge temperature diagrams for Seben samples.

CHAPTER 4

GEOTHERMOMETRY APPLICATIONS

4.1. Principles

Geothermometers are important geochemical tools for the exploration and development of geothermal resources. Geothermometry is used to estimate subsurface temperatures of the geothermal systems. Chemical geothermometers are based on temperature dependent chemical equilibrium between water and rock in deep reservoir conditions. The principal assumption during the use of these geothermometers is that the chemical composition of water is preserved during its rise to the site of collection at the surface. In this study, various silica and cation geothermometers were used for the estimation of the reservoir temperatures.

4.2. Silica Geothermometers

Silica geothermometers are based on the experimentally determined, temperature-dependent variations in the solubility of silica in water. Since silica can occur in various forms (quartz, chalcedony and cristobalite) different silica geothermometers have been developed. Equations for these geothermometers are listed in Table 4.1. Quartz is the stable form of silica and it has the lowest

Table 4.1. Temperature for silica geothermometers (S is SiO_2 concentration in ppm; temperature (T) is in °C).

Geothermometer	Equation	Reference
Quartz-no steam loss	$T = (1309 / 5.19 - \log S) - 273.15$	Fournier (1977)
Quartz-maximum steam loss at 100 °C	$T = (1522 / 5.75 - \log S) - 273.15$	Fournier (1977)
Quartz	$T = 42.198 + 0.28831S - 3.6686 \times 10^{-4} S^2 + 3.1665 \times 10^{-7} S^3 + 77.034 \log S$	Fournier and Potter (1982)
Quartz	$T = 53.500 + 0.11236S - 0.5559 \times 10^{-4} S^2 + 0.1772 \times 10^{-7} S^3 + 88.390 \log S$	Arnorsson (1985) based on Fournier and Potter (1982)
Chalcedony	$T = (1032 / 4.69 - \log S) - 273.15$	Fournier (1977)
Chalcedony	$T = (1112 / 4.91 - \log S) - 273.15$	Arnorsson et al. (1983)
Alpha-Cristobalite	$T = (1000 / 4.78 - \log S) - 273.15$	Fournier (1977)
Opal-CT (Beta-Cristobalite)	$T = (781 / 4.51 - \log S) - 273.15$	Fournier (1977)
Amorphous silica	$T = (731 / 4.52 - \log S) - 273.15$	Fournier (1977)

solubility. The quartz geothermometer seems to work best in the temperature range from 0 to 250 °C. Above 250 °C the equations depart from the experimentally determined solubility curve and should not be used.

When quartz geothermometer is applied to boiling hot springs, since the silica concentration in the residual liquid increases as water boils, effects of steam separation should be considered. Thus, it is necessary to correct for the amount of steam formation or the proportion of adiabatic vs. conductive cooling.

Another consideration is precipitation of silica prior to or after sample collection. Silica precipitation before sample collection can occur in the deep, hot part of the system as the solution cools if water temperature is above 250 °C. However, if water temperature is less than about 225 °C to 250 °C and cools fairly quickly, little quartz is likely to precipitate during upflow. In addition, ascending solution having reservoir temperature more than 225 °C will become supersaturated with respect to amorphous silica before reaching the surface owing to the decreased temperature. Amorphous silica precipitates much more quickly than quartz. After sample collection, precipitation or polymerization of amorphous silica can occur in water coming from reservoirs above 145 °C since the water will become supersaturated with respect to amorphous silica during cooling to 25 °C. Because of the precipitation of quartz at high temperature and polymerization and precipitation of amourphous silica at low temperature, the reservoir temperature will be underestimated.

Hot water can be mixed with cold water when ascending to the surface. A new water-rock chemical equilibrium may or may not be attained after mixing. If chemical equilibrium is attained after mixing, the silica geothermometer will give the temperature of that last equilibrium. If chemical equilibrium is not attained after

mixing, direct application of the silica geothermometer will give a calculated temperature that is too low.

4.3. Cation Geothermometers

Na-K Geothermometers

The Na/K ratio in geothermal waters is widely used as a geothermometer (Table 4.2). There is a tendency to use the Na/K ratio to estimate possible higher temperatures in deeper parts of a system where waters reside for relatively long periods of time. Application of Na-K geothermometer is limited to high temperature well waters (above about 180 °C). Na/K geothermometer generally gives unrealiable results at low temperatures (<100 °C) because at low temperatures the ratio of dissolved Na to K in the geothermal waters is controlled by leaching rather than chemical equilibrium (Fournier and Truesdell, 1973). All the Na-K geothermometers give almost the same result at about 300 °C. The main advantages of the Na/K geothermometer is that it is less affected by dilution and steam separation than other commonly used geothermometers, provided there is little Na^+ and K^+ in the diluting water compared to reservoir water.

K-Mg Geothermometer

K/Mg geothermometer of Giggenbach (1988) is based on calculating various temperatures for the relative concentrations of K and Mg (Table 4.2) which would be in equilibrium with the mineral assemblage K-feldspar, chlorite and

Table 4.2. Temperature equations for cation geothermometers (concentrations are in meq for Na-K-Ca-Mg geothermometer and in ppm for the others; temperature (T) is in °C).

Geother.	Equations	Reference
Na-K	T=[855.6/(0.857+log(Na/K))]-273.15	Truesdell (1976)
Na-K	T=[833/(0.780+log(Na/K))]-273.15	Tonani (1980)
Na-K	T=[933/(0.993+log (Na/K))]-273.15 (25-250 °C)	Arnorsson et al. (1983)
Na-K	T=[1319/(1.699+log(Na/K))]-273.15	Arnorsson et al. (1983)
Na-K	T=[1217/(1.483+log(Na/K))]-273.15	Fournier (1979)
Na-K	T=[1178/(1.470+log (Na/K))]-273.15	Nieva and Nieva (1987)
Na-K	T=[1390/(1.750+log(Na/K))]-273.15	Giggenbach (1988)
K-Mg	T=[4410/(14.00-log(K/$\sqrt{Mg}$))]-273.15	Giggenbach (1988)
Na-K-Ca	T=[1647/(log(Na/K)+B(log($\sqrt{Ca}$ /Na)+2.06)+2.47)]-273.15 β=1/3 if T>100 °C β=4/3 if T<100 °C β=1/3 if T<100 °C when [log ($\sqrt{Ca}$ /Na)+2.06]<0	Fournier and Truesdell (1973)
Na-K-Ca-Mg	$T = T_{Na-K-Ca} - \Delta t_{MG}$°C R = (Mg / Mg + 0.61Ca + 0.31K) x 100 **if R from 1.5 to 5** Δt_{MG}°C = -1.03 + 59.971 log R + 145.05 $(\log R)^2$ – 36711 $(\log R)^2$ / T - 1.67 x 10^7 log R / T^2 **if R from 5 to 50** Δt_{MG}°C=10.66-4.7415 log R+325.87$(\log R)^2$-1.032x$10^5$$(\log R)^2$/T-1.968x$10^7$$(\log R)^3$/$T^2$ **Note:** Do not apply a Mg correction if Δt_{MG} is negative or R<1.5. If R>50, assume a temperature = measured spring temperature. T is Na-K-Ca geothermometer temperature is Kelvin.	Fournier and Potter (1979)

muscovite assuming that all solids have pure end-member compositions and activity coefficients are unity (equal to 1).

When the results of K-Mg and other geothermometers (especially silica and Na-K-Ca) are similar, water rock equilibration is attained at the estimated temperature and there is little water-rock interaction during the ascent to the surface.

Na-K-Ca and Na-K-Ca-Mg Geothermometer

The Na-K-Ca geothermometer of Fournier and Trusdell (1973) was developed specifically to deal with calcium-rich waters that give anomalously high temperatures by the Na/K method. The Na-K-Ca geothermometer is affected by the changes in concentration of hot waters resulted both from boiling and from mixing with cold, dilute waters. The main effect of boiling is loss of CO_2 which can cause $CaCO_3$ to precipitate. Fournier and Potter (1979) showed that the Na-K-Ca geothermometer may also give anomalously high results when applied to the Mg-rich waters which owe their nature to the water-rock reactions occurring at relatively low temperatures. For such waters, an empirical Mg correction is applied to the Na-K-Ca geothermometer. Mg-corrected Na-K-Ca geothermometer is known as Na-K-Ca-Mg geothermometer (Fournier and Potter, 1979). Mg corrections in geothermal waters rapidly decrease as temperature increases. All the waters which have high Mg content have undergone a water-rock interaction at low temperatures. Only low-temperature waters require a Mg correction to give the correct temperature. Mg correction to high-temperature waters which have picked up Mg during upflow will yield too low reservoir temperatures.

Other Cation Geothermometers

Various other cation geothermometers were suggested for use in some specific cases. These are Na-Ca (Tonani, 1980) and K-Ca (Tonani, 1980). Na-Ca and K-Ca are affected by the changes in CO_2 partial pressure. Precipitation of calcium carbonate from an ascending fluid causes the Na-Ca and K-Ca geothermometer temperatures to be too high.

4.4. Results of Chemical Geothermometer Calculations

Silica Geothermometers

The results of silica geothermometers applied to the thermal waters of the study areas are given in Table 4.3. Among the silica geothermometers, Opal-CT, amorphous silica, cristobalite geothermometers give anomalously low temperature values (much lower than the discharge (measured) temperatures for most of the samples). Chalcedony geothermometer of Arnorsson et al. (1983) give results similar to discharge temperature. However, quartz geothermometer with and without steam loss (Fournier, 1977), quartz geotermometers of Fournier and Potter (1982) and quartz geothermometer of Arnorsson (1985) yield reasonable reservoir temperatures ranging from 88 to 91 °C for Kurşunlu, 85 to 88 °C for Bolu, 143 to 150 °C for Efteni, 77 to 86 °C for Mudurnu, 111 to 115 °C for Seben, 97 to 99 °C for Reşadiye and 67 to 72 °C for Gözlek areas. Compared to quartz geothermometers chalcedony geothermometers of Fournier (1977) displays relatively lower reservoir temperatures.

T.C. YÜKSEKÖĞRETİM KURULU
DOKÜMANTASYON MERKEZİ

Table 4.3. Results of silica geothermometry application of collected waters (°C).

Locality	Sample No	Disc. T °C	Q No Steam Loss[a]	Q Max Steam Loss[a]	Quartz[b]	Quartz[c]	Chal.[a]	Chal.[d]	Crist.[a]	Opal-CT[a]	Amor. Silica[a]
Kurşunlu	1a	57	88	91	89	89	58	60	38	*	*
Kurşunlu	1b	16	81	84	81	82	49	52	31	*	*
Bolu	2	45	85	88	86	86	54	57	35	*	*
Efteni	3a	44	150	143	150	145	124	122	99	50	28
Mudurnu	4a	38	77	81	78	78	46	49	28	*	*
Mudurnu	4b	40	83	86	83	83	51	54	33	*	*
Seben	5a	73	111	111	111	111	82	83	61	13	*
Seben	5b	58	115	114	115	114	86	86	64	17	*
Seben	5c	51	112	111	112	111	82	83	61	14	*
Reşadiye	6	47	97	99	98	98	67	69	47	1	*
Gözlek	7a	40	67	72	68	68	35	39	18	*	*

[a] Fournier (1977); [b] Fournier and Potter (1982); [c] Arnorsson (1985); [d] Arnorsson et. al. (1983).
* Calculated geothermometer is less than zero.

Cation Geothermometers

The results of cation geothermometers are given in Table 4.4. The reservoir temperatures computed from the cation geothermometers for each water are generally higher than those of silica geothermometers. Na/K geothermometers give temperatures ranging from 176 to 224 °C for Kurşunlu area, 107 to 169 °C for Efteni area, 154 to 197 °C for Seben, 139 to 195 °C for Reşadiye, 156 to 209 °C for Gözlek area. For Bolu and Mudurnu area, it yields very high temperatures around 300 °C. Although the Na/K geothermometer is based on the use of ratios rather than the absolute abundances of the ions, and hence it is less sensitive to the effects of mixing and/or boiling, it should be used with great caution because it may yield erroneous estimates for waters from low temperature environments. Additionally, Na/K geothermometer gives erroneous estimates for waters having high Ca contents like those in Bolu (Ca-SO_4 character) and Mudurnu (Ca-HCO_3 character). In order to eliminate the possible effects of Ca concentrations on Na/K geothermometer, Na-K-Ca geothermometer of Truesdell (1973) was used. For Bolu and Mudurnu it yields lower temperature than Na/K geothermometer results, 211 °C for Bolu area and 182 to 187 °C for Mudurnu field. It gives temperatures similar to Na/K geothermometer results for Kurşunlu, Efteni, Seben and Reşadiye. However, it is important to note here that in Kurşunlu and Reşadiye calcite precipitation is observed in the field. This means that the measured Ca contents of these waters are lower than those supposed to be in reservoir conditions. This in turn means that low Ca concentration results in high temperature estimates in the Na-K-Ca geothermometer (see Table 4.2). In this respect, Na-K-Ca geothermometer and the Na/K geothermometer (giving similar results with Na-K-Ca geothermometer) are

Table 4.4. Results of cation geothermometry application of collected waters (°C).

Locality	Sample no.	Disc. T °C	Na/K[a]	Na/K[b]	Na/K[c]	Na/K[c]	Na/K[d]	Na/K[e]	Na/K[f]	K/Mg[f]	Na-K-Ca[g]
Kurşunlu	1a	57	176	183	184	207	208	195	224	88	221
Kurşunlu	1b	16	143	148	152	182	181	168	198	89	187
Bolu	2	45	409	434	398	356	374	358	374	48	211
Efteni	3a	44	107	110	118	153	150	138	169	45	132
Mudurnu	4a	38	343	362	339	318	331	315	336	43	187
Mudurnu	4b	40	327	344	324	308	320	304	326	44	182
Seben	5a	73	154	159	163	191	190	177	207	74	175
Seben	5b	58	163	169	171	197	197	184	214	67	177
Seben	5c	51	160	166	169	195	195	182	211	66	174
Reşadiye	6	47	139	143	148	179	177	165	195	58	156
Gözlek	7a	40	156	162	165	192	192	179	209	50	153

[a] Truesdell(1976), [b] Tonani(1980), [c] Arnorsson et al. (1983), [d] Fournier(1979), [e] Nieva and Nieva (1987), [f] Giggenbach (1988), [g] Fournier and Trusdell (1973).

not much reliable for the studied fields. K-Mg geothermometer of Giggenbach (1988) gives estimates similar to chalcedony estimates and hence to discharge temperatures.

Given that Na/K and Na-K-Ca geothermometers yield overestimates and that K-Mg and chalcedony geothermometer yield results similar to discharge temperatures, it can be concluded that quartz geothermometer give more representative estimates for the reservoir temperature.

4.5. Na-K-Mg Diagram and Na-K-Mg-Ca Diagram

A further evaluation of the cation geothermometers is made on the Na-K-Mg diagram proposed by Giggenbach (1988) (Figure 4.1). This technique is devised giving an automatic indication as to the suitability of given water for the application of ionic solute geoindicators. The model is based on the following reactions:

$$\text{K-feldspar} + Na^{+} = \text{Na-feldspar} + K^{+}$$

and

$$2.8\text{K-feldspar} + 1.6H_2O + Mg^{2+} = 0.8\text{K-mica} + 0.2\text{chlorite} + 5.4SiO_2 + 2K^{+}$$

The corresponding concentration quotients of cations in these reactions are temperature dependent and used to drive following geothermometers (t_{kn} : K-Na geothermometer, t_{km} : K-Mg geothermometer) which are also presented in Table 4.2.

$$t_{kn} = 1390/(1.75 - \log(C_K/C_{Na})) - 273.15$$

$$t_{km} = 4410/(14.0 - \log(C^2_K/C_{Mg})) - 273.15$$

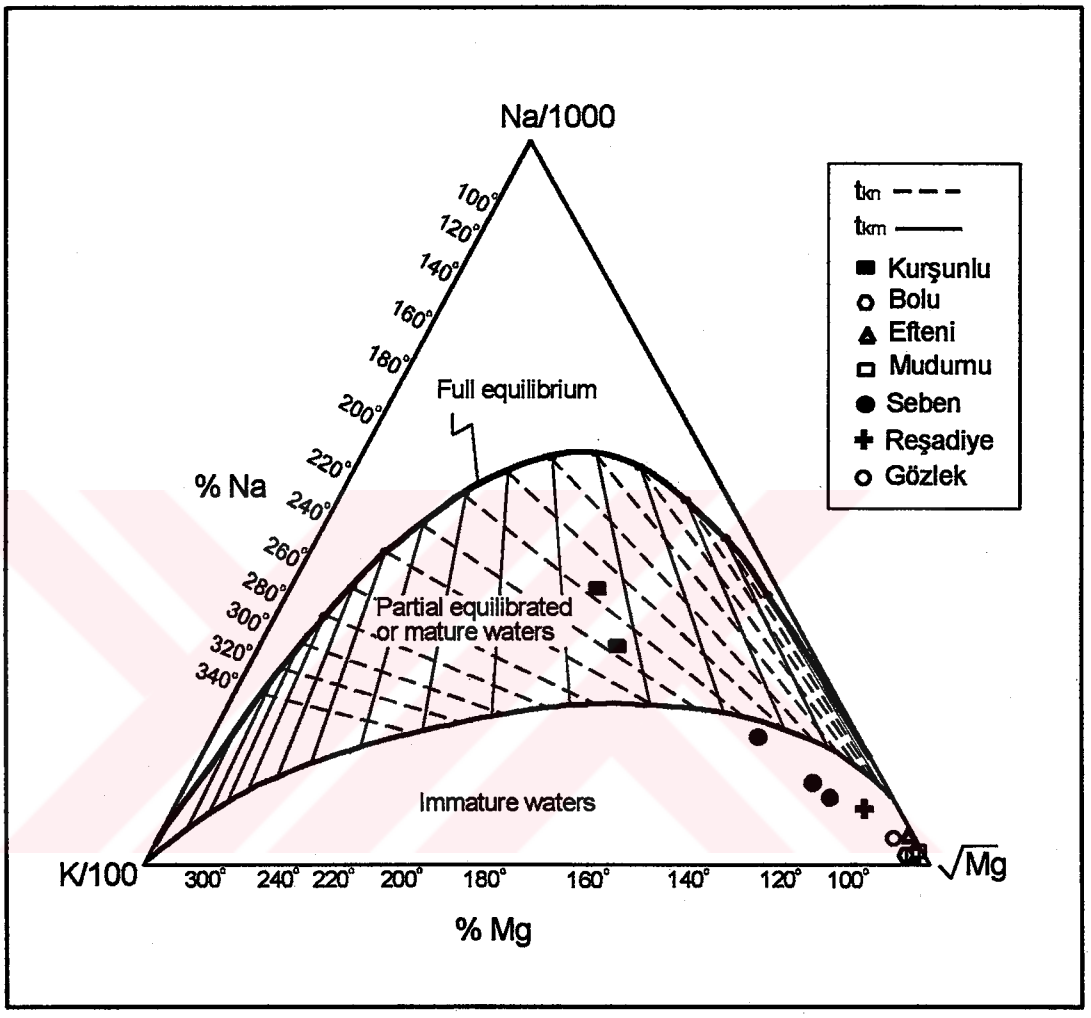


Figure 4.1. Graphical evaluation (Giggenbach, 1988) of the water-rock equilibration temperatures using relative Na, K and Mg concentrations (mg/kg) of thermal water in the studied areas.

A triangular diagram with Na/1000, K/100 and $\sqrt{Mg}$ corners graphically illustrates the Na-K-Mg geothermometer. The position of full equilibrium line changes with respect to assumed Na-K and K-Mg geothermometer equations.

In Figure 4.1, it can be seen that all waters except Kurşunlu hot water are immature water. Kurşunlu hot water is partially equilibrated (mature water). Seben hot waters are close to boundary between mature water and immature water. Application of Na/K and K/Mg geothermometer to immature water gives erroneous results. Therefore the results of these geothermometers for Bolu, Eften, Mudurnu, Reşadiye and Gözlek are doubtful and the interpretation of the temperature predictions of such areas should be made cautiously. On the other hand, for Kurşunlu and to a certain extend Seben temperature estimates can be performed with some degree of confidence.

The plot of 10Mg/(10K+Na) (Giggenbach, 1988) of waters from the study areas is presented in Figure 4.2.

Like the model given in Figure 4.1, the position of the samples do not indicate any equilibrium between the rock and waters.

4.6. Mixing Models

The reservoir temperature of thermal waters and the processes controlling the chemical composition of well and spring waters in respective geothermal fields are further examined with silica-enthalpy (Fournier, 1977) and cloride-enthalpy (Truesdell and Fournier, 1975) mixing models.

The enthalpy values used in both diagrams are the values, taken from the Steam Table in Henley et al. (1984), at the corresponding discharge temperatures.

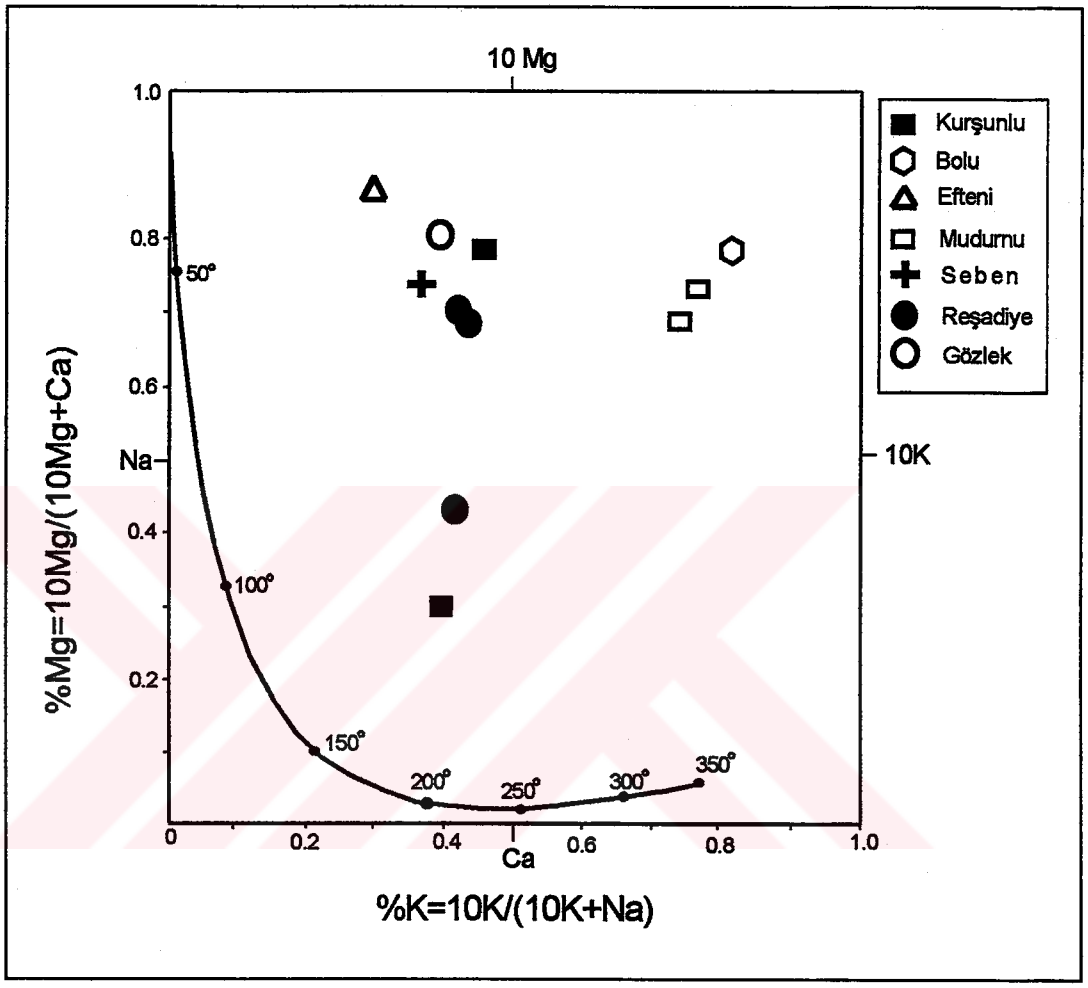


Figure 4.2. Plot of 10K/(10K+Na) vs. 10Mg/(10Mg+Ca) of thermal water (mg/kg) in the studied areas (Giggenbach, 1988).

T.C. YÜKSEKÖĞRETİM KURULU
DOKÜMANTASYON MERK

Silica –Enthalpy Mixing Model

The silica-enthalpy mixing model is applied to Seben, Mudurnu and Kurşunlu geothermal fields where adequate number of samples –cold, warm, hot waters- were collected. Since no silica analysis could be performed for samples collected in 2001, the data used in the silica-enthalpy mixing model are those obtained from samples collected in 2000. The diagrams belonging to respective fields are given in Figures 4.3, 4.4, and 4.5.

In silica-enthalpy diagram, the reservoir temperature can be estimated from the intersection of mixing line (joining cold water to hot water sample) with the quartz solubility curve (Fournier, 1977).

In Seben geothermal field, the mixing line, which connects the cold water sample (sample no:5d) to the hot sample (sample no:5a), intersects the quartz solubility curve at an enthalpy value of 625 J/g which corresponds to a reservoir temperature of 148-149 °C (Figure 4.3). This temperature estimate is based on the assumption that the steam formed during a possible boiling process did not separate from the residual liquid before mixing with the cold water component. If a possible steam loss is assumed to have occurred prior to mixing, then taking the enthalpy of water at the temperature of steam formation as 407 J/g (boiling at 97 °C at the elevation of Seben (see Appendix B)), the initial enthalpy is found as 515 J/g, corresponding to a reservoir temperature of 122-123 °C.

In Mudurnu geothermal field, the mixing line was drawn between the cold water sample (sample 4c) and hot water samples (sample 4a and 4b) and intersects the quartz solubility curve at an enthalpy of 421.4 j/g which corresponds to a reservoir temperature of 100-101 °C (Figure 4.4).

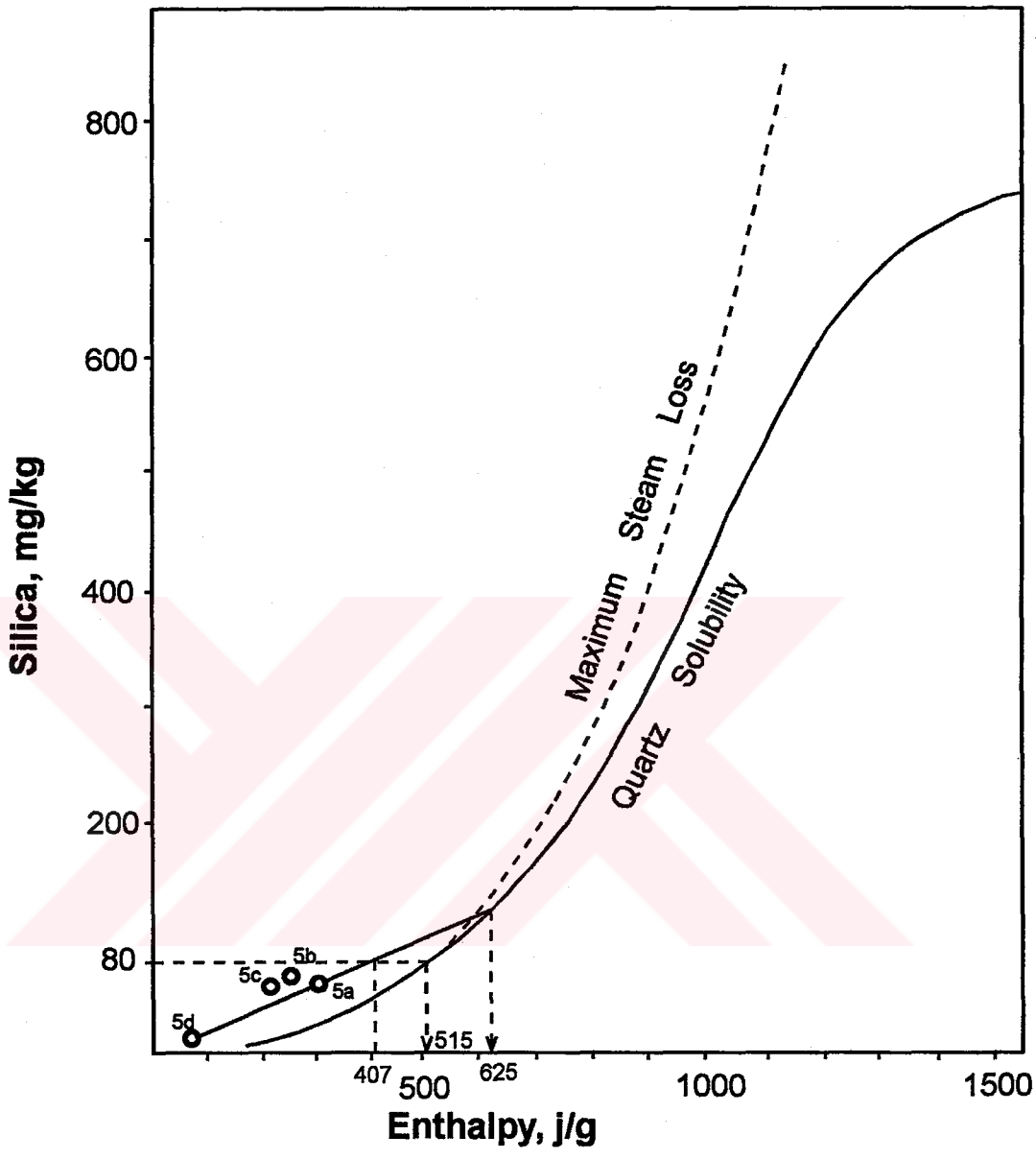


Figure 4.3. Enthalpy-silica mixing model for samples of Seben (quartz solubility curves are from Fournier, 1977).

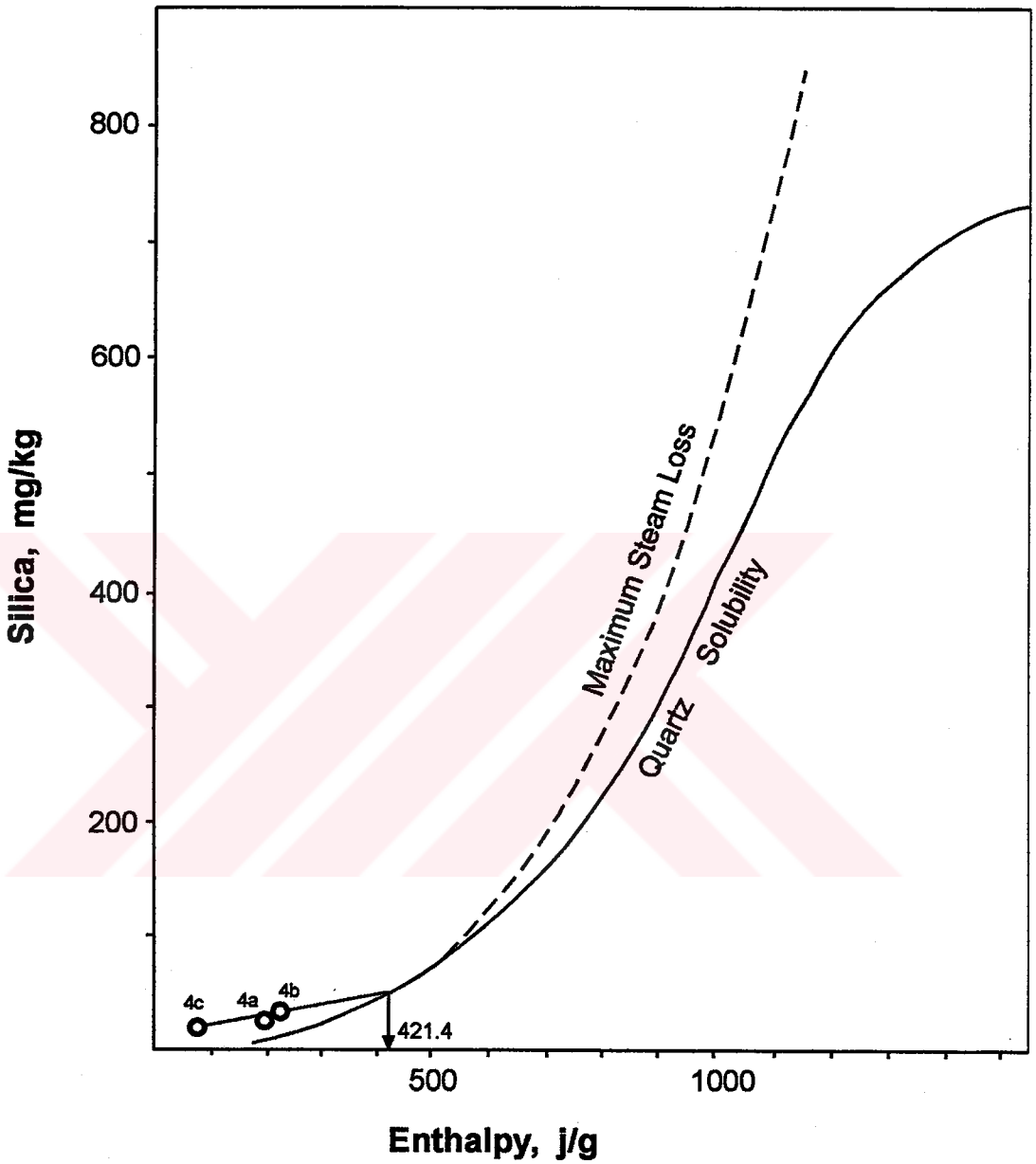


Figure 4.4. Enthalpy-silica mixing model for samples of Mudurnu (quartz solubility curves are from Fournier, 1977).

In Kurşunlu field the silica content of cold water sample (sample 1c) is higher than that of the mineral and hot water samples (sample 1b and sample 1a, respectively) indicating a possible silica precipitation for the latter two samples, either before or after sampling. Therefore, the mixing line was drawn between mineral and hot water samples. The line intersects the solubility curve at an enthalpy of 364,3 j/g which corresponds to a reservoir temperature of 87 °C (Figure 4.5). Possibly this temperature is an underestimate because of the silica precipitation.

Chloride-Enthalpy Model

The chloride-enthalpy mixing model, like silica-enthalpy model, can be applied to fields where adequate number of samples are available. In this respect, Seben , Kurşunlu and Mudurnu fields appear to be the most appropriate fields to be utilized in chloride-enthalpy mixing model. However, in the Mudurnu field cold water sample has Cl^- content higher than those of hot and warm waters (see sections 3.3.1 and 3.3.2. for possible explanations) and, hence, chloride-enthalpy mixing model is not applicable to this field. Therefore possible reservoir temperature estimates via chloride-enthalpy mixing model are made here only for Seben and Kurşunlu fields. The data used in these diagrams are the averages of those obtained from samples collected in 2000 and 2001.

In Seben geothermal field, the sample (sample no.5a) with the highest chloride content and enthalpy value is connected to the cold water sample (sample no.5d) and the mixing line is marked as ML1 in the figure 4.6. Sample 5b and 5c

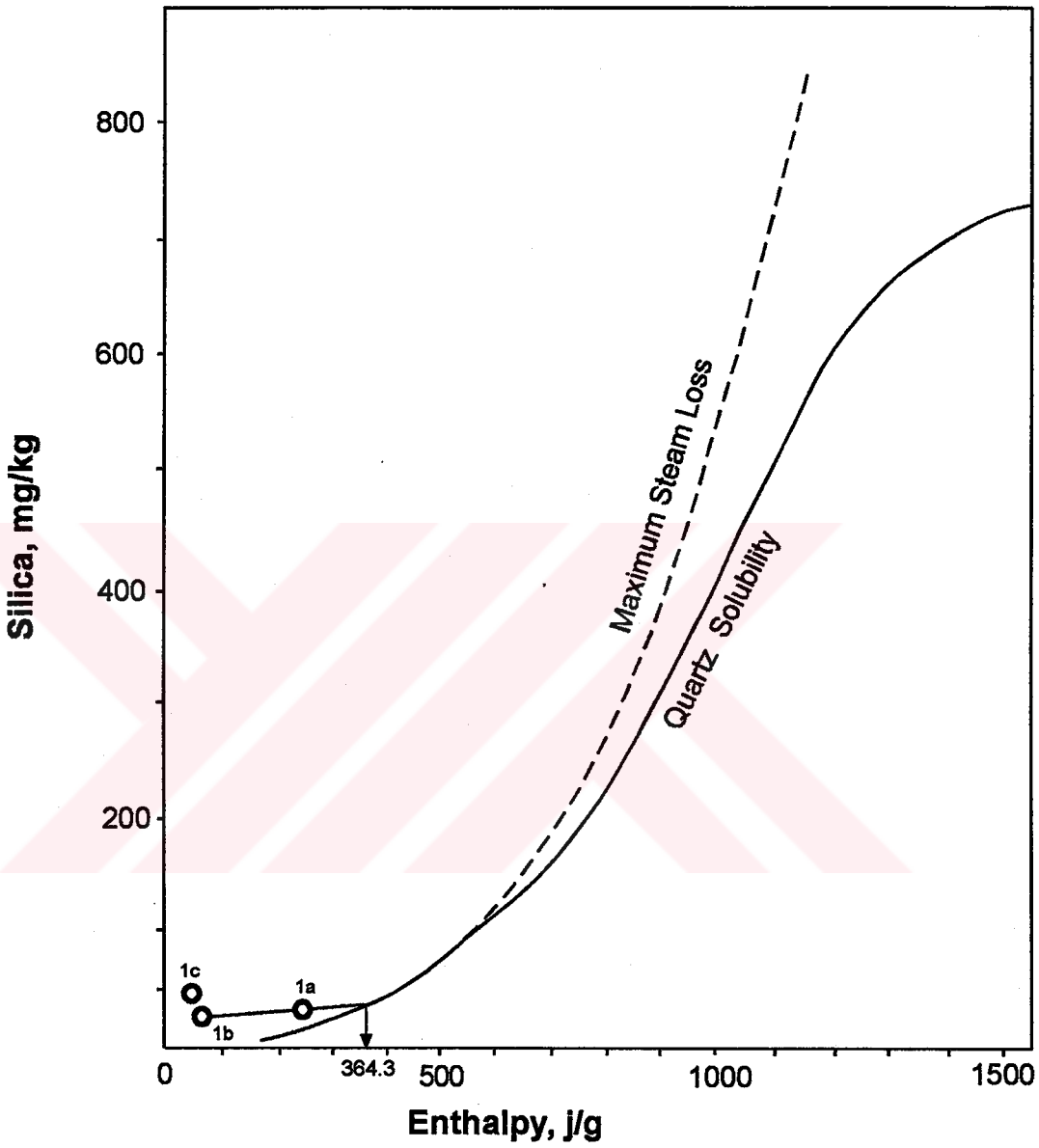


Figure 4.5. Enthalpy-silica mixing model for samples of Kurşunlu (quartz solubility curves are from Fournier, 1977).

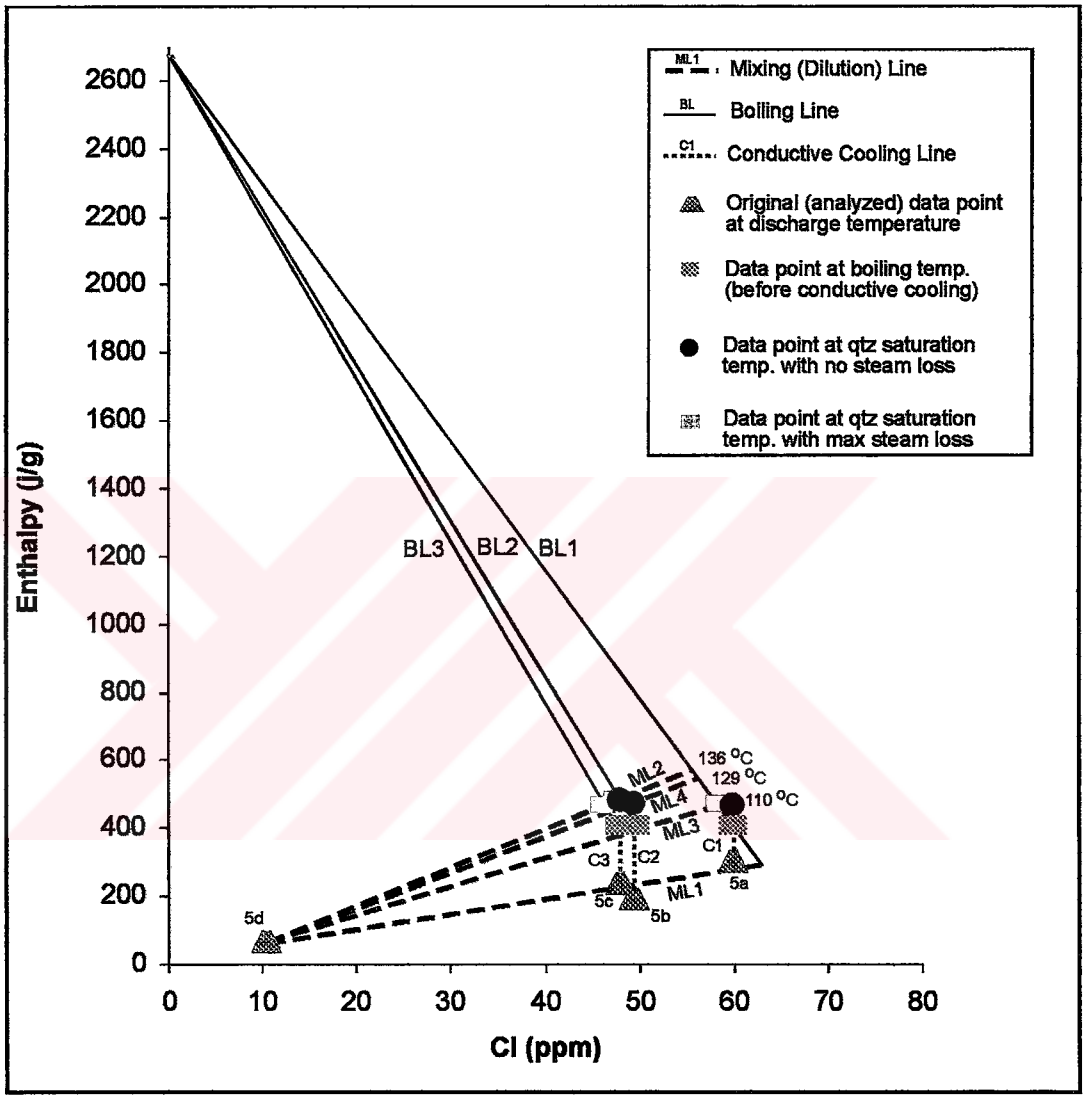


Figure 4.6. Enthalpy-chloride mixing model for samples of Seben.

coincide with this mixing line. It is probable that these samples originated by a mixing between the cold water and the hot water samples.

With regard to the estimation of reservoir temperatures, a number of possibilities can be considered in the figure. As a first approximation (boiling of deep reservoir fluid followed, in turn, by conductive cooling and mixing), it is assumed that sample 5a (with the highest Cl^- content) is produced by boiling of a deep reservoir fluid to 97 °C (temperature of boiling at the elevation of Seben), followed by conductive cooling to discharge temperature. Within this framework, the original data point for sample 5a is projected upwards to 97 °C, assuming conductive cooling to the discharge temperatures following this boiling process. The point at 97 °C is connected to the point with 2670 J/g and 0 ppm Cl^- (representing the steam phase at 97 °C), producing the boiling line BL1. As can be seen from the figure, the mixing line ML1 intersects this boiling line (BL1) at a temperature lower than the boiling temperature (97 °C) which makes it impossible to estimate the reservoir temperature.

The second approximation (mixing followed, in turn, by boiling and conductive cooling) assumes that the hot samples are produced by adiabatic and subsequent conductive cooling of mixed waters. In order to examine this process, the original data points are projected upwards to 97 °C assuming conductive cooling to the discharge temperatures following boiling. The points at 97 °C are then connected to the point with 2670 J/g and 0 ppm Cl^- (representative of steam at 97 °C), producing the boiling lines BL2 and BL3. On these lines (BL1, BL2 and BL3), the temperatures estimated through the use of the quartz geothermometer with maximum steam loss are marked. The data points obtained in this way are joined to the cold water sample, producing the mixing lines ML2 and ML3. The intersections

of these mixing lines with the boiling line BL1 correspond to reservoir temperatures of 110 °C and 136 °C respectively.

Another scenario (mixing followed by conductive cooling) can be that the hot water samples are mixed waters which cooled conductively to the discharge temperatures without any adiabatic cooling. To examine this process, the original data points (with discharge temperatures) are projected upwards to temperatures obtained from the quartz geothermometer with no steam loss. They have the same Cl^- content as the original data points. One of the mixing lines which pass through the data points at quartz (no steam loss) temperatures coincides with the mixing line ML2, the other is marked as ML4. These mixing lines intersects the boiling line BL1 at enthalpy values of 540 and 570 j/g which correspond to the reservoir temperatures of 129 and 136 °C, respectively.

In Kurşunlu geothermal field, the sample with the highest Cl^- content and enthalpy value (sample no.1a) is connected to the cold water sample (sample no.1c). The mixing line is marked as ML1 in the figure 4.7. Sample no.1b does not coincide with this line, suggesting that even if it was a product of mixing between hot and cold waters, this sample should have cooled conductively to its discharge temperature following mixing.

With regard to the estimation of reservoir temperature, as a first approximation (boiling of deep reservoir fluid followed, in turn, by conductive cooling and mixing) it is assumed that sample no.1a is produced by boiling of a deep reservoir fluid to 97 °C (boiling temperature at the elevation of Kurşunlu), followed by conductive cooling to discharge temperature. Within this framework, the original data point for sample no.1a is projected upwards to 97 °C. The point at 97 °C is connected to the point with 2670 j/g and 0 ppm Cl^- (representative of steam

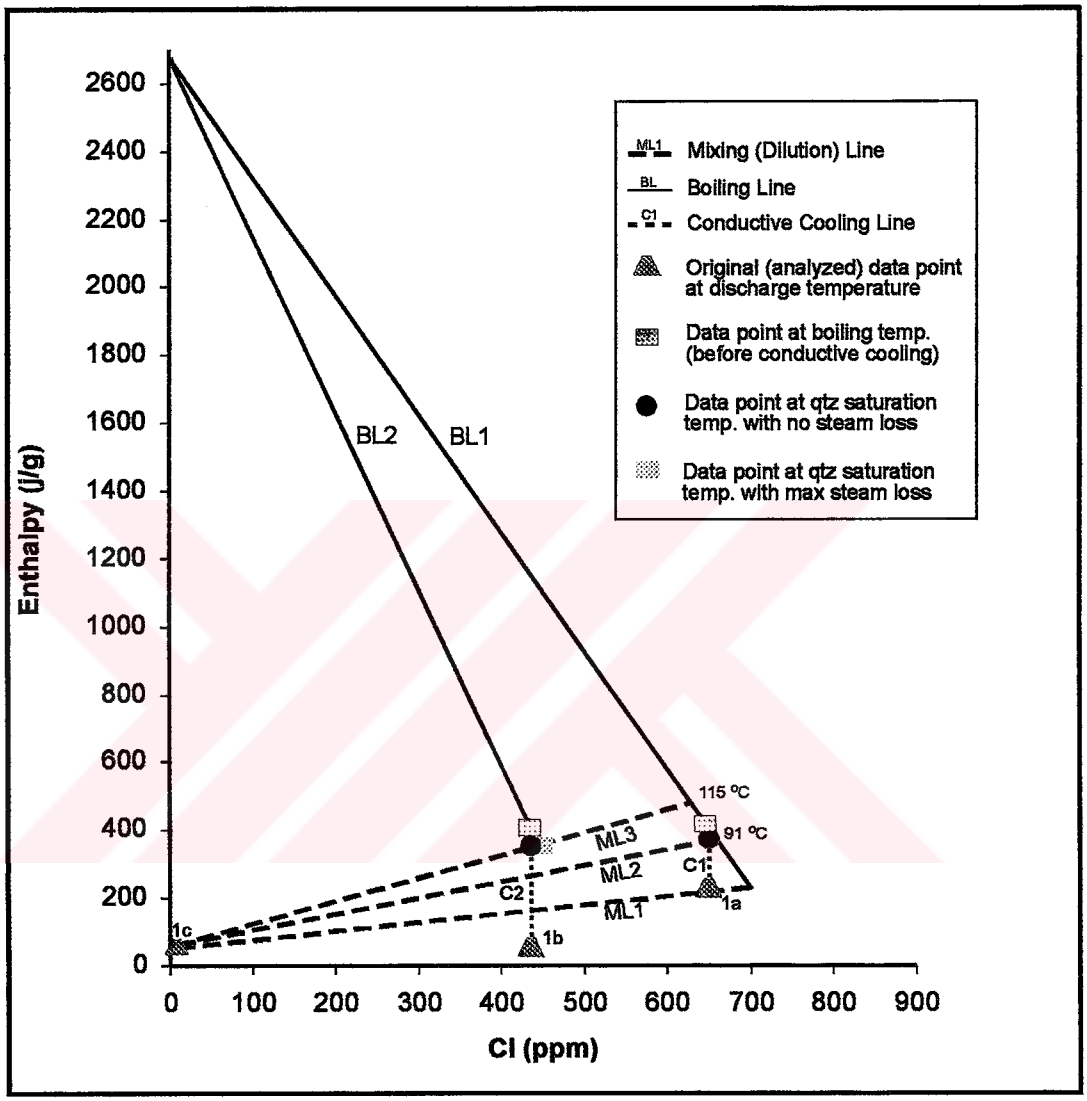


Figure 4.7. Enthalpy-chloride mixing model for samples of Kurşunlu.

at 97 °C), producing boiling line BL1. As can be seen from the diagram, the mixing line ML1 intersects this boiling line at a temperature lower than 97 °C leaving no possibility for a reservoir temperature estimate.

The second approximation (mixing followed, in turn, by boiling and conductive cooling) assumes that the warm-water is produced by adiabatic (and subsequent conductive) cooling of mixed waters (i.e. the original point is projected upwards to 97 °C producing boiling line BL2). However, since the temperature, estimated by quartz with max steam loss geothermometry, is lower than 97 °C (a possible precipitation - as discussed previously – resulting in underestimated quartz temperatures), this alternative does not work in Kurşunlu field.

As a third approximation (mixing followed by conductive cooling), the hot and warm water samples (samples 1a and 1b) are assumed to be products of conductive cooling of mixed waters. To examine this process, the original data points are projected upwards to temperature obtained by quartz geothermometer with no steam loss. Two mixing lines, ML2 and ML3, are obtained which intersect the boiling line BL1 at enthalpies of 480 and 380, respectively. The temperature corresponding to these enthalpy values are 115 °C and 91 °C, respectively.

In summary, chloride-enthalpy mixing model suggests reservoirs temperatures in the ranges of 91-115 °C for Kurşunlu and 110-136 °C for Seben geothermal fields.

CHAPTER 5

FLUID - MINERAL EQULIBRIA

5.1 Theory

The compositions of the geothermal fluids are mainly controlled by temperature-dependent reactions between minerals and fluids. Pressure, rock type, permeability, fluid composition, and duration of activity affect the formation of hydrothermal minerals in the geothermal systems. In order to determine the original reservoir temperatures of the geothermal systems, many hydrolysis reactions in the hydrothermal fluids (fluid-mineral equilibria in active geothermal systems) are used as geothermometers. By determining all the mineral phases that can be in equilibrium with a given geothermal fluid at a given temperature, the most probable reservoir temperature can be determined. This is the temperature at which the maximum numbers of mineral phases are in equilibrium with each other and with the geothermal fluid constituents. By definition, at equilibrium, $Q_k = K_k$, where Q_k is the activity quotient for the aqueous species arising from the dissolution of the mineral, k, and K_k is the equilibrium constant for the dissolution reaction; i.e.

$$K_k = \prod^{i} \frac{(a_{i,k})^{\nu_{i,k}}}{a_k} \quad , \qquad Q_k = \prod^{i} (a_{i,k})^{\nu_{i,k}}$$

Where,

a_i = activity of the species i in the equilibrium mass action expression for mineral k.

ν_{ik} = stoichiometric coefficient of species i in equilibrium mass action expression for mineral k.

a_k = activity of mineral k.

Since at equilibrium $Q_k = K_k$, log (Q/K)= 0 at the equilibrium temperature.

In a plot of log (Q/K) versus temperature, all minerals in equilibrium with the solution (i.e. log(Q/K) = 0) will converge to a value of zero at the same temperature. In non-equilibrium conditions, on the other hand, log (Q/K) will have either positive or negative values suggesting supersaturation or undersaturation of the geothermal fluid with respect to the concerned mineral, respectively.

Evaluation of the chemical equilibria between the minerals and the solution in the geothermal systems requires the determination of the activities of the aqueous species and solid phases, and a knowledge of the solubilities of the minerals found in the altered rocks (Arnorsson et al., 1982).

The computer program WATSPEC (Wigley, 1978) is one of the most commonly used program for mineral-fluid equilibrium studies. This program considers the most common species found in natural waters and the program is small and fast enough to be used on a quite small computer.

Starting from the chemical analysis and field measurements as temperature, pressure, pH and alkalinity, these suitable computer programs operate at any selected reference temperature of the speciation of the deep waters. Ionic speciation is the equilibrium distribution of aqueous species between free ions and ion pairs or complexes. Ionic speciation calculations are estimations of the distribution of aqueous ionic forms. For example, total calcium concentrations of all calcium species are expressed as:

$$\Sigma mCa = mCa^{++} + mCaSO^{\circ}_4 + mCaCO^{\circ}_3 + mCaHCO^{+}_3 + mCaOH^{+}$$

Calculation of ionic species concentrations is based on the dissolution reactions of related species in water.

$$H_2O \Rightarrow H^{+} + OH^{-}$$

$$H_2CO_3^{\circ} \Rightarrow HCO_3^{-} + H^{+}$$

$$HCO_3 \Rightarrow CO_3^{-2} + H^{+}$$

$$CaHCO_3^{+} \Rightarrow Ca^{2+} + H^{+} + CO_3^{-2}$$

$$CaCO_3^{\circ} \Rightarrow Ca^{2+} + CO_3^{-2}$$

$$CaOH^{+} \Rightarrow Ca^{2+} + OH^{-}$$

$$CaSO_4 \Rightarrow Ca^{2+} + SO_4^{2-}$$

Combining other free ions pairs, after T, pH and total concentrations input, n number of reactions with n unknown are obtained for ionic speciation calculated by the program WATSPEC.

WATSPEC program calculates the saturation indices with respect to a number of minerals. Saturation index (SI = Q/K) is a measure of the thermodynamic state of a solution relative to equilibrium with a specified solid-phase mineral (equilibrium saturation corresponds to Q = K, i.e. SI = 1 or log SI = 0 at

equilibrium; Q < K and SI < 1 or log SI < 0 is for solutions undersaturated, and Q > K and SI > 1 or log SI > 0 is for solutions supersaturated with respect to mineral).

5.2 Saturation Index Calculations for Geothermal Fields

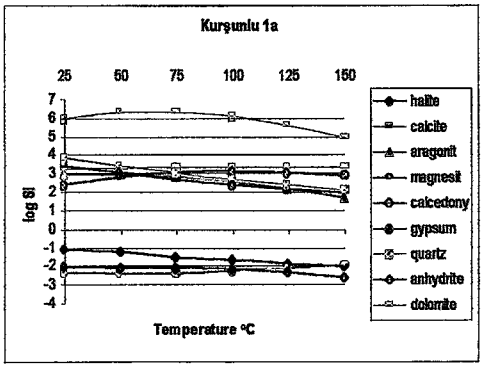
In order to use in a further evaluation of reservoir temperatures, and an assessment of the scaling potential during the possible development of the geothermal fields, saturation index calculations were performed in this study using the program WATSPEC. The calculations were carried out for only the hot waters using the averages of the analysis results for samples collected 2000 and 2001 (except for SiO_2 which was analyzed only for the samples collected in 2000).

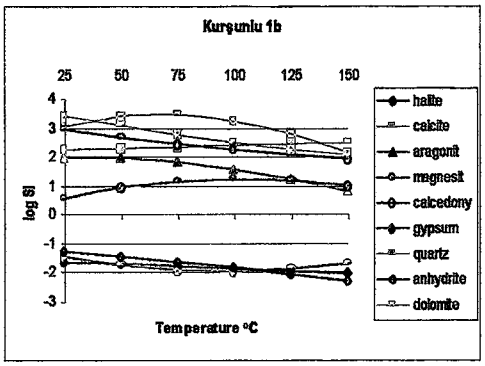
Only major ion concentrations and SiO_2 contents were analyzed and discharge temperature and pH values were measured within the scope of this thesis, saturation indices were calculated without redox potential.

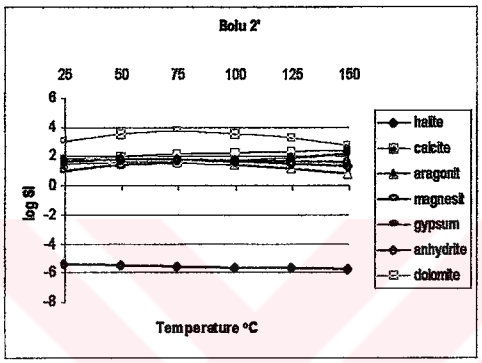
The saturation indices belonging to studied geothermal fields are given in Figure 5.1. It can be seen from the figure, all waters are supersaturated with respect to quartz, chalcedony and carbonates and undersaturated with respect to halite. The samples from Kurşunlu (samples 1a,1b), Efteni (sample 3a) and Gözlek are undersaturated, whereas all the others are supersaturated with respect to sulphate minerals, namely gypsum and anhydrite.

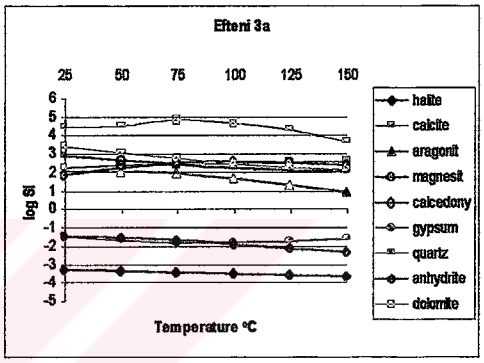
Regarding the reservoir temperature estimates, an inspection of log SI vs. T °C diagrams in Figure 5.1 shows that log Q/K curves for different minerals are dispersed and do not converge at log SI=0 line which represents the equilibrium condition. Therefore, from the SI curves of the minerals used in these calculations it is not possible to estimate the reservoir temperature at which the geothermal fluid

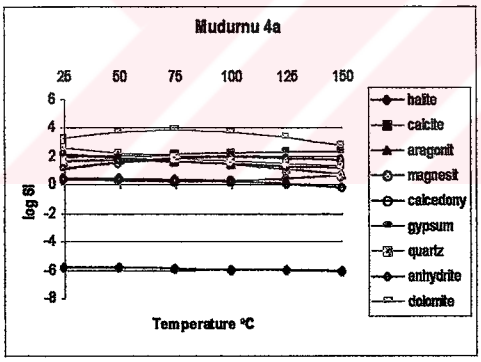
T.C. YÜKSEKÖĞRETİM KURULU
DOKÜMANTASYON MERKEZİ

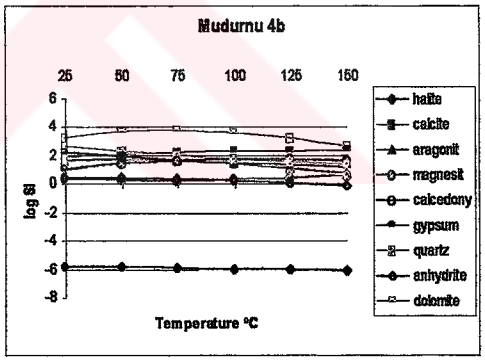

Kurşunlu 1a
log SI
Temperature °C
halite
calcite
aragonit
magnesit
calcedony
gypsum
quartz
anhydrite
dolomite

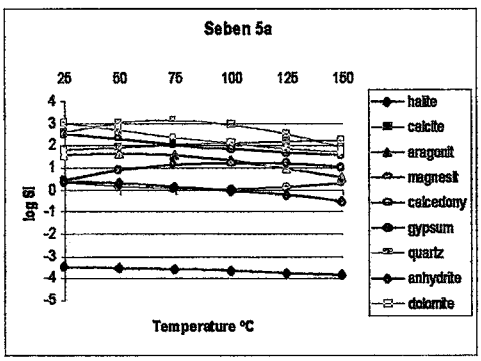

Kurşunlu 1b
log SI
Temperature °C
halite
calcite
aragonit
magnesit
calcedony
gypsum
quartz
anhydrite
dolomite

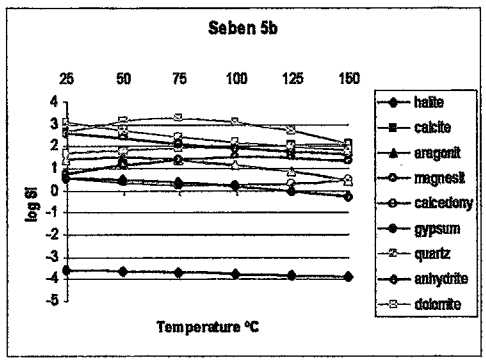

Bolu 2'
log SI
Temperature °C
halite
calcite
aragonit
magnesit
gypsum
anhydrite
dolomite


Efteni 3a
log SI
Temperature °C
halite
calcite
aragonit
magnesit
calcedony
gypsum
quartz
anhydrite
dolomite


Mudurnu 4a
log SI
Temperature °C
halite
calcite
aragonit
magnesit
calcedony
gypsum
quartz
anhydrite
dolomite


Mudurnu 4b
log SI
Temperature °C
halite
calcite
aragonit
magnesit
calcedony
gypsum
quartz
anhydrite
dolomite


Seben 5a
log SI
Temperature °C
halite
calcite
aragonit
magnesit
calcedony
gypsum
quartz
anhydrite
dolomite


Seben 5b
log SI
Temperature °C
halite
calcite
aragonit
magnesit
calcedony
gypsum
quartz
anhydrite
dolomite

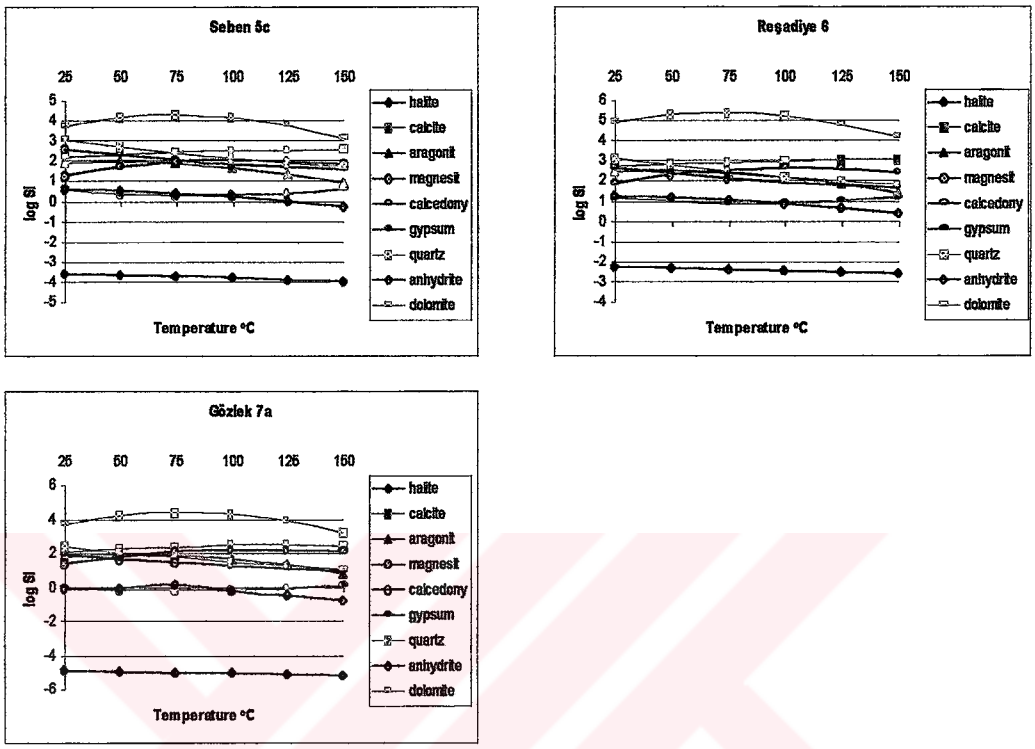


Figure 5.1. Mineral equilibrium diagrams for samples collected in June 2000 and April 2001.

and the minerals are supposed to be in equilibrium. It should be noted, however, that the minerals used in fluid-mineral equlibria calculations are rather limited in number and, since no Al analysis was done in this study, calculations with respect to feldspar minerals (which are the major rock forming minerals) could not be performed if these calculations could, however, be performed they would probably yield a reservoir temperature estimate.

Regarding the reservoir temperature estimates, since calcite and silica are supersaturated in all water samples, calcite and silica scaling could possibly arise during the utilization of thermal waters. However, except Kurşunlu and Reşadiye geothermal field, no calcite precipitation is observed during sampling.

CHAPTER 6

CONCLUSIONS

A total of 7 geothermal fields along 530 km long E-W transect of the North Anatolian Fault Zone were examined in this study for their geochemical characteristics and geothermal potential. The main conclusions drawn from this study are summarized as follows:

The thermal waters of Kurşunlu, Efteni, Seben, Reşadiye and Gözlek geothermal fields are Na-HCO_3 type waters, whereas Bolu has Ca-SO_4, and Mudurnu has Ca-HCO_3 type waters. Thermal waters appear to have acquired their chemical character mainly from their reservoir rocks that are dominantly limestones. The young volcanism confined to the pull-apart basins associated with NAFZ might also be responsible for the rise of CO_2 and H_2S gasses that gave the bicarbonate and sulphate rich character, respectively, to the waters in which they dissolve.

Subsurface phenomena could be examined in only three fields where it was possible to collect adequate number of samples including both hot and cold waters. The examination suggests the occurrence of both mixing and conductive cooling (between reservoir and surface) in Kurşunlu, Mudurnu and Seben geothermal fields.

Regarding the geothermal potential of the fields, cation geothermometers yield overestimated reservoir temperatures. Quartz geothermometers seem to yield more representative estimates which are –more or less- supported by the temperatures obtained from silica– enthalpy mixing model for Seben, Kurşunlu and Mudurnu fields, and from chloride-enthalpy mixing model for Seben and Kurşunlu fields. In this respect, the possible reservoir temperatures range from 88 to 115 °C for Kurşunlu, 85 to 88 °C for Bolu, 143 to 150 °C for Efteni, 77 to 101 °C for Mudurnu, 110 to 149 °C for Seben, 97 to 99 °C for Reşadiye and 67 to 72 °C for Gözlek fields.

Fluid-mineral equilibria calculations performed for carbonate, sulphate and quartz minerals could not yield any equilibrium temperature. In order to obtain reliable estimates of reservoir temperature, minor ions (e.g. Al) should be analysed to determine saturation state of minerals like feldspars, micas and clay minerals, which would give a possible equilibrium temperature.

The temperature estimates from chemical geothermometers and mixing models reveal that Kurşunlu, Efteni, Mudurnu, Seben and Reşadiye fields are more promising for geothermal energy development. Temperatures are high enough for conventional electric generation in Efteni and Seben whereas they are suitable for binary fluid electric generation in Kurşunlu, Mudurnu and Reşadiye. Moreover, all thermal waters in these fields can be used for soil warming, balneology, greenhouses or space-heating. However, since calcite and silica are supersaturated in all water samples, calcite and silica scaling could possibly arise during the utilisation of thermal waters.

REFERENCES

Arnorsson, S., 1985. The use of mixing models and chemical geothermometers for estimating underground temperatures in geothermal systems. Journal of Volcanology an Geothermal Research, 23, 209-335.

Arnorsson, S., Gunnlaugsson, E., and Svavarsson, H., 1982. The chemistry of geothermal waters in Iceland-I. Calculation of aqueous speciation from 0° to 370°C. Geochim. Cosmochim. Acta, 46, 1513-1532.

Arnorsson, S., Gunnlaugsson, E., and Svavarsson, H., 1983. The chemistry of geothermal waters in Iceland-II. Mineral equilibria and independent variables controlling water compositions. Geochim. Cosmochim. Acta, 47, 547-566.

Arpat, E. and Şaraoğlu, F., 1972. The East Anatolian fault system: thoughts on its development. Bull. Min. Res. Expl. Inst. Turkey, 78, 33-39.

Arpat, E. and Şaraoğlu, F., 1975. Türkiye'deki bazı önemli genç tektonik olaylar. Türkiye Jeoloji Kurumu Bülteni, 18, 91-101 (in Turkish).

Barka, A.A., 1992. The North Anatolian Fault Zone. Annales Tecton., 6, 164-195.

Canıtez, N. and Üçer, S.B., 1967. Computer determinations of the fault plane solutions in and near Anatolia. Tectonophysics, 4, 235-244.

Canik, B., 1971. Bolu Kaplıcalarının Jeoloji ve Hidrojeoloji Etüdü. MTA Raporu No. 5028 (in Turkish).

Canik, B., 1972. Düzce, Derdin Hamamı Civarının Jeoloji ve Hidrojeoloji Etüdü. MTA Raporu No.6359 (in Turkish).

Collocott, T.C. and Dobson, A.B. (eds.), 1975. Chambers dictionary of science and technology. W and R Chambers Ltd., Edinburgh, 1296 p.

Çemen, I., Gökten, E., Varol, B., Kılıç, R., Özaksoy, V., Erkmen, C., 2000. Turkish earthquakes reveal dynamics of fracturing along a major strike-slip fault zone. EOS, Trans., Am. Geophys. Union, 81, 309-313.

Dewey, J.F., Şengör, A.M.C., 1979. Aegean sea and surrounding regions: complex multiplate and continuum tectonics in a convergent zone. Geol. Soc. Am. Bull., Part I, 90, 84-92.

Erişen, B., Akkuş, İ., Uygur, N. and Koçak, A., 1996. Türkiye Jeotermal Envanteri. Maden Tetkik ve Arama Genel Müdürlüğü, Ankara, 480 p. (in Turkish).

Fournier, R.O. and Truesdell, A.H., 1973. An Emprical Na-K-Ca Geothermometer for Natural Waters. Geochim. Cosmochim. Acta, 37, 1255-1275.

Fournier, R.O., 1977. Chemical geothermometers and mixing models for geothermal systems. Geothermics, 5, 41-50.

Fournier, R.O., and Potter, R.W. II, 1979. Magnesium correction to the Na-K-Ca chemical geothermometer. Geochim. Cosmochim. Acta, 43, 1543-1550.

Fournier, R.O., 1979. A revised equation for the Na-K geothermometer. Geothermal Resource Council Transections, 3, 221-224.

Fournier, R.O. and Potter, R.W., 1982. A Revised and Expanded Silica (quartz) Geothermometer, Geotherm. Resourc. Counc. Bull., 11, 10, 3-12.

Fournier, R.D., 1991. Water geothermometers applied to geothermal energy. In: D'Amore, F. (Co-ord.), Application of Geochemistry in Geothermal Reservoir Development. UNITAR, USA, 37-69.

Giggenbach, W.F., 1988. Geothermal Solute Equilibria. Derivation of Na-K-Ca-Mg Geoindicators. Geochim. Cosmochim. Acta., 52, 2749-2765.

Jackson, J.A. and McKenzie, D.P., 1984. Active tectonics of the Alpine-Himalayan belt between Western Turkey and Pakistan. Geophys. J.R. Astr. Soc., 77, 185-264.

Henley, R.W, Truesdell, A.H., Barton, P.B. and Whitney, J.A., 1984. Fluid-Mineral Equilibria in Hydrothermal Systems. Reviews in Economic Geology-Volume 1, Society of Economic Geologists, 267 p.

Koçak, A., 1974. Çavundur (Kurşunlu-Çankırı) Kaplıca Bölgesinin Hidrojeoloji Etüdü Raporu. MTA Raporu No. 6373(in Turkish).

Koçyiğit, A., 1990. Tectonic setting of the Gölova basin, total offset of the North Anatolian Fault Zone, Eastern Pontide, Turkey. Annales Tecton., 4, 155-170.

Koçyiğit, A., 1988. Tectonic setting of the Geyve basin: age and total displacement of the Geyve fault zone. METU Pure Appl. Sci., 21, 81-104.

Mc Kenzie, D.P., 1972. Active tectonics of the Mediterranean region. Geophys. J. R. Astron. Soc., 30, 109-185.

Mutlu, H. and Güleç, N., 1998. Hydrogeochemical outline of thermal waters and geothermometry applications in Anatolia (Turkey). Journal of Volcanology and Geothermal Research, 85, 495-515.

Müftüoğlu, E. and Akıncı, K., 1989. Bolu-Seben Kesenözü Kaplıcası ve Çevresi Jeotermal Enerji Aramaları Sismik Etüd Raporu. MTA Raporu No. 8856 (in Turkish).

Nieva, D. and Nieva, R., 1987. Developments in geothermal energy in Mexico, part 12. A cationic geothermometer for prospecting of geothermal resources. Heat Recovery Systems and CHP, 7, 243-258.

Özcan M. and Ünay T., 1978. Bolu-Seben-Kösenözü Kaplıcası ve Çevresi Jeotermal Enerji Aramaları Rezistivite Etüdü Raporu. MTA Raporu No. 8269 (in Turkish).

Piper, A. M., 1944. A Graphic Procedure in the Geochemical Interpretation of Water Analysis, Trans. Amer. Geophys. Union, 25, 914-923.

Rotstein, Y. and Kafka, A.L., 1982. Seismotectonics of the southern boundary of Anatolia, Eastern Mediterranean region: subduction, collision, and arc jumping. J. Geophys. Res., 87, B9, 7694-7706.

Schoeller, H., 1977. Geochemistry of Groundwaters. In: Groundwater Studies and International Research and Practice, UNESCO, Paris, Ch. 15, 1-18.

Seymen, İ, 1975. Tectonic characteristics of the North Anatolian Fault Zone in Kelkit Valley. Ph. D. Thesis. İstanbul Technical University Publications, 192p.

Shapiro, L., 1975. Rapid analysis of silicate, carbonate and phosphate rocks: U.S. Geological Survey Bulletin, 1401, revised ed., 76 p.

Şahinci A., 1971. Mudurnu Kaplıcası Hidrojeoloji Etüd Raporu. MTA Raporu No. 4367 (in Turkish).

Şaroğlu, F., 1988. The age and offset on the North Anatolian Fault. METU J. Pure Appl. Sci., 21, 65-79.

Şaroğlu, F., Emre, Ö. And Kuşçu, İ., 1992. Türkiye Diri Fay Haritası, MTA.

Şengör, A.M.C., 1979. The North Anatolian Transform Fault: its age, offset and tectonic significance. J. Geol. Soc., London, 136, 269-282.

Şengör, A.M.C. and Yılmaz, Y., 1981. Tethyan evolution of Turkey: a plate tectonic approach. Tectonophysics, 75, 181-241.

Şengör, A.M.C. and Canıtez, N., 1982. The North Anatolian fault. In: Berckhemer, H., Hsu, K. (Eds.), Alpine-Mediterranean Geodynamics. Am. Geophys. Union, Geodynamics Series, 7, 205-216.

Şengör, A.M.C., Görür, N. And Şaroğlu, F., 1985. Strike-slip faulting and related basin formation in zones of tectonic escape: Turkey as a case study. In: Biddle K.T., Christie-Blick N. (Eds.), Strike-slip Faulting and Basin Formation. Soc. Econ. Paleontol. Mineral. Sp. Pub., 37, 227-264.

Şentürk Ö., and Ünay T., 1976. Amasya-Terziköy ve Gözlek Kaplıcaları Sıcak Su Aramaları Rezistivite Etüdü Raporu. MTA Raporu No. 5672 (in Turkish).

Tatar, Y., 1978. Tectonic study of the Erzincan-Refahiye section of the North Anatolian Fault Zone. Hacettepe Univ. Earth Sci., 4, 201-236.

Tonani, F., 1980. Some Remarks on the Application of Geochemical Techniques in Geothermal Exploration. in Proceedings, Adv. Eur. Geoth. Res., Second Symp., 428-443.

Toprak, V., 1988. Neotectonic Characteristics of the North Anatolian Fault Zone between Koyulhisar and Suşehri (NE Turkey). METU J. Pure Appl. Sci., 21, 155-168.

Truesdell, A.H. and Fournier, R.O., 1975. Calculation of Deep Temperatures in Geothermal Systems from the Chemistry of Boiling Spring Waters of Mixed Origin, Proc. Second U.N. Symposium on Geothermal Resources, San Francisco, CA, 837-844.

Truesdell, A.H., 1976. Summary of Selection III Geochemical Techniques in Exploration. in Proceedings, Second United Nations Symposium on the Development and Use of Geothermal Resources. San Francisco,CA, 1975, 1, 1iii-1xiii.

Tüysüz, O., Barka, A.A. and Yiğitbaş, E., 1998. Geology of the Saros Graben: its implications on the evolution of the North Anatolian Fault in the Ganos-Saros region, NW Turkey. Tectonophysics, 293, 105-126.

Ünlü M.R. and Balkaş Ö., 1975. Kösenözü Kaplıcası-Belören (Ankara-Bolu İli) Alanının Jeolojisi ve Jeotermal Olanakları. MTA Raporu No.3228 (in Turkish).

Weast, R.C.(ed.), 1974-75. Handbook of Chemistry and Physics. CRC Press, Ohio.

Wigley, T.M.L., 1978, WATSPEC: A computer program for determining the equilibrium section of aqueous solutions, Univ. Of East Anglia Pub., Norwich-England, 1-45.

Yücel B., Alkaş İ., and Ünlü M.R., 1994. Bolu Sıcaksu Sondajı (B-1) Kuyu Bitirme Raporu. MTA Raporu No. 9831 (in Turkish).

APPENDIX A

METHODS OF ANALYSES

Preparation of Quartz Powder

First a quartz crystal was broken into pieces using a hammer. Then they were placed into the jaw crusher and obtained smaller chips. Finally, the chips were ground by means of the shatter box. In case of contamination, all tools were cleaned by the help of an air pump. Obtained powder is washed with diluted HCl acid at 1:1 ratio or with concentric HCl acid. This mixture was heated on a hot plate. Then it was filtered and washed with distilled water 5 or 6 times. When acid was removed completely, powder was dried in a furnace at 110 °C. After drying, the sample was placed into desiccator until it gets normal temperature.

Preparation of Standard SiO_2 Solution

The method was taken from Shapiro (1975) after some modifications.

Reagents:

1) NaOH Pellets
2) H_2SO_4 (3N)

Procedure:

- 0.1 gram of the sample and 32 pellets (0.75 gram) of NaOH were put in a nickel crucible.
- The nickel crucible containing all these ingredients was melted over a small flame and then heated until it took a bright red colour and next, the melt on the sides of the crucible was swirled. The melt was then cooled. When it is cooled, 2 litre of H_2O was added to them.
- After cooling stage, in order to take the melt into a dry beaker, each crucible was heated by adding distilled water on it. To facilitate the dissolving procedure, the crucibles were heated and alternatively cooled by washing process by the help of a wash bottle.
- 40 ml of H_2SO_4 (3N) was added to the dissolved solution and the contents of the beaker were filtered into 1-litre flasks. The filtrate was completed to 1 litre by volume with distilled water and mixed. They were then immediately transferred to plastic bottles to be used for silica analysis.

SiO_2 Analysis

SiO_2 was determined by the help of the spectrophotometer using standard solution SiO_2, by the molybdenum – blue method.

Reagents:

1- Dilute HCl + NH_4 – Molybdate (Ammonium molybdate acid mixture)

2 gram NH_4 Molybdate was dissolved in about 70 ml of distilled water and 6 ml of concentrated HCl was added to the solution. The solution was then completed upto 250 ml by distilled water.

2- 10 % Oxalic Acid Solution

10 gram of oxalic acid was dissolved in 100 ml of distilled water.

3- Dilute H_2SO_4

200 ml of H_2SO_4 was diluted to 1 litre.

4- Metol + Na_2SO_3 (Metol – sodium sulphide solution)

3 gram Na_2SO_3 anhydrite was dissolved in 230 ml of distilled water and 5 gram of metol was added. The mixture was then completed upto 250 ml by distilled water. Solution was filtered and kept in a dark bottle.

5- Reducing Solution

85 ml of metol – sodium sulphide (Na_2SO_4) solution was mixed with 50 ml of oxalic acid solution and 100 ml of dilute H_2SO_4 was added to the. Volume was then completed to 250 ml in a volumetric flask.

Procedure:

- In different 100 ml volumetric flasks, 2 ml of solution of each sample was transferred with a 2 ml pipette. Also, 2 ml of distilled water and 2 ml of silica standard were transferred to the flasks, too.
- 10 ml of HCl + NH_4 Molybdate was added to each flask.
- All the flasks were kept in place for about 15 minutes.
- 15 ml of reducing solution was added to the contents of each flask.
- All the flasks were completed to 100 ml using distilled water and they are shaken well.
- All the flasks were left for a period of about 12 hours, then the results were read at 812 μm wavelength on the spectrophotometer.

T.C. YÜKSEKÖĞRETİM KURULU
DOKÜMANTASYON MERKEZİ

- The blank solution was used to standardize the instrument at minimum absorbance. Absorbance of all the solutions wee read 3 times and averages were taken. Dividing the weight percentage of known rock standard and absorbance value of standard, a factor was obtained. For each sample this factor was multiplied by the corresponding absorbance value, giving the weight percentage of SiO_2.

  The concentration of SiO_2 in the samples was determined by using the formula:

  SiO_2 % = [(sample absorbance x standard concentration) / standard absorbance] x 100

Sulfate Analysis

Sulfate was analysed using SulfaVer Method by the HACH DR/2000 Direct Reading Spectrophotometer. Sulfate ions in the sample reacted with barium in Sulfaver 4 Sulfate Reagent and formed insoluble barium sulfate turbidity. The amount turbidity formed was proportional to the sulfate concentration. Finally result was obtained in mg/l.

Chloride Analysis

Chloride was analysed using Mercuric Thiocyanate Method by HACH DR/2000 Direct Reading Spectrophotometer. Chloride in the sample reacted with mercuric thiocyanate to form mercuric chloride and liberate thiocyanate ion. Thiocyanate ions reacted with the ferric ions to form an orange ferric thiocyanate

complex. The amount of this complex was proportional to the chloride concentration. The result was read as mg/l.

Alkalinity Analysis

Alkalinity analysis was performed by Titration method (HACH Digital Titrator-MK120). The sample was titrated with sulfuric acid to a colorimetric end point corresponding to a specific pH. Phenolphthalein alkalinity was determined by titration to a pH of 8.3, as evidenced by the colour change of phenolphthalein indicator, and indicates the total hydroxide and one half the carbonate present. Total alkalinity was determined by titration to a pH between 3.7 and 5.1, and includes all carbonate, bicarbonate and hydroxide.

Total Hardness

Total hardness analysis was performed by Titration method (HACH Digital Titrator-MK120). After the sample was buffered to pH 10.1, ManVer 2 Hardness Indicator was added, and formed a red complex with a portion of the calcium and magnesium in the sample. EDTA titrant reacted first with the free calcium and magnesium ions, then with those bound to the indicator, causing it to change to a blue colour at the end point.

Calcium Hardness

Calcium hardness analysis was performed by Titration method (HACH Digital Titrator-MK120) like total hardness. Calcium was titrated with EDTA, after

removing magnesium interference by pH adjustment. After all calcium in the sample was complexed by EDTA, CalVer 2 indicator changed colour from red to blue, signalling the end point.

Then Ca and Mg concentrations were calculated as mg/l using the hardness relationships:

mg/l Ca = mg/l Ca or Ca Hardness as $CaCO_3$ x 0.4

mg/l Mg = mg/l Total Hardness as $CaCO_3$ – mg/l Ca Hardness as $CaCO_3$

mg/l Mg = mg/l Mg hardness as CaCO3 x 0.842 x 0.29

APPENDIX B

CALCULATION OF BOILING TEMPERATURE

Boiling temperature was calculated using the formula (Collocott and Dobson, 1975):

Altitude = [32 (500 + T1 + T2) (B1-B2)] / (B1 + B2)

Where ;

T1 = Temperature at sea level (T °C)

T2 = Temperature at the station of interest (T °C)

B1 = Barometric pressure at sea level = 0.760 mmHg

B2 = Barometric pressure at the station of interest (mmHg)

The elevations for the fields of concern ranges between 900 m and 1000 m. Since as elevation difference of 100 m results in 1 °C change only, 900 m is accepted as the average elevation. Temperatures at sea level and at the station of interest are taken to be the mean annual temperatures. Using these data and the formula above, B2 value (barometric pressure at the station) is found as 0.68. The boiling temperature corresponding to this pressure is then obtained as about 97 °C from Handbook of Chemistry and Pyhsics (Weast, 1974-1975).

The boiling temperatures in Kurşunlu and Mudurnu geothermal field were calculated using the same procedure.

APPENDIX C

CALCULATION OF CHARGE BALANCE ERROR (CBE) AND TOTAL DISSOLVED SOLIDS (TDS)

Charge Balance Error:

An aqueous solution must be electrically neutral, or the sum of all cation equivalents must equal the sum of all anion equivalents. The charge-balance error is given by the equation:

$$CBE = \frac{\sum m_c z_c - \sum m_a z_a}{\sum m_c z_c + \sum m_a z_a} x100$$

where,

m_c and m_a are the concentrations of the cations and anions, respectively, in mol/l ;

z_c and z_a are the absolute values of the charges of the cations and anions, respectively.

A reasonable limit for accepting an analysis as valid is ± 5 %.

Total Dissolved Solids (TDS):

Represents the total amount of solids in mg/l remaining when a water sample is evaporated to dryness. In principle, it is the sum of all dissolved constituents.

APPENDIX D

EXAMPLE OUTPUT FILE FOR PROGRAM WATSPEC

SAMPLE NUMBER 1

INPUT DATA

(Moles per litre of solution: Equivalents per litre for alkalinity)

CaTOT	MgTOT	NaTOT	KTOT	ClTOT	ALKAL
0.00117000	0.00070000	0.12147000	0.00639000	0.01836000	0.10540000
SO4TOT	AlTOT	FeTOT	SrTOT	BaTOT	LiTOT
0.00007000	0.00000000	0.00000000	0.00000000	0.00000000	0.00000000
NO3TOT	SiO2TOT	BTOT	BrTOT	H2STOT	NH4TOT
0.00000000	0.00062000	0.00000000	0.00000000	0.00000000	0.00000000

****

Ph= 7.33 Pe= --- Temperature (deg C)= 55.50 Density (gm/cc)= 1.00
-LOG(PCO2)= 0.42 -LOG(PO2)= --- -LOG(PCH4)= ---
Ionic Strength= 0.12475
Total Dissolved Solids (gm/lt soln)=10.23
Total Inorganic Carbon Molality= .1117709
Ion Balance Error (%)= 3.15
Cation Excess (charge*moles)= 7.779613E-03
H20 Activity= 0.9956

****

INDIVIDUAL SPECIES MOLALITIES

OH-	2.362724E-06	CO3--	3.351443E-04	HCO3-	9.913103E-02
SO4--	5.491462E-05	Cl-	1.851862E-02	Ca++	5.785874E-04
CaOH+	1.355915E-08	CaCO3o	8.538149E-05	CaHCO3	5.172172E-04
CaSO4o	8.970952E-07	Mg++	4.394565E-04	MgOH+	8.307911E-08
MgCO3o	2.700563E-05	MgHCO3	2.401052E-04	MgSO4o	5.865904E-07
Na+	.1179865	NaCO3-"	9.992532E-04	NaHCO3"	3.697424E-03
NaSO4-	1.305888E-05	NaClo	2.955423E-05	K+	6.453163E-03
KSO4-	1.266211E-06	KClo	1.63172E-06	Ba++	0
BaOH+	0	Sr++	0	SrOH+	0
Li+	0	LiOHo	0	LiSO4-	0
H4SiO4	6.185304E-04	H3SiO4	7.879362E-06	H2SiO4	1.410091E-08
Al+++	0				
AlOH++	0	AlOH2+	0		
AlOH4-	0	AlSO4+	0	AlSO42	0
Fe+++	0	FeOH++	0	FeOH2+	0
FeOH3o	0	FeOH4-	0	FeCl++	0
FeCl2+	0	FeCl3O	0	FeSO4+	0
Fe++	0	FeOH+	0	FeOH2o	0
FeOOH-	0	FeSO4o	0	NH4+	0

T.C. YÜKSEKÖĞRETİM KURULU
DOKÜMANTASYON MERKEZİ

NH3aq	0	NH4SO4	0	NO3-	0
H+	5.792467E-08	H2SO4o	1.823039E-20	HSO4-	2.636202E-10
HClo	9.095597E-15	H2Saq	0	HS-	0
S--	0	Br-	0	H3BO3o	0
H2BO3-	0	H2CO3	6.738382E-03	O2aq	0

****

INDIVIDUAL SPECIES ACTIVITIES

OH-	1.729463E-06	CO3--	1.14137E-04	HCO3-	.0757283
SO4--	1.790645E-05	Cl-	1.361377E-02	Ca++	2.00108E-04
CaOH+	1.047436E-08	CaCO3o	8.786964E-05	CaHCO3	3.995471E-04
CaSO4o	9.23238E-07	Mg++	1.597376E-04	MgOH+	6.47335E-08
MgCO3o	2.779262E-05	MgHCO3	1.779629E-04	MgSO4o	6.036846E-07
Na+	8.935449E-02	NaCO3-"	7.633507E-04	NaHCO3"	3.805173E-03
NaSO4-	9.975954E-06	NaClo	3.041549E-05	K+	4.743975E-03
KSO4-	9.672855E-07	KClo	1.679271E-06	Ba++	0
BaOH+	0	Sr++	0	SrOH+	0
Li+	0	LiOHo	0	LiSO4-	0
H4SiO4	6.365554E-04	H3SiO4	5.84008E-06	H2SiO4	4.802215E-09
Al+++	0				
AlOH++	0	AlOH2+	0		
AlOH4-	0	AlSO4+	0	AlSO42	0
Fe+++	0	FeOH++	0	FeOH2+	0
FeOH3o	0	FeOH4-	0	FeCl++	0
FeCl2+	0	FeCl3O	0	FeSO4+	0
Fe++	0	FeOH+	0	FeOH2o	0
FeOOH-	0	FeSO4o	0	NH4+	0
NH3aq	0	NH4SO4	0	NO3-	0
H+	4.677352E-08	H2SO4o	1.876166E-20	HSO4-	1.976593E-10
HClo	9.360658E-15	H2Saq	0	HS-	0
S--	0	Br-	0	H3BO3o	0
H2BO3-	0	H2CO3	6.934749E-03	O2aq	0

****

MINERAL SATURATION INDICES

ADULARIA	---	ALBITE	---	ANHYDRIT	-3.641
ANORTHIT	---	ARAGONIT	0.775	BARITE	---
BOEHMITE	---	BRUCITE	-3.969	CALCITE	1.123
CA-MONT	---	CELESTIT	---	CALCEDN	0.017
CHLORITE	---	DOLOMITE	2.203	GIBBSITE	---
GOETHITE	---	GREIGITE	---	GYPSUM	-3.737
HALITE	-4.559	HALLOYST	---	HEMATITE	---
HUNTITE	1.404	HYDROMAG	1.012	ILLITE	---
KAOLINIT	---	K-MICA	---	MACKINAW	---
MAGNESIT	0.920	MAGNETIT	---	MIRABILT	-7.042
NESQUEHO	-2.224	PHLOGOPT	---	PYRITE	---
PYROPHYL	---	QUARTZ	0.390	SIDERITE	---
STRONTNT	---	TALC	0.496	THENARDT	-6.627
WITHERIT	---				